University of Sassari

Department of Biomedical Sciences

PhD School in Life Sciences and Biotechnologies

Director: Prof. Leonardo A. Sechi

Cycle XXXIV

Development of suitable tools to produce a DISC vaccine to control African Swine Fever

Supervisor:

Prof. Marco Pittau

PhD Candidate:

Dott.ssa Roberta Piredda

Academic Year: 2020-2021

...A mio Nonno A.P...

Roberta Piredda

Development of suitable tools to produce a DISC vaccine to control African Swine Fever

PhD School in Life Sciences and Biotechnologies
University of Sassari

TABLE OF CONTENTS

Abstract

African Swine Fever is a highly contagious, lethal, and economically devasting infectious disease that affects bush pigs, warthogs, domestic pigs, and wild boars. ASF is present in Africa, eastern and western Europe, Asia, and Sardinia, where it is endemic since 1978. The etiological agent of ASF is the *African Swine Fever Virus* (*ASFV*), a large, enveloped virus assembled by an icosahedral structure containing a double-strand DNA genome. The lack of a vaccine limits the options to control the disease. For this reason, it is important the development of a vaccine capable of infecting and inducing a long last immunity as well as avoiding the arise of side effects and the risk of possible recombination with the wild type virus to eradicate the disease. Therefore, the main goal of the present project is the development of a DISC vaccine specific for *ASFV* Sardinian isolates. Vaccines' production requires the development of suitable continuous porcine cell lines genetically stable to support viral replication. The natural target cells for *ASFV* are cells derived from monocytes, in particular macrophages. At present, there are not monocyte/macrophage continuous cell lines permissive to virus replication. In the natural host, *ASFV* replicates in endothelial cells as well. This work showed the development of an immortalized Porcine Aortic Endothelial Cell (iPAEC) line using E6-E7 oncogenes derived from *OaPV3* ovine papillomavirus. This allowed us to obtain a suitable continuous cell line derived from porcine that may be used to develop a DISC vaccine. Analysis on iPAEC cells showed that they are capable to support viral replication revealing a highly susceptibility to *ASFV* infection. In addition, the production of a DISC vaccine requires the deletion of selected *ASFV* genes. This project showed the design of synthetical target late genes and their expression in Cos-1 cell lines. The presented work allowed us to set up a strategy to develop helper cell lines expressing mutagenized genes and capable to support replication of defective viruses. The methodology here described represents a new suitable tool for vaccines development.

Roberta Piredda

Development of suitable tools to produce a DISC vaccine to control African Swine Fever

PhD School in Life Sciences and Biotechnologies
University of Sassari

1. Introduction

1.1 African swine fever: a general overview

African swine fever (ASF) is one of the most important infectious and hemorrhagic diseases that affects both domestic and wild suids and it must be notified to the World Organization of Animal Health (OIE) to immediate restrictions on pigs and pork trade. For this reason, ASF is considered an economically devasting disease. ASF is present in many African, eastern, and central European countries, Asia, and Sardinia. The etiological agent of ASF is the ASF virus (*ASFV*), a DNA virus which is one of the two members of the family *Asfarviridae*. ASF was described for the first time in 1921 in Kenya (*Montgomery, 1921*) and since then it has spread rapidly to other African countries. From Africa *ASFV* escaped in 1957 to reach Portugal by contaminated waste containing infected pig products used to feed pigs. After this invasion, which was rapidly controlled, *ASFV* re-entered Portugal in 1960 spreading to the whole Iberian Peninsula, where it persisted for more than 30 years (*Arias and Sanchez-Vizcaıno, 2002*). During this period, *ASFV* spreads sporadically to other countries in Europe and America. ASF has been eradicated from all these countries except from Sardinia, where it is endemic since 1978 after its spread from Iberian Peninsula by contaminated waste (*Sanchez-Vizcaıno and Arias, 2012; Costard et al., 2013*). Sardinia is the only Italian region in which ASF is endemic, and this is due, probably, to socio-economics influences, to prevalent free-range livestock and to the high number of wild boars circulating in the region. In 1994 ASF started to spread from the African continent to west African countries and some islands that were free of the disease. The spread was probably due to a combination of factors including increasing pigs' production on the continent, the presence of asymptomatic pigs that could act as reservoirs to spread the virus, and globalization. These factors combined with the economic crisis of the present century could be the origin of the virus spread to eastern Europe (*Penrith and Vosloo, 2009; Sanchez-Vizcaıno et al., 2013*). In fact, in 2007 *ASFV* entered Georgia via contaminated food used for pigs alimentation and from that moment it spreads rapidly affecting neighboring countries such as Armenia, Azerbaijan and the Russian Federation where *ASFV* affects both domestic pigs and wild boars and has spread to the north and west. In 2012 the first outbreaks were registered in Ukraine and in Belarus in 2013 (*Sanchez-Vizcaıno et al., 2013*). ASF continued to spread reaching the European Union frontiers in

2014, when several wild boars were found dead in Lithuania and Poland. Since then, several cases have been reported in Estonia and Latvia and over and over in Lithuania and Poland (*OIE, 2014*), and this devasting disease continues to be reported in 16 countries (during 2020-2021). The critical situation of ASF in east and central Europe raises a serious risk to other EU countries, which could suffer the severe consequences of trade restrictions, as has already happened with Russian Federation bans. Despite that, two European countries have reported eradication of the disease, such as Czech Republic (April 2018) and Belgium (March 2020). In August 2018, the virus has reached China, representing the first appearance of ASF in Asia. Since then, the disease continued to spread in the Region, affecting 16 countries in 2021. In September 2019, ASF occurred for the first time in Oceania, followed by Papua New Guinea (March 2020), and in July 2021 the virus reappeared in the Americas after an absence of almost 40 years, first in Dominican Republic and later in Haiti (*OIE, 2021*) (Figure 1). Recently, in January 2022, ASF appeared in different Italian regions, such as Piemonte, Liguria and Campania.

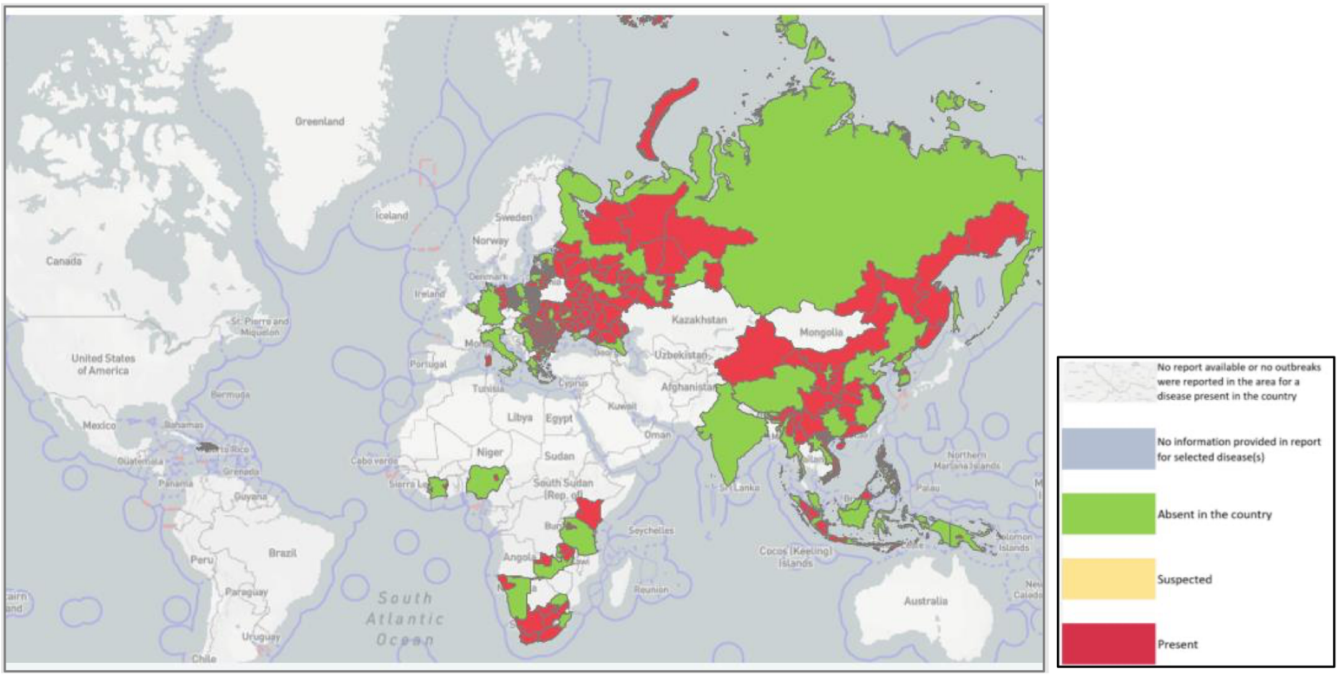

Figure 1 *ASF distribution in 2020-2021 (OIE, 2021)*

The main routes for ASF spread involve the transport of infected animals and infected products that could be imported illegally or may involve the transport of wastes containing contaminated pig

products. Other sources of infection are related to contaminated objects, including livestock vehicles or infected materials. In addition, natural ranging of wild boars is one of the most serious problems for the European Union due to the proximity to affected territories, as demonstrated by the recent cases detected at EU frontiers. Other important causes for *ASFV* transmission are infected ticks because the virus can also be transmitted by arthropods, or airborne transmission, even though at a local level, and should be potential sources for ASF infection in distant countries that are disease-free. ASF is principally characterized by the presence of hemorrhagic lesions of skin and internal organs of the infected animals, even though clinical signs could be different depending on different property as, for example, the virulence of the viral isolate, the route and dose of infection and the host characteristics. Therefore, every animal that present fever in a high-risk area, should be tested for ASF. *ASFV* strains are usually classified as high, moderate, and low virulent (*Pan and Hess, 1984*). High virulent strains are usually responsible for the per-acute (pigs dead 1and 4 days post infection) and acute forms (animals dead 3 and 8 dpi) of the disease, characterized by a mortality rate of the 100% of the infected animals, while moderate virulent strains are involved in the acute and sub-acute forms (animals die after 20 dpi). Chronic, or asymptomatic, ASF has been associated with infection by moderate-to-low virulence isolates (*Mebus and Dardiri, 1979; McVicar, 1984*), which were only described in Spain, Portugal, and the Dominican Republic when ASF infection was endemic. In this form the majority of the infected animals survives becoming asymptomatic carrier of ASF. No vaccine is available to prevent virus infection, for this reason, prevention is based on avoiding introduction of the disease. The main control measures are to monitor the entry of pigs and pig products and to forbid the use of waste for feeding pigs. Especially food waste from infected areas must be incinerated and never used to feed pigs (*Sanchez-Vizcaıno and Arias, 2012*). An important risk for ASF-free territories near affected areas is the contact between wild boars and domestic pigs. It is also important separating domestic free-ranging pigs from wild boars, as well as increasing biosecurity by fencing pig farms. Another important measure to control the disease is the presence of an early detection strategy that includes raising consciousness between veterinarians and farmers by providing them with updated information on risks. The control measures for ASF are based on rapid detection and diagnosis, culling animals in infected holdings, and forbidding movements of pigs and pig-derived products in affected areas. It is also necessary to investigate the involvement of wild boars and ticks in disease appearance (*Sanchez-Vizcaıno et al., 2014*). All these control measures are

difficult to apply in Sardinia where there is a high number of wild boars that live in close contact with domestic pig populations, supporting virus spread. The only effective weapon capable to counteract virus spread would be the development of an effective and safe vaccine, that is still not available. In 2017, the European Commission for health and food safety, has elaborated a document containing the guideline to work together to create a vaccine against *ASFV* (*Blueprint and Roadmap on the possible development of a vaccine for African Swine Fever prepared by the African Swine Fever EU Reference Laboratory on Commission Request*).

1.1.1 Epidemiology

The natural hosts of *ASFV* are African sylvatic suids such as bush pigs (*Potamochoerus porcus* and *P. larvatus*) and warthogs (genus *Phacochoerus*). Nevertheless, also wild boars and domestic pigs are susceptible to virus infection. On the other hand, different soft ticks species (genus *Ornithodoro*s) constitute viral vectors, where the virus can survive for more than five years (*Oleaga-Pèrez et al., 1990*). In general, wild boars are more resistant to *ASFV* infection than domestic pigs, albeit they show a similar pathology and epidemiology (*Sánchez-Vizcaíno, 2006*). Normally, sylvatic suids do not exhibit clinical evidence acting as a reservoir of virus in Africa (*De Tray, 1957*). In this area ASF is characterized by low virus levels into tissue and by a low or not observed viremia (*Plowright, 1981*). Based on that, they are not able to support virus transmission by direct contact and/or through soft ticks (*Jori e Bastos, 2009*). However, transmission occurs in newborn warthogs with high level of viremia (*Thomson, 1985*). For this reason, warthogs role is essential for the sylvatic cycle of *ASFV*, supporting the persistence of the disease into the entire Continent and bringing about serious obstacles to ASF eradication. On the other hand, in west Africa sylvatic suids and soft ticks play only a minimal role, since the virus spread is due especially to illegal trade of suids and infected pig products (*Penrith e Vosloo, 2009*). Based on the presence of reservoir animals, soft ticks, and their interaction with domestic suids, five possible epidemiological situations have been described. The most ancient scenario describes virus transmission in eastern and southern Africa, where sylvatic swine and soft ticks (species *O. Moubata*) act as a virus reservoir. In fact, *ASFV* transmission in domestic pigs is due, principally, to infected ticks and by the ingestion of warthog flesh with an acute infection (*Wilkinson, 1986*). The second scenario describes the typical situation that is present in west Africa.

In this area, transmission occurs via direct contact between domestic pigs or via indirect contact between swine and infected products, without soft ticks' involvement. In addition, the lack of veterinary services and the concealment of animals at the first stage of pathology, encourages virus spread in the country, and in neighboring regions (*Beltràn-Alcrudo et al., 2009*). The third situation appeared in the period 1960-1995, when the disease was present in the Iberian Peninsula. Domestic pigs and wild boars contracted the disease that was principally transmitted via contact between animals and infected pork flesh. In this situation, also soft ticks *O. erraticus* played an important role in *ASFV* transmission. For this reason, the simultaneous participation of infected wild boars and soft ticks has made the eradication of ASF difficult, especially for the existence of free-range livestock in which *O. erraticus* was the major cause of the disease re-emerge (*Boinas et al., 2011*). Despite that, ASF eradication occurred thanks to specific programs of disease control, which involved anti-tick antibodies detection in wild boars, the disposal of carcasses or the isolation of animals in the areas where ticks were present (*Arias e Sánchez-Vizcaíno, 2002b*). A similar situation occurred for the fourth scenario, during the disease spread in Central and South America (1968-1980). In these countries *ASFV* infected only domestic pigs, with no virus reservoirs, supporting an early eradication of the disease. (*Simeòn-Negrìn e Frìas- Lepoureau, 2002; Lyra, 2006*). The last situation is currently happening in Russia region and Trans-Caucasian countries where ASF affects domestic pigs (79,8%), due to the movement of infected animals and their products, and wild boars (20,2%), due to direct contact with domestic pigs (*OIE, 2011a; efsa, 2010a*). No ticks involvement was registered (*EFSA, 2010a*).

1.1.2 ASF clinical signs

ASF is a hemorrhagic disease that shows typical hemorrhagic lesions in the per-acute form and acute form but not in the sub-acute, chronical, and asymptomatic forms. Different clinical signs characterize the disease, and they depend on the strain virulence, host, viral load, and route of infection. In acute forms, clinical signs resemble those of other hemorrhagic diseases, such as Classical Swine Fever, Salmonellosis or Red Fever. For this reason, a laboratory diagnosis is necessary to confirm ASF.

Per-acute form

It is produced by high virulent strains, and it is characterized by high fever (41-42°C), lack of appetite, lethargy, tachypnea, and acute hyperemia. Death occurs within 1-4 days from the onset of clinical signs, without any organ lesions.

Acute form

Animals present a high fever (40-42°C), lack of appetite, lethargy, apathy, an early leucopenia due to a lymphocytopenia and a monocytopenia, and they tend to gather. A dramatic pulmonary oedema is present with an impaired respiratory function. The infected swine present a cutaneous erythema, especially in the ears area, tail, distal ends, chest, abdomen, and perineal area (Figure 2, A). Tiny necrotic clusters and subcutaneous hematomas are also described. (Figure 2, B-C). Other clinical signs that have been described are a serous rhinal drainage, epistaxis, vomit, abdomen pain, constipation or diarrhea that is initially mucoid but may rapidly evolve in hemorrhagic. In pregnant sow abortion may occurs. Approximately 90-100% of swine dead within the first week, showing lather around snout and jaws. Splenomegaly and diffused petechiae are also observed in several organs.

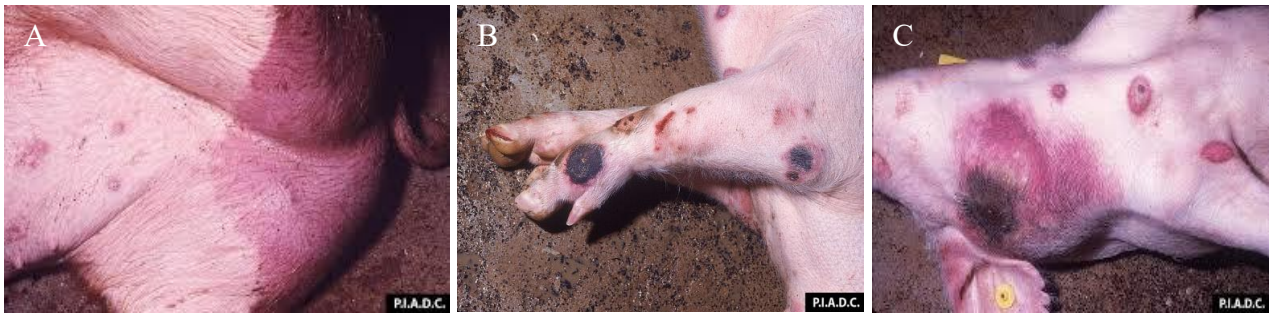

Figure 2 *Clinical signs in ASF acute form.* Imagine A shows the presence of cutaneous erythema. Pictures B and C show the presence of necrotic clusters and subcutaneous hematomas (*Sànchez-Vizcaino et al., 2015*).

Sub-acute form

Clinical signs are the same as the acute form but less pronounced, although vascular modifications are more intense. Swine dead within 7-20 days from the onset of the clinical signs, with a mortality rate of 30-70%. Surviving animals recover after 3-4 weeks, though they may eliminate virus until 6 weeks after infection.

Chronical form

This form is caused by low virulence strains, and it has been described only in some region characterized by the endemic presence of the virus, such as Spain, Portugal, and Dominican Republic. Nevertheless, it has not been described in Africa and Sardinia, where the virus has been present for a long time. This form is characterized by the persistence of cutaneous necrotic lesions, growth rate, weight loss, respiratory signs, abortion, and a low mortality rate. Vascular lesions are also present caused by secondary bacterial infections (*Sànchez-Vizcaino et al., 2015*).

1.2 *African Swine Fever Virus*

African Swine Fever Virus (ASFV) was discovered in 1921 in Kenya (*Montgomery, 1921*). *ASFV* is a large, enveloped, icosahedral double-stranded DNA virus with a linear genome that varies in size from 170 to 190 kbp depending on the strain, and contains terminal inverted repeats and covalently closed terminals (*Sogo et al., 1984; González et al., 1986; Tulman et al., 2009, Rodriguez et al., 2012*). It is the only know arbovirus with a DNA genome (*deoxyvirus*) and one of the two recognized members of the family *Asfarviridae,* genus *Asfavirus*. In fact, recently another member relating to this family has been discovered, the *Abalone Asfa-Like Virus (AbALV)* (*Matsuyama et al., 2020*). *ASFV* infects tissue macrophages, blood monocytes and specific lineages of reticular, polymorphs, and megakaryocytic cells (*Casal et al., 1984; Wilkinson, 1989*), while some virus replication has been described in endothelial cells (*Wilkinson and Wardley, 1978*), hepatocytes (*Sierra et al., 1987*), renal cells (*Gomez-Villamandos et al., 1995*) and neutrophils (*Carrasco et al., 1996*). *ASFV* also replicates in soft ticks of the genus *Ornithodoros*, which act as virus reservoirs. These ticks are involved in the epidemiological cycle of ASF in eastern and southern Africa (*Ornithodoros moubata*) and in the Iberian Peninsula (*Ornithodoros erraticus*). Other *Ornithodoros spp.* have been demonstrated to be susceptible to ASF infection (*European Food Safety Authority, EFSA, 2010*). *ASFV* is extremely resistant at pH and temperature variations, and it can remain infective for 100 days in the environment, 18 days at room temperature, and 7 days at 4° C. *ASFV* genome encodes for 151-167 open reading frames (ORF) that are densely distributed, separated by short intergenic regions. The virus particle contains more than 50 structural proteins that are immunogenic. At least six of the major *ASFV* structural proteins (p150, p37, p35, p34, p15, and p14) are synthesized as polyprotein precursors (pp220 and pp62), which is an unusual feature in a DNA virus. The viral architecture consists of a nucleoid that contains virus genome surrounded by the core shell, and it is organized in proteins layer. It is wrapped by an inner lipid envelope, an icosahedral capsid formed by protein subunits, and an outer lipid envelope. *ASFV* morphogenesis takes place in cytoplasmic areas, the viral factories (VFs), where occurs viral DNA replication. The VFs contain abundant membrane-like structures, which represent the first morphological evidence of virus assembly. By assembling the exterior capsid layer, viral membranes cover the core material obtaining a polyhedral shape (*Germán Andrés, 2017*).

1.2.1 Structure and morphogenesis of ASFV particle

The *ASFV* particle has an icosahedral morphology with an average diameter of 200 nm and is composed by several concentric layers: an internal core formed by the nucleoid containing DNA, coated by a thick protein layer named core shell, an inner lipid envelope surrounding the core and the capsid, which is the outermost layer of the intracellular virions (*Carrascosa et al., 1984; Andres et al., 1997*). The extracellular virions possess an outer envelope originated from the plasma membrane (*Breese and DeBoer, 1966*). The virions also contain the transcriptional enzymes for the synthesis, capping and polyadenylation of early RNA (*Salas, 1999*). There are 19 genes that are known to encode for structural proteins (Figure 3) and their localization in the different domains of the virus particle has been identified (*Yanez et al., 1995; Dixon et al., 2012*).

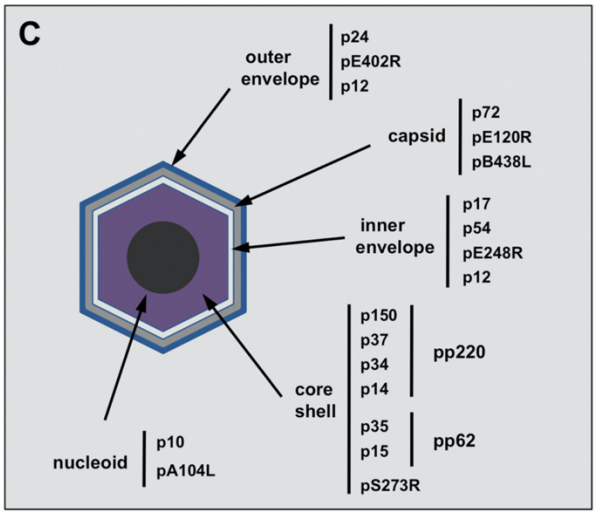

Figure 3 *Localization of different ASFV structural proteins in ASFV particle (Salas and Andrès, 2012)*

The outer envelope of extracellular virus is plasma membrane like, and p12, that is necessary for virus attachment, is localized into this structure (*Carrascosa et al., 1993*). In this region there was found another virus protein, virus homologue of cellular CD2 (pE402R) (*Dixon et al., 2012*), mediating hemadsorption of infected cells (rosette formation) (*Rodríguez et al., 1993*). p72, encoded by gene *B646L*, is the major component of the icosahedral capsid (*Garcia-Escudero et al., 1998*) and it takes up approximately one third of the virus particle mass. Another component of the capsid is pE120R

involved in the transport of mature virions from the VFs to plasma membrane (*Andres et al., 20017*). Into the capsid is found another important structural protein, p49, encoded by gene *B438L*, that is responsible for vertices assembly. The inner envelope is derived from the endoplasmic reticulum, and it contains different membrane proteins, such as p54, p17 and pE248R. The core shell is a thick protein layer of approximately 30 nm that is an independent domain of the virus core surrounding the central nucleoid (*Andres et al., 1997, 2002*). Its major components are the cleaved products of polyproteins pp220 and pp62 (*Li and Hochstrasser, 1999; Andres et al., 2001a*). The nucleoid is an electrodense structure of 80 nm containing the viral genome (*Andres et al., 1997*) and nucleoproteins such as the DNA-binding protein p10 (*Munoz et al., 1993, Andres et al., 2002b*) and protein pA104R (*Borca et al., 1996; Andres et al., 2002b*), which is similar to the histone-like proteins of bacteria. The nucleoid also contains the enzymes necessary for the synthesis and modification of early RNAs that includes the multi-subunit RNA polymerase, poly A polymerase, capping enzymes and early transcription factors (*Salas, 1999; Salas and German Andrès, 2002*). *ASFV* enters host cells by clathrine-mediated endocytosis or by micropinocytosis (Figure 4). Once inside the endosome, because of its acid environment, *ASFV* loses his capsid establishing into the cytoplasm to replicate. The *ASFV* particles are assembled into the VFs that are located close to the cell nucleus and the microtubule organizing center (MTOC). Extracellular *ASFV* particles have an outer envelope derived from plasmatic membrane, and an inner envelope originating from ER-membranes.

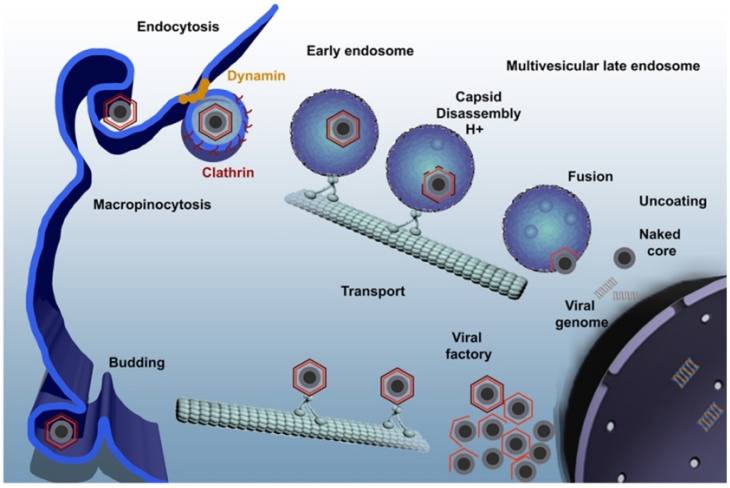

Figure 4 *African swine fever virus infectious cycle. ASFV can enter swine macrophages by clathrin-mediated endocytosis and actin-driven micropinocytosis (Galindo and Alonso, 2017).*

During the morphogenesis process there is a gradual increase in the size of the VFs occupying the cytoplasm that became larger (*Brookes et al., 1996; Sala and Andrès, 2013*). In this area the lack of cellular organelles is observed, and VFs were cover by the ER membranes and rolled up in a shell assembled with vimentin. The first step of *ASFV* particles morphogenesis (Figure 5) is the accumulation within the VFs of viral membranes, which are the precursors of the inner envelope. The second step is capsid formation that occurs with a process requiring ATP and Calcium (*Cobbold et al., 2000; Salas and Andrès, 2013*). The capsid is a layer with a hexagonal pattern that represents its surface, instead their vertices have a pentagonal pattern (*Carrascosa et al., 1984, Salas and Andrès, 2013*). p72 is the major capsid component, but its assembly is also due by pB602L, a non-structural protein that is necessary for p72 folding (*Cobbold et al., 2001; Epifano et al., 2006, Salas and Andrès, 2013*) and by p49, a minor capsid component involved in vertices formation (*Epifano et al., 2006b, Salas and Andrès, 2013*). Together with the capsid assembly, the core shell is formed. The last step in morphogenesis process is the nucleoid development. There are evidences that pronucleoids are first pre-formed in the VFs and then are encapsidated onto the empty particles through a single vertex (*Brookes et al., 1996, 1998; Salas and Andrès, 2013*). Once the *ASFV* particles are mature, they exit from the host cells releasing extracellular virions surrounded by the outer envelope (*Breese and DeBoer, 1966; Salas and Andrès, 2013*).

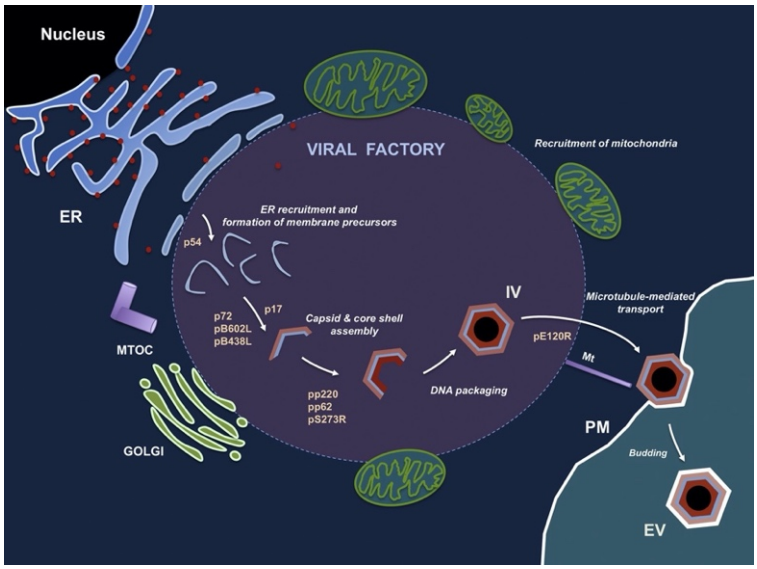

Figure 5 *Model of ASFV assembly (Salas and Andrès, 2012)*

1.3 *ASFV* Genome and its replication

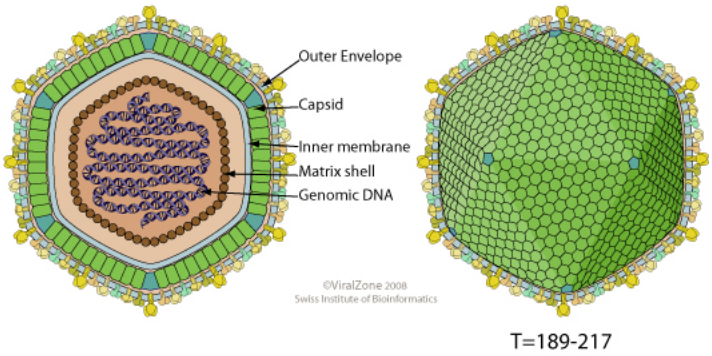

Figure 6 *Structure of ASFV particle, including his genomic DNA (https://viralzone.expasy.org/12, Swiss Institute of Bioinformatics, 2008)*

The *ASFV* genome is a linear double-stranded DNA molecule of approximately 170-193 kbp (*Yanez et al., 1995; Chapman et al., 2008; de Villiers et al., 2010*) that encodes for 151-167 proteins. Differences in genome length and genes number are due to gain or loss of multigene families (MGF) expressed by the virus. There are some smaller length variations due to a divergence in number of short tandem repeats either within genes or intergenic regions (Figure 7) (*Dixon et al., 1990; Lubisi et al., 2007*). The complete genome sequence of the tissue culture adapted *BA71V* was the first to be determined, and from that several other virus strains have been sequenced (approximately 200 different strains). Genes were named based on EcoRI restriction enzyme digestion, gene orientation (Left or Right), and number of amino acids of encoded proteins. Recently, a new nomenclature was proposed for multigene family according to their family name and their position into the genome (*Chapman et al., 2008*). Upstream of each gene there is a short sequence that contain the promoter which is recognized by the viral RNA polymerase complex. The genome termini are cross-linked and are present in two forms that are inverted and complimentary to each other. Their structure resembles that of *Poxvirus* genomes although the sequences are different. The *ASFV* genome consists of an average of approximately 61–62% A + T nucleotides (*Yanez et al., 1995*).

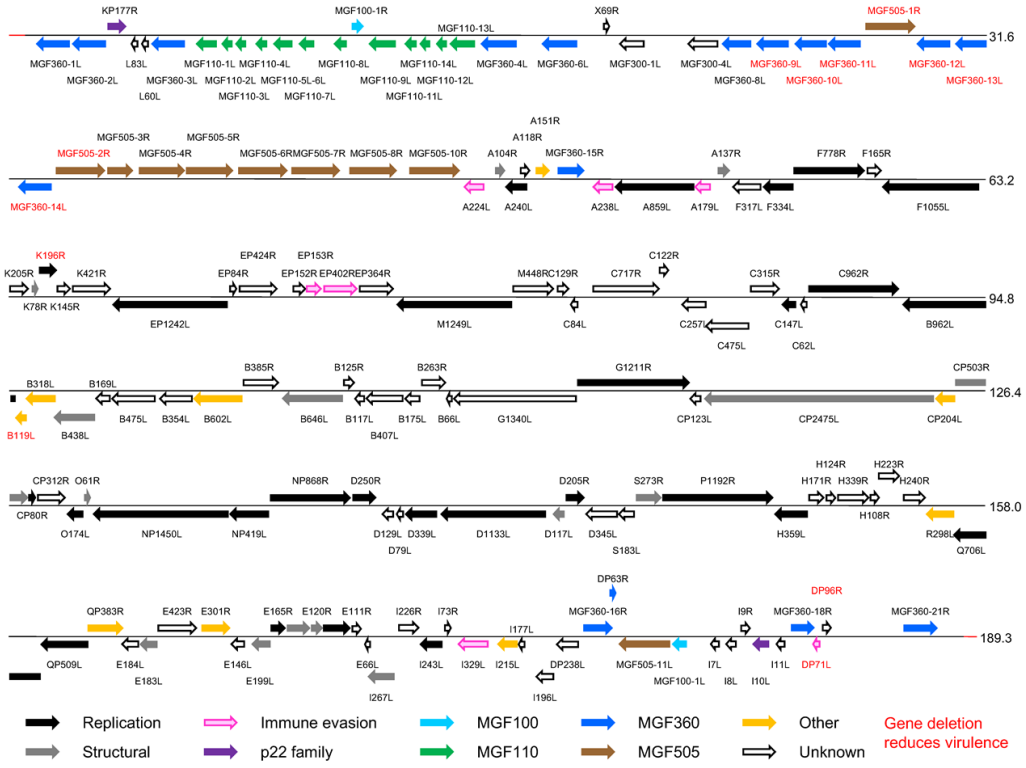

Figure 7 *Organization of ASFV isolate Georgia 2007/1 genome. The colored arrows indicate Open reading frames (ORFs) (Dixon et al., 2013).*

ASFV DNA replication took place in VFs. This process requires enzymes that are expressed immediately after virus entrance into the cytoplasm by partially uncoated core particles. Early transcription utilizes enzymes packaged in the core and encoded by virus (*Kuznar et al., 1980b; Salas et al., 1983; Dixon et al., 2012*). An early stage of DNA replication occurs also in the nucleus, and it took place at 6 h post-infection and declines to almost zero by 12 hpi (*Tabares and Sanchezbotija, 1979; Garciabeato et al., 1992b; Rojo et al., 1999; Dixon et al, 2012*). Genome fragments synthetized in the nucleus are relatively short and do not reach higher molecular weight or genome length fragments, quite the opposite, short fragments generated during cytoplasmatic DNA synthesis may reach higher molecular weight fragments. In the nucleus viral DNA is located close to the nuclear membrane. The role of the early nuclear phase of DNA replication is unknown. It has been postulated that the nucleus may provide transcripts or other factors required for virus replication. The similarities in *ASFV* genome structure to that of *Poxviruses* indicates that *ASFV* may have a replication model similar to that of vaccinia virus (*Moyer and Graves, 1981; Baroudy et al., 1982; Dixon et al., 2012*).

1.4 Genotype classification of *ASFV*

The phylogenetic analysis of *B646L* gene, that encode the major capsid protein p72, *E183L* gene, that encode the envelope protein p54, and the central variable region (CVR) of the *B602L* gene, has been used to classify *ASFV* into 23 genotypes (from I to XXIII). All genotypes are present in eastern and southern Africa where the sylvatic cycle, involving warthogs and soft ticks of the *Ornithodoros moubtata* species, is present (*Lubisi et al., 2005, 2007; Boshoff et al., 2007*). Analysis of isolates circulating in domestic pigs identified that genotype I spread through central and western Africa and then spread to Portugal in 1957 and 1960, and from there to other European countries, such as Sardinia, the Caribbean Island and Brazil (*Dixon and Wilkinson, 1988; Lubisi et al., 2005, 2007; Nix et al., 2006; Gallardo et al., 2011b; Dixon et al., 2012*). Until recently, genotype I was the only one found in central and western Africa, but genotype IX has now been identified in Republic of Congo (*Gallardo et al., 2011b; Dixon et al., 2013*). Genotype II is one of the genotypes circulating in south-eastern Africa in pigs in Mozambique and Zambia and has also been introduced to Madagascar (1998), Mauritius, Georgia and in the Caucasus (*Rowlands et al., 2008; Lubisi et al., 2009; Chapman et al., 2011; Dixon et al., 2012*). From Georgia ASF has spread to neighboring countries including the Russian Federation, Armenia, Azerbaijan, and Ukraine. Currently, complete genome sequences are available only for 6 of the 23 p72 genotypes (*Dixon et al., 2012*).

1.4.1 Sardinian ASFV isolates

All Sardinian *ASFV* isolates are members of p72 genotype I and IA, but they have shown minor genetic variations in two different regions of the genome, within the *B602L* and *EP402R* genes (*Giammarioli et al., 2011; Sanna et al., 2017*). A 6-amino acid repeat at the C-terminus of the CD2v protein, and 13 tetrameric repeats in the *B602L* ORF have been lost in 1990 by Sardinian *ASFV* isolates. Based on these characteristics, the isolates were placed into two temporally different subgroup: the first includes isolates identified during 1978-1990 period, and the second that consists of all isolates from 1990 until today. The first sequenced Sardinian *ASFV* isolate is the *47/Ss/08*, found in 2008 in Sassari area, and it is similar to Spanish strain. Its genome is made up of 184,638 nucleotides and with a GC content of 38.5% (*Granberg et al., 2016*). Beyond that, other *ASFV* strains

have been collected in Sardinia during the endemic period (1978-2014) (Table 1), and all the isolates show a high genomic stability (*Torresi et al., 2020*). Among them, the complete genome was sequenced also for another isolate, virus *26544/OG1*0, collected in 2010 in Nuoro territory. Its genome is 182,906 bp long with an average of 38.6% GC content and contains 164 ORFs (*Bacciu et al., 2016*).

Virus designation	Year	Province	Host species	GenBank accession no.
56/Ca/78	1978	Cagliari	Domestic pig (Sus scrofa domesticus)	MN270969
57/Ca/79	1979	Cagliari	Domestic pig (Sus scrofa domesticus)	MN270970
139/Nu/81	1981	Nuoro	Domestic pig (Sus scrofa domesticus)	MN270971
140/Or/85	1985	Oristano	Domestic pig (Sus scrofa domesticus)	MN270972
85/Ca/85	1985	Cagliari	Domestic pig (Sus scrofa domesticus)	MN270973
141/Nu/90	1990	Nuoro	Domestic pig (Sus scrofa domesticus)	MN270974
142/Nu/95	1995	Nuoro	Domestic pig (Sus scrofa domesticus)	MN270975
60/Nu/97	1997	Nuoro	Domestic pig (Sus scrofa domesticus)	MN270976
26/Ss/04	2004	Sassari	Domestic pig (Sus scrofa domesticus)	MN270977
72407/Ss/05	2005	Sassari	Wild boar (Sus scrofa)	MN270978
47/Ss/08	2008	Sassari	Domestic pig (Sus scrofa domesticus)	KX354450
26544/OG10	2010	Nuoro	Domestic pig (Sus scrofa domesticus)	KM102979
97/Ot/12	2012	Olbia-Tempio	Domestic pig (Sus scrofa domesticus)	MN270979
22653/Ca/14	2014	Cagliari	Domestic pig (Sus scrofa domesticus)	MN270980

Table 1 *ASFV Sardinian isolates until 2014 (Torresi et al., 2020)*

1.5 Similarities between *ASFV* and other virus families

ASFV is a member of the *Asfarviridae* family. The *Asfarviridae* represents a family inside the nucleocytoplasmic large DNA virus (*NCLDV*) superfamily, which is composed of a monophyletic class of viruses that infect a wide range of eukaryotic hosts. Both families have in common part of their replication cycle in the cytoplasm, even though the *NCLDV* is independent from the nucleus. It probably means that they should encode conserved proteins that mediate most processes essential for virus replication and transcription (*Iyer et al., 2001, 2006*). First virus families proposed in the *NCLDV* included the *Asfarviridae* and the *Poxviridae* in which different members infect insects, reptiles, birds, and mammals; the *Iridoviridae* which infects insects and cold-blooded vertebrates; the *Phycodnaviridae* which infects algae (*Iyer et al., 2001*). After that, the *NCLDV* were expanded to other newly discovered virus families including the *Mimiviridae* and *Marseillevirus* which infect acanthamoeba and the *Ascoviridae* which infects insects, especially Noctuids. Comparing the genome sequences of different *NCLDV* families were identified 9 genes that were present in all families and a variety of others that were present in more than one family, producing a map of about 40 genes that originate from a putative common ancestor. As expected, the *NCLDV* superfamily shares additional genes that are not present in other large DNA virus families, such as a Superfamily 3 helicase fused to DNA primase, a packaging ATPase and a disulphide oxidoreductase involved in morphogenesis. As well as individual *NCLDV* virus families encode unique genes earned to facilitate replication in particular environmental niches (*Iyer et al., 2006; Koonin et al., 2009; Koonin and Yutin, 2010; Yutin et al., 2009*). Metagenomic sequencing projects of virus fractions from different environmental niches, have identified gene fragments that share high sequence similarity with a variety of genes, including hallmark genes of the *Asfarviridae* family. In addition, the Heterocapsa circularisquama DNA virus (*HcDNAV*), that infects marine dinoflagellates, encodes a DNA polymerase B similar to that of *ASFV*, suggesting that it may be more closely related to the *Asfarviridae* than to the *Phycodnaviridae* as was originally believed. Recently, a new virus closely related to *Asfarviridae* family has been discovered, and it was named *Abalone Asfa-Like Virus* (*AbALV*), the putative causative agent of abalone amyotrophia. This new virus shares approximately 58 proteins with the *NCLDV* family (with 47 of them shared with *ASFV)* (*Matsuyama et al., 2020*), and for this it has been proposed as a new member of the *Asfarviridae* family.

1.6 *ASFV* late genes selected for the project

Different *ASFV* genes have been selected for the present study, such as *B438L*, *B119L*, *B318L*, *B962L* and *E120R*. All these genes are expressed late during *ASFV* infection, encoding, therefore, for their late proteins. *B962L* ORF is the last of four overlapping genes (*B438L*, *B119L* and *B318L* (Figure 8)) in a genome region encoding for capsid proteins (p72, p49), their folding and post-translational modifications.

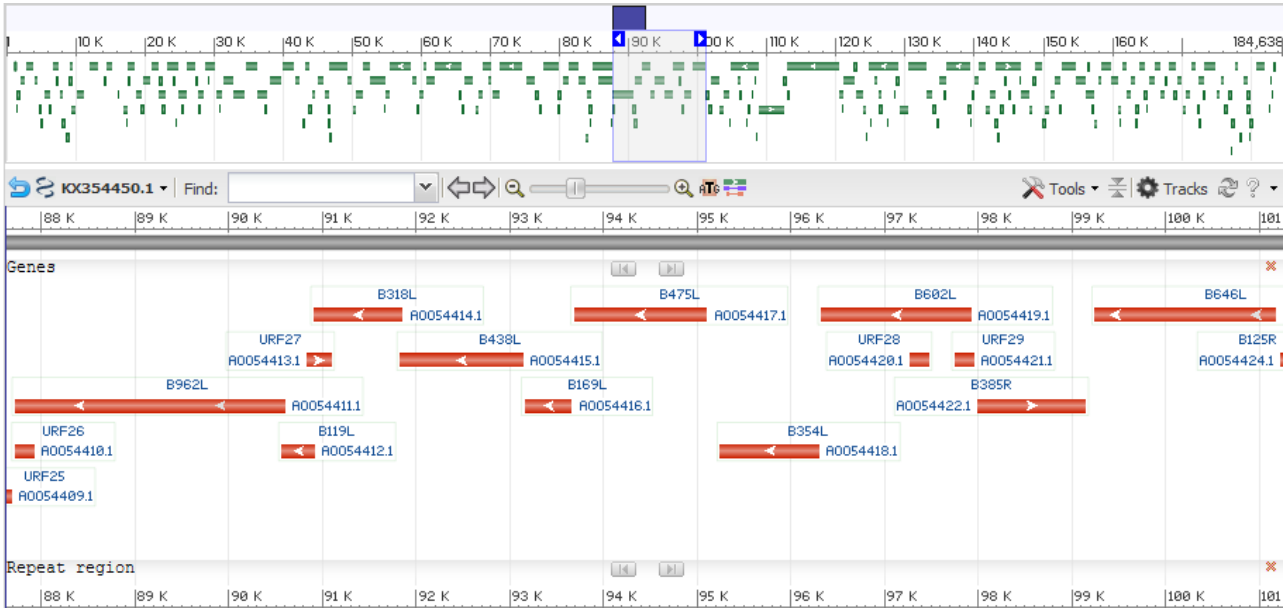

Figure 8 *ASFV isolate 47/Ss/2008 complete genome indicating ORFs B962L, B318L, B119L, B438L (NCBI, KX354450 key access number)*

The *B438L* ORF encodes for pB438L composed of 438 amino acids with a predicted molecular mass of 49,3 kDa (*Galindo et al., 2000*), which is expressed at late times pi. pB438L, also called p49, is localized at the VF and contains a cell attachment RGD (Arg-Gly–Asp) motif (*Yànez et al., 1995*). During the infection, p49 is associated with membranes acting as an integral membrane protein, and it is able to form disulfide-linked homo- or heterooligomers in the virus particle. It has been shown that, in the absence of p49, aberrant tubular structures without icosahedral morphology are generated (*Epifano et al., 2006*) (Figure 9). For this reason, it has been suggested that p49 is necessary for the generation of the capsid vertices, and it is essential for *ASFV* infectivity.

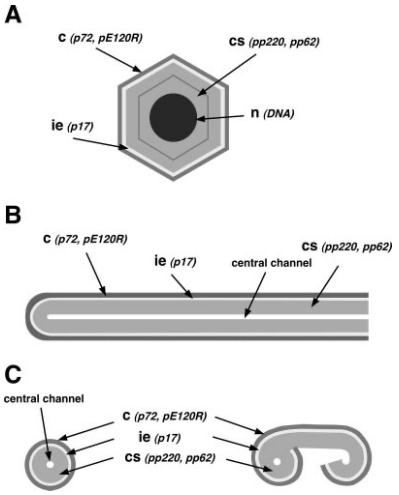

Figure 9 *Representation of structures generated in presence (**A**) or absence (**B**, **C**) of p49.* **(A)** Normal icosahedral particle. **(B)** Longitudinal section of a tubular particle. **(C)** Cross section of a tubular particle (left) and a bilobulate structure (right). c indicates the capsid, ie is the inner envelope, cs the core shell and n is the nucleoid (*Epifano et al., 2006*).

The *B119L* ORF encodes a 119-amino-acid protein of 14 kDa that conserves the PCXXC active-site motif and several residues that participate in FAD (Flavin Adenine Dinucleotide) binding in Alrp and Erv1p (*Gross et al., 2002*). It has been shown that pB119L is a flavoprotein member of the Erv1p/Alrp family, and it is considered as a nonstructural protein localized at VF and expressed at a late stage in *ASVF*-infected macrophages, and it is necessary for correct virus assembly (*Lewis et al., 2000*). pB119L is a FAD-linked sulfhydryl oxidase, which is present in infected cells especially in an oxidized state containing a disulfide bond and forms noncovalent dimers. In addition, it has been supposed that *ASFV B119L* gene is also involved in virus morphogenesis, because its deletion from the virus genome powerfully affects virions maturation and virus production in infected macrophages (*Rodríguez et al., 2020*) (Figure 10).

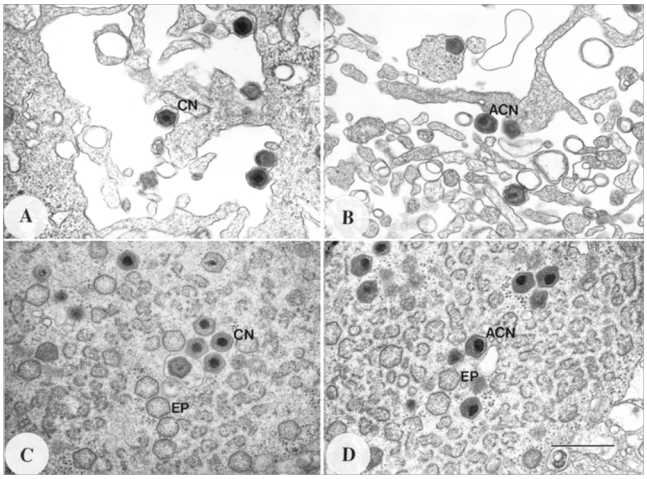

Figure 10 *Macrophages infected with an ASFV wild type (**A** and **C**) and with an ASFV strain with B119L deletion.* The imagines **B** and **D** show the presence of virus particle with acentric nucleoids (ACN) that is arranged over two vertices of the icosahedral shell, despite the imagines **A** and **B** where virus particles have a normal appearance *(Rodríguez et al., 2020).*

The *B318L* ORF encodes a polypeptide with a predicted molecular weight of 35,904 localized into cytoplasmic viral assembly site. It is a gene expressed at a late stage of virus infection that encodes for a late protein, pB318L, an *ASFV* trans-prenyltransferase, and it is classified as a putative class III membrane protein. Until today, *ASFV B318L* is the only viral prenyltransferase gene that has been identified, thought it has properties that are quite the opposite from those described for the FFP (Farnesyl Pyrophosphate) synthase or GGPP (Geranylgeranyl Pyrophosphate) synthase involved in the synthesis of the prenyl donors for protein prenylation. As pB318L is associated with viral membranes precursors derived from the ER, it has been supposed that it may be involved in the synthesis of ubiquinone prenyl chain to produce an extra amount of this compound and this could be necessary to protect virus membranes and its DNA against oxidation to prevent cell death by apoptosis of the infected cell (*Alejo et al., 1999*). *B962L ORF* is located in the central region of the *ASFV* genome and encodes for a putative DNA helicase of 962 amino acids, with a molecular mass of 109,6 kDa (*Yanez et al., 1993*). *B962L* is expressed late during *ASFV* infection, after the start point of viral DNA replication. pB962L contains amino acid motifs that are characteristics of helicases superfamily II, and it is able to form hexameric structures with a ring shape form and a modified AAA^{+} core involved in DNA binding or protein-protein interaction (*Singleton et al., 2007*). Until

today no function has been associated to *ASFV B962L*, and it has been supposed that *ASFV* pB962 key role is the viral DNA packaging inside the icosahedral capsid during replication final stages (Figure 11), but additional data would be necessary to support such a proposal (*Yanèz et al., 1993; Brookes et al., 1998*).

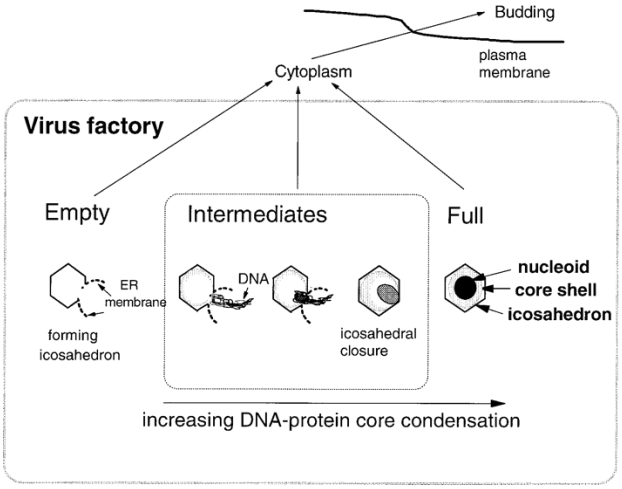

Figure 11 *Model of DNA packaging and ASFV particle assembly in the VF (*Brookes et al., 1998*)*

ORF *E120R* encodes for a protein of 120 amino acids characterized by a molecular mass of 14,5 KDa and with hydrophilic and acid properties. pE120R, named also p14.5, is a structural protein synthesized at a late phase of the viral infectious cycle after the beginning of DNA replication recruiting during capsid formation. In vitro analysis revealed that pE120R interacts with p72 (*Andrés et al., 2001*), and this elucidates the external localization of that protein in the virus particle. In addition, this protein interacts with DNA, and it was described as a DNA-binding protein. These characteristic properties suggested that pE120R may be involved in condensation or encapsidation of the viral DNA (*Martínez-Pomares et al., 1996*). A consecutive study by Andrés et al. in 2001 using a recombinant virus lacking *E120R* gene has shown that pE120R in necessary for virus egress and its expression is important for intracellular particles transport to the plasma membrane (Figure 12) (*Andrés et al., 2001*).

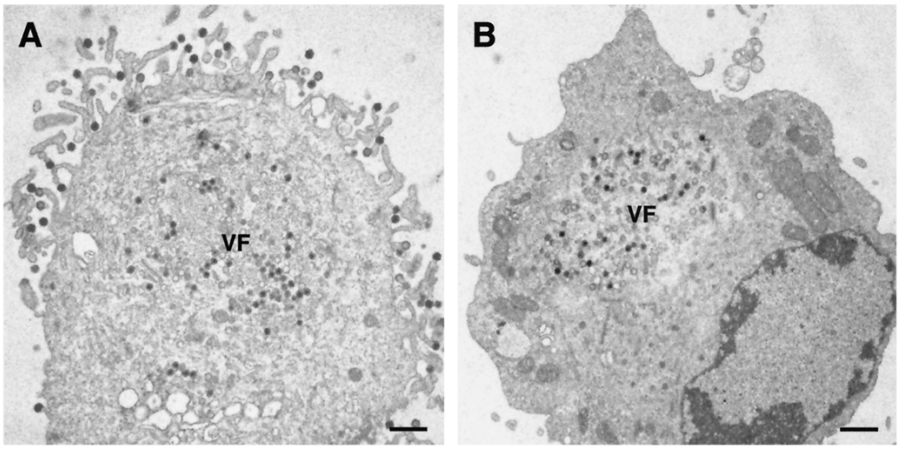

Figure 12 *Role of pE120R in intracellular particles transport.* Imagine **A** shows as, in the presence of the protein, viral particles move from VF to plasma membrane; instead, imagine **B** shows as, in pE120R absence, particles are assembled in the VF, but they cannot be transported (*Andrés et al., 2001*).

A more recent study has revealed that *E120R* can afford to suppress the host antiviral response via the inhibition of IFN-β production. In fact, the protein interacts with interferon regulatory factor 3 (IRF3), a key transcription factor that is important for type I IFN induction and is essential for genes expression in different innate immune response stages (*Canivet et al., 2018; Liu Huisheng et al., 2021*). Therefore, pE120R interferes with IRF3 recruitment to TBK1 (TANK-binding kinase 1) decreasing interferon production though suppressing IRF3 phosphorylation. The present study has shown a novel system used by *ASFV* to elude the host antiviral response, and *E120R* could be considered as a new target in *ASFV* vaccines development (*Liu Huisheng et al., 2021*).

1.7 Clustered Regularly Interspaced Short Palindromic Repeats/Cas9 technology

Clustered Regularly Interspaced Short Palindromic Repeat (CRISPR)-*Cas9* is an RNA-guided gene-editing platform that make use of an endonuclease (Cas9) and a synthetic guide RNA (sgRNA) to introduce a double strand break at a specific location within the genome (Figure 13). The CRISPR system is a prokaryotic adaptive immune system that uses the RNA-guided DNA nuclease Cas9 to silence viral nucleic acid and it has been shown to act as a gene editing tool in various organisms including mammalian cells. CRISPR technology consists of a short non-coding guide RNA (gRNA) made up of a target complementary CRISPR RNA (crRNA) and an auxiliary transactivating crRNA (tracrRNA). Basically, the crRNA defines Cas9 genomic target, while the tracrRNA acts as a scaffold to connect the crRNA to Cas9 and actively contributing to the conversion of mature crRNA from pre-crRNA derived from CRISPR arrays. The gRNA is able to guide the Cas9 endonuclease to a specific genomic locus through base pairing between the crRNA sequence and the target sequence and cleaves the DNA to create a double-strand break. The gRNA is made through a fusion of the natural crRNA and tracrRNA components and it is required for Cas9 to specifically bind and cleave a target DNA sequence. gRNA contains a 18-20 base variable sequence that can be changed to target any DNA sequence that is located immediately upstream of a PAM (Protospacer Adjacent Motif), a short DNA fragment of approximately 3-5 nucleotides (5'-NGG-3') that is required as a signal to bind Cas9 endonuclease (*Ran et al., 2013*).

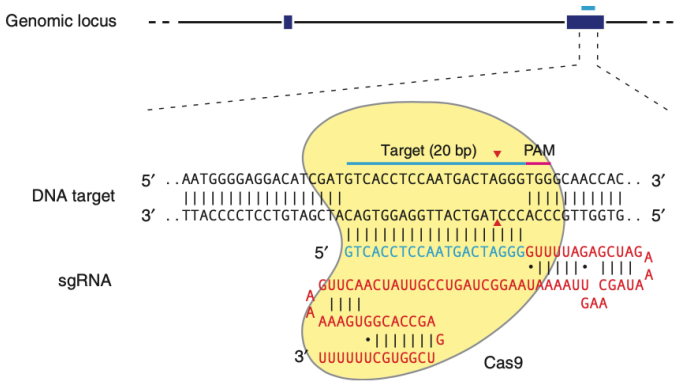

Figure 13 *Schematic representation of CRISPR-Cas9 system (Ran et al., 2013).*

1.8 Papillomaviruses and their transforming properties

In the present project we decided to use a protocol that was previously described by our research team to immortalize Primary Lamb Keratinocytes (PLK-1) (*Tore et al., 2019*), using oncogenes *E6* and *E7* deriving from two ovine papillomaviruses, *OaPV3* and O*aPV4*. Papillomaviruses are known to possess the ability to transform cells inducing their immortalization. For example, the first immortalized cell line, HeLa (epithelial cells from cervical carcinoma), has been naturally immortalized thanks to the presence of *HPV18* papillomavirus. Since the HeLa cells have been discovered, other cell lines have been immortalized using that system, and today we know that tumors transforming properties may be used to immortalize different primary cells and develop new stable and continuous cell lines. Papillomaviruses (PVs) are icosahedral double-stranded DNA virus. Usually, they infect skins and mucous squamous stratified epithelium of different vertebrates, in which they may cause cellular proliferation or persist asymptomatically. PVs are extremely species-specific, and the majority of them were identified in human. However, the direct link between PVs and neoplasia was discovered for the first time in animal papillomavirus, especially in cottontail rabbit papillomavirus (*CRPV*), bovine papillomaviruses (*BPVs*), and canine oral papillomavirus (*COPV*) (*Campo, 2002*). Most of PVs do not have any role in tumor progression and they are in healthy skin and mucosae located (*McMillan, 2006*). Different studies suggested that these viruses are extremely capable to adapt themself to the host environment, and they are controlled by the immune system with a limited virions production (*Doorbar, 2016*). A recent study has shown *FcaPV2* genes expression in oral and cutaneous SCC (Squamous Cellular Carcinoma), and E6 and E7 proteins transforming properties through pRB and p53 interaction, suggesting that virus may have an important role in SCC develop in feline species (*Altamura G. et al., 2016*). E6 ed E7 are the most important oncoproteins in papillomaviruses that are able to evade DNA reparation processes and apoptosis (*Tommasino, 2017*), causing cellular transformation and immortalization.

Transforming properties of E6

E6 cutaneous oncoproteins role in cells transformation is still not clear. Several studies suggested that their first function is p53 inactivation through indirect manner. Its inactivation is really recurring during tumor develop, and it have a key role in viruses caused transformation. For example, the E6 oncoprotein of different *beta-HPV* and *BPV1* bound LXXL motif of the *Mastermind-like 1*(MAML1), that is a core component of the canonical Notch signaling pathway (*Brimer et al., 2012*). In keratinocyte cells, the Notch signaling pathway has a crucial role during cell cycle arrest and differentiation, and its inactivation due to E6 oncoprotein may support viral life (*Rangarajan et al., 2001*).

Transforming properties of E7

E7 oncoproteins in *HPV* have the capability to bound protein pRb through LxCxE motif located into CR2 region (*Sullivan CS, et al., 2002; Ahuja D, et al., 2005; DeCaprio JA, et al. 2009*). pRb is a tumor suppressor factor involved in cell cycle control allowing the progression into G1/s phase. In quiescent cells, pRb is linked to E2F family transcriptional factors inhibiting them. pRB phosphorylation due to cyclin-dipendet kinasy (CDK) activity causes the interruption of pRb-E2F complex, leading to activate E2F transcriptional factors (*Tommasino, 2014*). pRb degradation and the consequently transcriptional activation by E2F are two key mechanisms by which viruses may preserve the DNA synthesis in differentiated epithelial cells (*McLaughlin-Drubin e Munger, 2009*).

2. Aim of the project

The present project is part of a collaboration between Institute of Infectious Diseases and Virology of the Department of Veterinary Medicine of University of Sassari, Istituto Zooprofillattico Sperimentale della Sardegna G. Pegreffi (Sassari), Institute of Molecular Biology Severo Ochoa of Madrid and Istituto Zooprofilattico Sperimentale Umbria e Marche (Perugia).

The lack of a vaccine limits the options to control the disease, for this reason it is extremely important the development of a vaccine capable of infecting and inducing a long last immunity as well as avoiding the risk of possible recombination with the wild type circulating virus in order to eradicate the disease. Therefore, the main goal of the project is the development of a DISC (Disabled Infectious Single Cycle) vaccine specific for *ASFV* Sardinian isolates. To carry out the aim, different objectives have been set up:

- Immortalization of Porcine Aortic Endothelial Cells (PAEC) by ovine papillomaviruses (*OaPV3* and *OaPV4*) oncoproteins *E6* and *E7*.
- Evaluation of the stability of *ASFV* Sardinian isolates cultivated on iPAEC cells and their susceptibility to virus infection.
- Design of different synthetic *ASFV* selected late genes.
- Stable expression of mutagenized *ASFV* genes in Cos-1 and iPAEC cell lines.
- Establishment of a cellular platform expressing different *ASFV* late proteins using CRISPR-Cas9 system to produce helper cells utilized to develop DISC vaccines.

3. Materials and methods

3.1 Immortalization of Porcine Aortic Endothelial cells

This step of the project was carried out in our laboratory of Veterinary Virology and Infectious Diseases of University of Sassari. Vaccine production require the development of suitable continuous cell lines genetically stable to support viral replication. It is important that such cell lines originate from naturally host species and from tissues involved in infection. The natural target cells for *ASFV* are cells derived from monocytes, in particular macrophages, primary cell lines difficult to obtain and to cultivate as does not exist a monocyte/macrophage continuous cell line capable to sustain virus replication. In the natural host, *ASFV* replicates in endothelial cells as well. For this reason, in this study primary Porcine Aortic Endothelial Cells (PAECs) have been set up and then their immortalization was performed. To this aim an immortalization tool that use *E6* and *E7* oncogenes derived from different ovine papilloma virus, *OapV3* and *OaPV4*, was applied.

3.1.1 Porcine Aortic Endothelial cells isolation

Primary Porcine Aortic Endothelial Cells (PAECs) were isolated thanks to a collaboration with Istituto di Clinica Ostetrica (Department of Veterinary Medicine, University of Sassari). Cells were collected from porcine aorta (10-14 cm of length) during slaughter process, according to animal welfare protocols. The aorta was washed in PBS (Dulbecco Phosphate Buffer Saline) without calcium and magnesium, supplemented with 1% penicillin/streptomycin (Euroclone) and 2,5 μg/ml of amphotericin B (Euroclone), to remove the residual blood. All the collateral arteries and an aorta end were closed with surgical suture thread (Ethicon-Somerville, Bridgewater, NJ) to obtain an aortic closed duct (Figure 14). The vessel cavity was filled with two different enzymatic solution.

Collagenase

The first method utilized 20 ml of collagenase H type 1 solution (0,1% in Dulbecco's Modified Eagle Medium, DMEM) and 1% Penicillin/Streptomycin. Then, the aorta was incubated at 37°C for 8-10

minutes, and later the enzymatic solution was harvested and deactivated by an equal volume of Porcine Endothelial Cell Growth Medium (Cell Application), centrifugated at 1200 rpm for 5 minutes at RT. The obtained cellular pellet was washed in sterile PBS, resuspended in cell medium, and cells were cultured in T25 tissue culture flask.

Dispase

The second method utilized 20 ml of dispase solution (25 U/ml in Dulbecco's Modified Eagle Medium, DMEM) with 1% Penicillin/Streptomycin. The aorta was incubated in enzymatic solution for 5-6 minutes at 37°C, then the suspension was collected and deactivated with an equal volume of cell medium, centrifugated at 1200 rpm for 5 minutes at RT, as described before. Cellular pellet was resuspended and cultured in T25 flask.

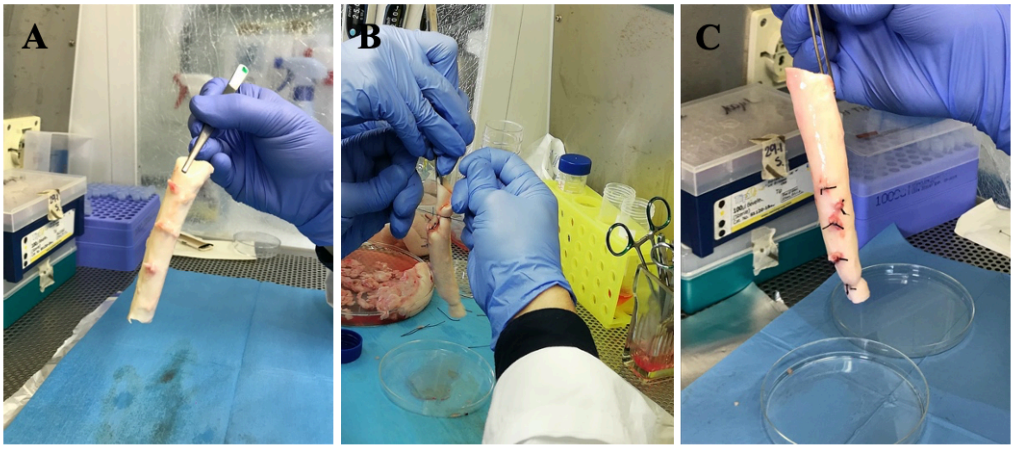

Figure 14 *PAEC isolation procedure.* **A**: porcine aorta; **B**: occlusion of the aorta extremity; **C:** collateral arteries closed by surgical suture thread.

3.1.2 Cell Culture

Porcine Aortic Endothelial Cells (PAEC) were cultured in Porcine EC Growth Medium (Cell Applications) supplemented with 20% of Fetal Bovine Serum (FBS) (Euroclone) and 1 µl/ml of amphotericin B (Euroclone). Phoenix cells are renal embryonal cells derived from human and immortalized by E1a adenovirus. They are usually employed to generate retroviral particles thanks

to their high capacity of being transfected. Phoenix cells were cultured in Dulbecco's Modified Eagle's Medium (DMEM) (Euroclone) supplemented with 10% of FBS, 100 units/mL penicillin, 100µg/mL streptomycin (Euroclone), 1% of L-glutamine (Euroclone) and 1 µl/ml of amphotericin B. Cos-1 cells derive from fibroblasts of green monkey (*Cercopithecus aethiops*) kidney, transformed with *SV40* virus. They were cultured in DMEM supplemented with 5% of FBS, 2mM L-glutamine, 100U/ml of gentamycin (Euroclone) and 0,4 mM of non-essential amino acids (Sigma). Cells were incubated at 37 °C with 5% of CO_2 in a humidified air (95%).

3.1.3 Plasmid design

For the project we employed two vectors developed before in our laboratory by our team, *pLXSN + OaPV3_E6E7* and *pLXSN + OaPV4_E6E7* expressing, respectively, genes *E6-E7* of *OaPV3* ovine papillomavirus 3 strain (Figure 15) and genes *E6-E7* of *OaPV4* ovine papillomavirus 4 strain (Figure 16). All plasmids used have been created with Snapgene® software (GSL Biotech LLC).

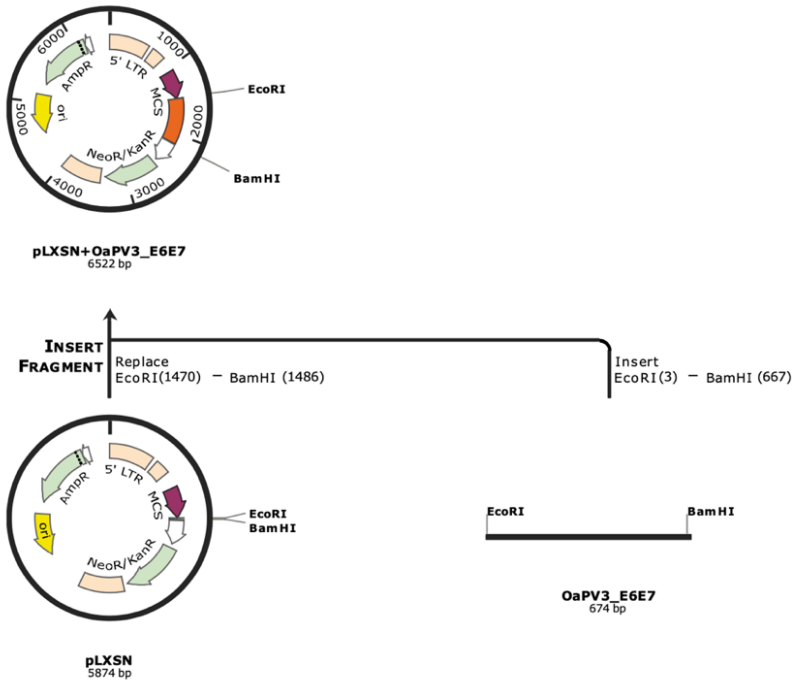

Figure 15 *pLXSN + OaPV3_E6E7*

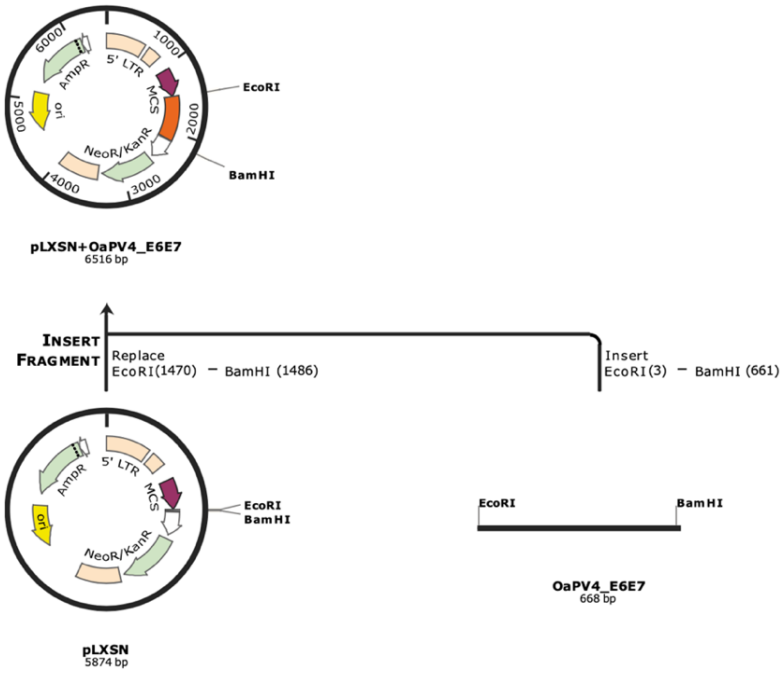

Figure 16 *pLXSN + OaPV4_E6E7*

3.1.4 Transfection of Phoenix cells

Phoenix cells were transfected using Calphos Mammalian Transfection kit (Clontech). Cells are seeded in 10 cm dishes the day before in order to have 50-70% of cell confluence prior to use. Before starting transfection, the old medium was removed from Phoenix cell cultures, and 5 ml of fresh complete DMEM supplemented with 5 µl of 25mM Cloraquine (25 µM as final concentration) were added. In the meantime, transfection solutions were prepared in 15 ml tubes (10 µg plasmid DNA + ddH2O up to 440µl, 62 µl of $CaCl_2$ 2M, 500 µl of HBS2X dropwise) using three different vectors:

- *pLXSN + OaPV3_E6E7*
- *pLXSN + OaPV4_E6E7*
- Empty *pLXSN* (used as a control)

Plasmid suspensions were added to cells dropwise and homogenously and incubated overnight. 24-hours after transfection medium was removed from cells and they were washed twice with PBS before adding 5ml of fresh complete DMEM. After 48- and 72-hours post infection (pi), medium of the Phoenix dishes (the supernatant contains retroviral particles) was collected and filtered through 0.2 µm filter twice. 5 µg/µl of PolyBren was added into each 5 ml retroviral suspension.

3.1.5 Infection of PAEC cell line

Primary Porcine Aortic Endothelial cells were seeded in 10 cm plates two days before infection. Old medium was removed from PAEC, and filtered retrovirus suspension was added to. 3-hours pi retroviral suspension was removed from the cells and fresh medium was replaced (Porcine EC Growth Medium).

3.1.6 Selection of transduced cells

Selection of transduced cells was started 24 hpi. Cells were splitted according to cell confluence and fresh medium supplemented with 0,7 mg/ml of G418 selective antibiotic was added. Selection was continued until death of control cells (not-infected PAEC).

3.1.7 Immunofluorescence

PAEC characterization was carried out using CD31 antibody. It is also known as Pecam-1 (Platelets Endothelial Cell Adhesion Molecule-1), and it is a specific endothelial marker expressed into cell junctions. $3{,}5x10^5$ Porcine Aortic Endothelial Cells were seeded in SPL Cell Culture borosilicate chamber slides (Euroclone) and let grow until 70-80% of confluence was reached. Afterwards, cells were washed twice with 1X PBS and fixed in 4% paraformaldehyde (PFA) at RT for 10 minutes. Fixed cells were incubated with 2% BSA (Bovine Serum Albumin, Sigma) in PBS for 30 min in a humid chamber. Primary antibody mouse-anti-pig CD31 was diluted 1:100 in 1% PBS/BSA and incubated with cells o/n at 4°C. Two or more washes with 1X PBS were performed before incubation with secondary antibody Donkey anti-Mouse IgG (H+L) Highly Cross-Adsorbed Secondary Antibody, Alexa Fluor 647 (fuchsia) or Alexa Fluor 488 (green) (Biorad) diluted 1:400 in 1% PBS

for 1 hour in the dark at RT. Two washes with 1X PBS were performed before incubation with DAPI (1µg/mL in milliQ) for 1 min. Cells were washed other two times before slide assembly in a ProLongTM Gold Antifade kit (Thermo Fisher Scientific) and analyze with confocal laser scanning microscope Leica SP5 associated with a Leica LAS AF Lite software for pictures acquisition.

3.1.8 RNA extraction from immortalized Porcine Aortic Endothelial Cells

RNA was extracted from iPAEC (immortalized Porcine Aortic Endothelial Cells) pellet using the RNeasy Mini Kit (Qiagen), following vendor's recommendations. RNA was treated by using the DNA-free™ DNase Treatment and Removal Reagents kit (Ambion), and retrotranscribed using the GoScript™ ReverseTranscription System (Promega), following manufacturer's instructions.

3.1.9 RT-PCR

cDNA of *E6E7* expressing iPAEC was used for RT-PCR to check *E6-E7* gene transcription. RT-PCR was performed with HotStarTaq DNA Polymerase (Qiagen) according to following conditions.

Primers

- OaPV3_E6E7_EcoRIF (5' GAGAATTCATGGAGGGAAGCCCTCGTAC 3')
- OaPV3_E6E7_BamHIstopR (5' AAGGATCCCTATGCAGCACACGGCGGAC 3')

Component	Volume	Final Concentration
10X PCR buffer	2,5 µL	1X
10 mM dNTP Mix	0,5 µL	200 µM
10 µM Primer Forward	0,75 µL	0,3 µM
10 µM Primer Reverse	0,75 µL	0,3 µM
cDNA	1 µL	
HotStarTaq DNA Polymerase (5U/ µl)	0,125 µL	0,625 U
dd H2O	19,375 µL	

PCR profile		
Initial activation step	94°C 15’	
Denaturation	94°C 30’’	35 cycles
Annealing	60°C 30’’	
Extension	72°C 30’’	
Final extension	72°C 10'	

PCR fragments were analyzed by agarose gel and purified with the DNA Clean & concentrator™ Kit (Zymo Research), according to manufacturer instructions. Purified samples were sequenced by BMR genomics (Padova).

3.1.10 Agarose gel electrophoresis

Agarose gels were prepared using a microwave to dissolve the agarose powder in 1X TAE buffer according to desired percentage. After boiling, GelRed® (Biotium) or GelGreen® (Biotium) was added to final 1X concentration and mixed. GelRed® (Biotium) was used for analytical visualization while GelGreen® (Biotium) was used for excision and purification of DNA fragments. The melted agarose was poured into a gel casting tray containing a comb. When solidified, the gel was placed in

the running chamber filled with 1X TAE buffer. DNA samples supplemented with loading buffer were loaded into wells together with 1kb plus DNA ladder (Invitrogen). Agarose gel electrophoresis was performed at 80V, and DNA was visualized with the GelDoc EZ® system (Biorad).

3.2 iPAEC infection with Sardinian *ASFV* isolates and evaluation of their susceptibility.

This step has been developed in collaboration with the Istituto Zooprofilattico Sperimentale della Sardegna G. Pegreffi (Sassari).

3.2.1 Primary cultures of porcine macrophages

Primary macrophages were isolated from peripheral blood samples derived from healthy swine of approximately 4-12 months old come from Azienda Sperimentale di Surigheddu (Sassari), a property of Istituto Sperimentale Zooprofilattico della Sardegna. Selected animals have been periodically checked in order to verify the absence of *ASFV* infection, according to animals' welfare protocols. Blood was collected and supplemented with heparin (100 U/ml), then was processed to set up macrophage cultures, according to Malmquist test (*Malmquist et al., 1960*). Blood was centrifugate at 700g for 30 minutes at 4°C, and serum was stored at 4°C to add it to macrophages culture medium, instead red blood cells were diluted in PBS 1/10 and stored at 4°C. Buffy coat was removed and incubated for 10 minutes at RT in hemolysis sample, and centrifugated at 700g for 10 minutes at 4°C. This step was carried out three times to obtain a cell pellet without red blood cells, and it was washed in PBS. Cells were counted using trypan blue (Sigma) to verify their viability and resuspended in RPMI (Roswell Park Memorial Institute)-164 medium (Euroclone) supplemented with 100 U/ml penicillin, 100 μg/ml streptomycin, 20% of autologous serum, seeded into 96-multiwell-plate or in T25 flasks at 37°C with 5% of CO_2 in a humidified atmosphere for 48 hours to allow monocyte/macrophages to attach. Once they are attached to the plate, they may be used to cultivate viruses.

3.2.2 ASFV isolates

For the project two *ASFV* isolates were selected, the high virulent Sardinian isolate *2008 (47/Ss/08)* isolated in the region of Sassari, and an attenuated isolate *NH/P68* isolated in Portugal in 1968. Both viruses belong to Genotype I, and Sardinian isolate has hemo-adsorbing ability while *NH/P68* not (*Gallardo et al; 2009; Franzoni et al;2017*). Both *ASFV* isolates were amplified in vitro using macrophage cultures. Macrophages were inoculated with 0.5 ml of each virus and incubated for 2 hours at 37°C. Then, culture medium supplemented with 1% of erythrocyte diluted 1/10 in PBS was added only to hemo-adsorbing virus (*2008*). After 3 days of incubation at 37°C, flasks were freezed and unfreezed for three times at -80°C, and then supernatant was collected, centrifugated at 3000g for 15 minutes and stored at -80°C.

3.2.3 Virus titration

Virus titration was realized on porcine monocyte/macrophage with serial dilutions of the isolates. 5 days pi the viral titer was calculated based on hemo-adsorbing properties for *2008* isolate or by direct immunofluorescence for *NH/P68*. The hemo-adsorbing event was estimated calculating the formed rosette, that happen when erythrocytes stick to the infected macrophage. Otherwise, the viral titer of *NH/P68* isolate was evaluated via direct immunofluorescence, using a polyclonal antibody anti-p72 conjugated with a fluorochrome (supplied by Istituto Zooprofilattico of Perugia). Medium was removed and macrophages washed three times with PBS and fixed with a EtOH/methanol solution for 15 minutes at 4°C. Fixed cells were incubated for 1 hour with the antibody diluted 1:200 in PBS and then analyzed by fluorescent microscope (*Axiovert 200, Zeiss, Germany*). Viral titer was established using Spearman–Kärber formula to calculate the 50% endpoint by serial dilution.

3.2.4 Infection of COS-1 and iPAEC cells with ASFV isolates

Cos-1 and iPAEC cells were mock infected or infected with isolates *2008* and *NH/P68* with different MOI (Multiplicity of infection): 3, 1 and 0.2. After 1 hour and half of incubation, viruses were removed, and cells were washed with PBS and culture medium was replaced. Cells were stopped at 2-, 4-, 24-, 48-, 72- and 96-hours pi. Experiments with MOI 1 and 3 were carried out in triplicate,

while experiments with MOI 0.2 in duplicate. At a later time, cells pellet and supernatant were collected. Supernatant was centrifugated for 5 minutes at 2000 rpm and stored at -80°C, while cellular pellet was stored in RNA later or fixed.

3.2.5 Flow cytometry assay

Cellular pellet collected before was fixed using Leucoperm (solution A), following manufacturer's instruction (Bio-Rad Antibodies). Then, cells were permeabilized using Leucoperm (solution B), following manufacturer's instruction. Subsequently, cells were washed with PBS, and incubated with antibody anti-p72-coniugated-FITC (clone 18BG3, Ingenasa, Madrid, Spain) for 30 minutes in the dark at RT. Then, cells were washed twice with PBS, centrifugated at 800g and resuspended in PBS supplemented with 2mM EDTA in specific tubes and analyzed by FACS Celesta (BD Biosciences). Analysis of data was performed using BD FACS Diva Software/BD (Biosciences). Gates for late *ASFV* protein p72 were set using mock-infected controls.

3.2.6 DNA extraction and Real-Time PCR

DNA was extracted from cellular pellet (viral intracellular DNA) and supernatant (viral extracellular DNA) of Cos-1 and iPAEC cells at 2h, 4h, 24h, 48h, 72h e 96h pi and from their mock-infected controls. For DNA extraction the PCR Template Preparation Kit (Roche) was used with an automatic extractor, the MagMax™ Express 96 (Applied Biosistem) following manufacturer's instructions. Real-Time PCR was performed using a protocol described by OIE handbook (*OIE, 2012; King et al., 2014*) shown in the table. The protocol utilizes a TaqMan probe FAM marked that is specific to the ORF encoding for protein p72, situated between nucleotide 267- 291 of the *ASFV* sequence presents in Gene Bank (accession number AY578692). The probe is located inside the region between primers RealPSAs (5' CTG CTC ATG GTA TCA ATC TTA TCG 3') and RealPSAa (5' GTA ACC ACA AGA TCR GCC GT 3'). After amplification, a threshold cycle (CT) value was assigned to each PCR reaction, and the analysis was evaluated using $\Delta Ct = Ct\ (sample) - Ct\ (mock)$ formula.

Component	Final concentration
Primer sense	50 pmol
Primer anti-sense	50 pmol
probe	5 pmol
TaqMan® master mix (Applied biosystem)	1x
Nuclease-free-water	
DNA template	3 µl

3.3 Establishment of a cellular platform expressing different *ASFV* late proteins using CRISPR-Cas9 system to produce helper cells to develop DISC vaccines.

This project step was carried out in our department (Veterinary Infectious Diseases and Virology), and it should have been continued at the Institute of Molecular Biology Severo Ochoa of Madrid, but unfortunately due to pandemic situation, it was not possible.

3.3.1 Design of selected late ASFV genes

Different late genes were selected to the aim of the project, such as *B438L*, *B119L*, *B318L*, *B962L* and *E120R* (Figure 17, 19, 21*)*. Nucleotide sequences of the genes were got from gene bank (NCBI), and they belong to *47/Ss/08 ASFV* Sardinian isolate (KX354450 key access number) or *26544/OG10 ASFV* Sardinian isolate (KM102979 key access number). Subsequently, selected gene nucleotide sequences were mutagenized in order to delete PAMs on both strands (NGG/CCN), since they are required as a signal to bind Cas9 endonuclease in CRISPR-Cas9 technology. PAMs were removed changing only a nucleotide in the sequence without any amino acid variation (Figure 18, 20, 22). This step is necessary to develop helper cells, stable cell lines that will express mutagenized genes. Cells will be infected with *ASFV* Sardinian isolates in which will applicated CRISPR-Cas9 system to interrupt a viral gene without interrupt the mutagenized one integrated into cell line. By this way,

defective viral particles will be produced, and they will be able to survive and infect without replicate (methodology to design a DISC vaccine).

B962L

>KM102979.1 ASFv 26544/OG10 from Italy, B962L

ATGGGAAAACCGACTTTATTGGAGCCTGGTCATCTCTATAACGTGCCCGCTGAGCACAAGAATGATGTTCCTATTCATTACATCATCACGT
GGATAAAACAACGTCTCCCGGAGTTTGGAGGGGCCATTCCAACCTCCCTCGCAGACCGGGTGCTCATTATAAAGTCACGCACTGGATCC
GGAAAATCCACGGCCCTGCCCGTACACGTGTTCAGAATTCTGAGAAATGAAAACACGCATTCTTTCCAAAAATACTTGGGACGCTCGGT
TATTTGTACCCAGCCAAGAGTCCTAACCGCAGTGACCCTCGCCAAAGACATCGGCGCCTCAACCCACTACCCCGACATGATATTAGGCCA
AACAGTGGGCTACCAGACGAAGCCTCTGACGGAAAAACCCAATCGGGGCCTTATCTATGCAACCGCGGGGGTTCTGTTGGCGCAGCTA
CATACAATGACGGATGATGAGATAGCTTCCCGCTATGCCTTTATGATTATAGATGAGGCCCATGAGCGAGCCCTAGGCATCGACCTTATGC
TCATGTATATTAAAAGTATGCTTCAGCGCATGTTGCAAAGAGGAAGCATAGGGGCGCTGCGTATTCCCTTTGTAATTTTAACCTCCGCCAC
CATTGATACCCATAAATACTCAACCTATTTTGGTATCGGAAAAGAAAACATTATTTTGGTGGAAGGACGACAGTACGGTGTGGAAACCCA
CTGGCCGCTGTATAACACCAACAACTACATTAAGACCGCCTGCGAAACGGCTCTCACTATTCATAAAGAAAACATTCATGATCGTCCCACG
GAAGCAGATATTTTAATTTTCATGCCCGGTATGGCTGAAATACGCTTCCTTTCGATGTTGCTGAATAATGCAAATATGGACCTTGCCAAAG
AAAAGCTGCCGTTAATGTTGATTTTGCCGATCGATAGT/GAGGCGATTGCGCAGGAAAATGAGGCCTACCTTGGCCTGAAAGCGGAAAT
TAAGAATCTGTGGGTGAAAAATCCCTTAACCGCTAAAGTGGAAAAACCTTTAAGAAGGGTCATTGTTTCCACGGTTGTTGCGGAAACGG
GCCTTACCATTGAAACGCTGAAGTACGTCATAGATCCCGGGTGGAACAGAAGCATTGAAACCTACTACCCTGAATGGGCGGGAGGGCT
CATTACGCGCCCCGCGGCTCAAAGCCGTATCGAGCAAAGAAAGGGACGCGTAGGGAGAGTATTTCCTGGGCACTTTTACCCGCTTTAC
ACAAAACACGTCTTTGAGCAAATACCAGCGCAGCAGTATCCTGAAATCATTACGGAAGGCCCTGGGGCCATTTTTCTTAGCATTGTCGTA
GAAACGATTAAAAAAAATAAGGAAGGCGTGTTTAAGGCAGAGGAGATTGATATGCTGGATCCTCCCCCCACGGATGCGCTGGCATCAG
CCATTGAGCGAGCCATTGTGGCAGGCCTTTTAACCAGAGGAGAAAAAGGTCTTCAACTCACGCAGCTCGGAGACATTGCCTCTCGCTTT
TCGTTTTTATCTATAGAAGAAGCGCGCATGTGCTTTTCGGGTTATTTCTGGCAAGCCGCCATTTCTGACATTGCAACCATCCTAGCCGTCG
TGTCTGTTGCGGACAAAAAACTTACGAATCTATTGGACAGTAAACAACGGAACGGAGCTATGCTTGCTGAAGCGGTTTTGGCAGGCATT
CCGCCGTTTCTACAAAATATTGACAATGCTTACACCAACATCCATCTTCTATTGGCAGATGATCTTTTGGAGGGGCTCTTTATTTTTGAAGG
CTTCCAACATGCCATCGTATACTTTATCAATAATAAGGTTAATAATGTAGCTAAACATCTTCGCGAATGGTGCGAAAAAAAAATGCTAAAAT
ATTCTTCTATGGTGCAGATTTTGGCGCGCCGCGAAGATATTTTAAACGAGCTGGCCATTGTAGGATTGAACCCCTTCCACCAATGGCAAA
ACCGCTTGGCCTCCGCCAATGCAGAAACCTTTTTAAAACGTGTTTGTACTTTGAAACAGTGTATGTATGAGGCATACCGCCTTAATTGTTT
CTGCTACGACAAACATAGGCTTCTTTATACTGGAAGAAATGGAATACACTTTTCTTACCACGATGCGGTGATTAAAAATCCTTCGTGCATT
GTAACGCCTAGGATTATGCTATCTCCCGTTTCTAAACAGTATATGGAATGGAGATTAGAGCCAAGCTTTGTGTCCGTCCTCGATGGATTCG
TAAACGTGGACATAAACTTTCTTTCGCCACGTCAGGAAATTCCAAATATTTTGGGAGGCGTCGAGGACGAAGAGGAGGAGCCCCCTCT
CCCCATTCAGGTATTTTTACATAAATACGTAAAGACCCATTTTCACTTCTCCGGGAAATCCTTTAAAGAGTTGAAAATGAAGCCTAGTCAG
ATGATTAAGTTTCCCGAAACAACCTTAATCAACATGATTCCCGATATACCTAAAAACGTGGTGCAAACCTACTTGGAAATAAATGTTTGTC
ATCAATACTCGTTTAAGCGTCTCATTTATTGTGAAACGTTTTATACCGATATGGACGATGTCCAGCATGAAAACTCTGTGGAGCTCATAGG
GTTACCTATGGCGGCGCATCATCTTACGATAAACGATTTTAACAAGCTTTACCATCTGTTGAAACCTGATGGTTTTCTTATCGTGTATGACC
TTCATAAAGGTCAGGAAGCCTTCTGGCTTCACAGCCTGCAGGACGCGCTTGGGCACCATACTATTCGTAGAGACATGGATTTCCATACCA
TCCCCGAATGGGAAACCATATTTAAAGAATGCGGATTCACACCGATTTTTAGTAAACAGCCTTCGGAGCACGAACTGTTCATCGTATTTAA
AAAATAA

Figure 17 *B962L gene sequence.*

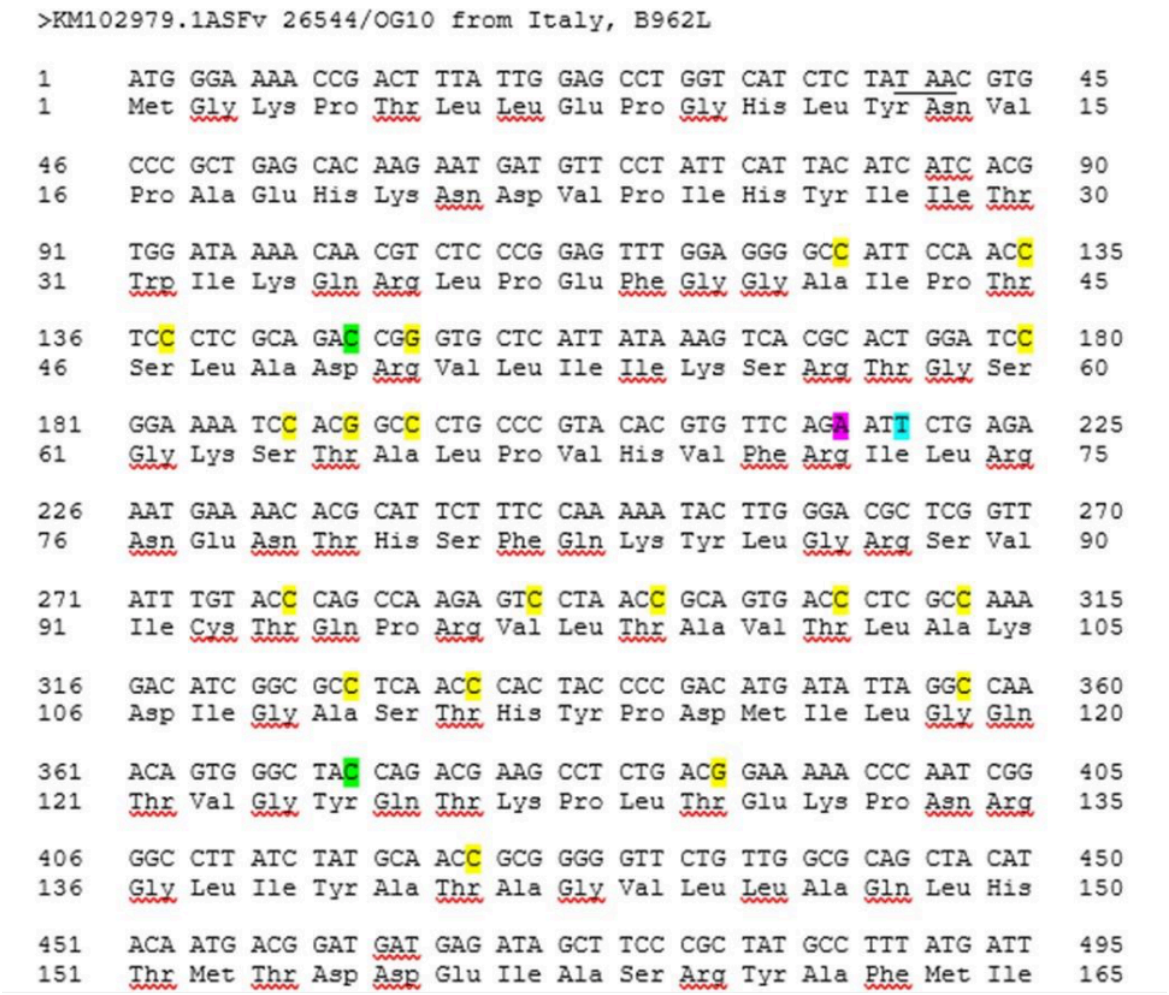

Figure 18 *B962L mutagenized gene sequence (954 bp)*. Some A were changed in C, some T were changed in C, a G was changed in A and a C was changed in T.

>KM102979 ASFV 26544/OG10 from Italy, B318L-B119L
AAGGACCATTCCCTGCGGGGAGACAACTCAGCATGTTGCATCTCATCTATATCTCCATCATTGTAGTTCTTAT
TATTATTTTAATATCCTATACGCGCAAACCTAAGTATTTTAGAATCACAGCTCCGCGTAGTGTCGCGCTTTTT
CATGGAATACATCCACTGAATCCTAAAAATTATAAAACCTTTAGTAAAGAGTTTGAGACCATCTTAAACAATG
CTATTGAAGATGGGGACTTTAAGGGACAACTAACAGAGCCTTGCTCTTACGCTCTAAGAGGTGGGAAGTATAT
CCGTCCCATTATCCTGATGGAAATTGTTCGGGCCTGTCAGTTGCAACATTCCTTTGGGGCGCCTATTTATCCG
GCAGAGGCTGCCCTAGCAGTGGAGTACTTTCACGTAGCTTCTTTGATTATCGACGATATGCCCTCCTTTGACA
ACGATGTGAAGCGGCGAAATAAAGATACAGTGTGGGCCCGCTTTGGCGTAGCCAAGGCGCAGATGAGCGCTCT
GGCGCTAACCATGCAAGGATTTCAAAACATTTGCCGGCAAATCGACTGGATTAAGGAACACTGTCCAAGGTTT
CCGGATCCCAACCAACTGGGAGCGCTGCTGTGTACCTTTGTAAGCCACTCTCTAAACAGCGCGGGTTCCGGTC
AGTTAGTAGACACTCCAGAAAAAACCATTCCCTTTTTTAAGATCGCGTTTATTATGGGCTGGGTTTTGGGCAC
AGGAACGATTGAAGACATTGGGATGATTGAAAGGGCTGCCCACTGTTTTGGACATGCCTTTCAGTTAGCGGAT
GACATTAAGGACCATGACACAGATACTGGCTGGAATTACGCCAAAATACATGGAAAACAAAAAACATTTGACG
ATGTGGCGCAATCCCTTCAAGAGTGCAAAAAAATTCTCCATGGAAAAAAAATATTTACCTCTATATGGAATGA
GATTTTTCAAAAGGTTATAAATGTTGCATTGGGGACCTAAATACTGGCGATCCTTGCATCTATATGCTATCTT
TTTTTCAGACGCTCCTAGCTGGAAAGAAAAATATGAAGCCATCCAATGGATACTGAACTTTATCGAGTCTCTG
CCATGCACCAGGTGTCAGCACCACGCCTTTTCGTATCTTACAAAAAATCCCTTGACATTAAACAACTCGGAGG
ACTTTCAGTACTGGACCTTCGCGTTCCATAACAACGTAAATAACCGGCTTAATAAAAAAATAATTTCTTGGTC
AGAGTATAAAAATATTTATGAACAATCAATCCTTAAAACAATAGAATATGGGAAAACCGACTTTATTGGAGCC
TGGTCATCTCTATAACGTGCCCGCTGAGCACAAGAATGATGTTCCTATTCAT

Figure 19 *B318L-B119L gene sequence (1318 bp)*

>dePAM B318L-B119L OG10
ACgaattc**AGCATGg**TGCATCTCATCTATATCTCTATCATTGTAGTTCTTATTATTATTTTAATATCTTATAC
GCGCAAACCTAAGTATTTTAGAATCACAGCTCCGCGTAGTGTCGCGCTTTTTCATGGAATACATCCACTGAAT
CCTAAAAATTATAAAACTTTAGTAAAGAGTTTGAGACCATCTTAAACAATGCTATTGAAGATGGGGACTTTA
AGGGACAACTAACAGAGCCTTGCTCTTACGCTCTAAGAGGTGGGAAGTATATCCGTCCCATTATCCTGATGGA
AATTGTTCGAGCTTGTCAGTTGCAACATTCTTTTGGGGCGCCTATTTATCCGGCAGAGGCTGCTCTAGCAGTG
GAGTACTTTCACGTAGCTTCTTTGATTATCGACGATATGCCCTCTTTTGACAACGATGTGAAGCGACGAAATA
AAGATACAGTGTGGGCTCGCTTTGGCGTAGCTAAGGCGCAGATGAGCGCTCTGGCGCTAACCATGCAAGGATT
TCAAAACATTTGCCGACAAATCGACTGGATTAAGGAACACTGTCCAAGATTTCCGGATCCCAACCAACTGGGA
GCGCTGCTGTGTACTTTTGTAAGCCACTCTCTAAACAGCGCGGGTTCTGGTCAGTTAGTAGACACTCCAGAAA
AAACTATTCCCTTTTTTAAGATCGCGTTTATTATGGGCTGGGTTTTGGGCACAGGAACGATTGAAGACATTGG
GATGATTGAAAGAGCTGCTCACTGTTTTGGACATGCTTTTCAGTTAGCGGATGACATTAAGGACCATGACACA
GATACTGGCTGGAATTACGCTAAAATACATGGAAAACAAAAAACATTTGACGATGTGGCGCAATCTCTTCAAG
AGTGCAAAAAAATTCTCCATGGAAAAAAATATTTACTTCTATATGGAATGAGATTTTTCAAAAGGTTATAAA
TGTTGCATTGGGGACCTAAATACTGGCGATCTTTGCATCTATATGCTATCTTTTTTTCAGACGCTCCTAGCTG
GAAAGAAAAATATGAAGCTATCCAATGGATACTGAACTTTATCGAGTCTCTGCCATGCACTAGATGTCAGCAC
CACGCTTTTTCGTATCTTACAAAAAATCCCTTGACATTAAACAACTCGGAAGACTTTCAGTACTGGACTTTCG
CGTTCCATAACAACGTAAATAATCGACTTAATAAAAAAATAATTTCTTGGTCAGAGTATAAAAATATTTATGA
ACAATCAATTCTTAAAACAATAGAATATGGGAAAACTGACTTTATTGGAGCTTGGTCATCTCTATAAAActcg
agTT

Figure 20 *B318L-B119L mutagenized sequence*. *B318L* and *B119L* overlap and probably they are transcribed together. All G were changed in A, and C in T. Possible PAMs sequence are highlighted.

>gi|723633498|gb|KM262845.1|:153635-154031 African swine fever virus strain NHV, complete genome
GTATTGTTATAGTGATGGCAGATTTTAATTCTCCAATCCAGTATTTGAAAGAAGATTCGAGGGACCGGACCTC
TATAGGTTCTCTAGAATACGATGAAAATTCCGACACGATTATACCGAGCTTCGCAGCAGGCTTGGAAGACTTT
GAACCCATTCCCAGCCCTACCACATCAACTTCCCTGTATTCACAATTGACCCACAACATGGAAAAAATCGCGG
AGGAAGAGGATATTAATTTTCTACACGATACTAGGGAGTTTACTTCACTGGTCCCCGATGAGGCAGACAATAA
ACCGGAAGATGACGAAGAAAGCGGTGCAAAACCTAAAAAGAAAAAACGTTTGTTTCCAAAATTAAGCTCGCAT
AAATCGAAGTAAAAATTGAAGCGAAAAAAAAG

Figure 21 *E120R gene sequence (365 bp)*

>KM262845.1:153649-154011 African swine fever virus strain NHV, complete genome

1	ATG GCA GAT TTT AAT TCT CCA ATC CAG TAT TTG AAA GAA GAT TCG	45
1	Met Ala Asp Phe Asn Ser Pro Ile Gln Tyr Leu Lys Glu Asp Ser	15
46	AGG GAC CGG ACC TCT ATA GGT TCT CTA GAA TAC GAT GAA AAT TCC	90
16	Arg Asp Arg Thr Ser Ile Gly Ser Leu Glu Tyr Asp Glu Asn Ser	30
91	GAC ACG ATT ATA CCG AGC TTC GCA GCA GGC TTG GAA GAC TTT GAA	135
31	Asp Thr Ile Ile Pro Ser Phe Ala Ala Gly Leu Glu Asp Phe Glu	45
136	CCC ATT CCC AGC CCT ACC ACA TCA ACT TCC CTG TAT TCA CAA TTG	180
46	Pro Ile Pro Ser Pro Thr Thr Ser Thr Ser Leu Tyr Ser Gln Leu	60
181	ACC CAC AAC ATG GAA AAA ATC GCG GAG GAA GAG GAT ATT AAT TTT	225
61	Thr His Asn Met Glu Lys Ile Ala Glu Glu Glu Asp Ile Asn Phe	75
226	CTA CAC GAT ACT AGG GAG TTT ACT TCA CTG GTC CCC GAT GAG GCA	270
76	Leu His Asp Thr Arg Glu Phe Thr Ser Leu Val Pro Asp Glu Ala	90
271	GAC AAT AAA CCG GAA GAT GAC GAA GAA AGC GGT GCA AAA CCT AAA	315
91	Asp Asn Lys Pro Glu Asp Asp Glu Glu Ser Gly Ala Lys Pro Lys	105
316	AAG AAA AAA CGT TTG TTT CCA AAA TTA AGC TCG CAT AAA TCG AAG	360
106	Lys Lys Lys Arg Leu Phe Pro Lys Leu Ser Ser His Lys Ser Lys	120
361	TAA 363	
121	End 121	

A
T

Figure 22 *E120R mutagenized gene sequence*. G nucleotides were changed in A and C in T.

Once mutagenized genes were designed, they were insert into *pEX-A128* vector and synthetized by Eurofin Genomics (Germany), including enzymatic cut sites and Kozac sequence (A/G NN ATG G).

B962L enzymatic cute sites:

- gaatcc: EcoRI 5' cut site
- ctcgag: XhoI 3' cut site

B318L-B119L enzymatic cute sites:

- gaattc: EcoRI 5' cut site
- ctcgag: XhoI 3' cut site

E120R enzymatic cut sites:

- gaattc: EcoRI 5' cut site
- ggatgc: BamHI 3' cut site

3.3.2 Transformation of One ShotTM TOP10™ chemically competent E. coli cells with pEX-A128 + dePAM genes constructs

pEX-A128 + dePAM genes were used to transform One Shot™ TOP10™ chemically competent *E. coli* (Invitrogen) cells. 1 µl of each plasmid (20 ng/µl) was added in a vial containing competent *E. coli* cells. *pUC19* vector was used as a positive control. Cell vials were incubated on ice for 30 minutes, and then they were undergone to thermic shock at 42°C for 30 seconds and immediately replaced on ice for 5 minutes. 250 µl of S.O.C. medium was added in each vial, and samples were incubated at 37°C, 250 rpm, for 1 hour to allow cells antibiotic expression. Transformed cells were seeded in LB (Luria Bertani) agar plates (Tryptone 10g, Yeast extract 5g, NaCl 10g, bacteriological agar 10g, dH2O up to 1L) containing 100 µg/ml of ampicillin. Plates were incubated at 37°C o/n. The day after, colonies were collected from each plate and placed in 3,5 ml of liquid LB (Tryptone 10g, Yeast extract 5g, NaCl 10g, dH2O up to 1L) containing ampicillin (100 µg/ml) and incubated o/n at 37°C and 220 rpm.

3.3.3 Extraction of plasmids

Small-scale and large-scale preparations of plasmid DNA were performed with Zyppy™ Plasmid Miniprep Kit (Zymo Research) and Zymopure ™ Plasmid Maxiprep Kit (Zymo Research) respectively, according to manufacturer's instructions.

3.3.4 Enzymatic digestions

The obtained plasmid preparations were digested with their specific digestion enzymes. All digestions were performed with NEB restriction enzymes (New England Biolabs). Samples were incubated at 37°C for 2 hours.

Digestion mixture for pEX-A128 + dePAM_B962L

(20000U/ml) EcoRI HF (high fidelity): 0,3 µl

(20000U/ml) XhoI HF: 0,3 µl

10X cutsmart buffer: 3 µl

Plasmid DNA (500 ng)

H_2O: up to 30 µl

Digestion mixture for pEX-A128 + dePAM_B318L-B119L

(20000U/ml) EcoRI HF: 0,3 µl

(20000U/ml) XhoI HF: 0,3 µl

10X cutsmart buffer: 3 µl

Plasmid DNA (500 ng)

H_2O: up to 30 µl

Digestion mixture for pEX-A128 + dePAM_E120R

(20000U/ml) EcoRI HF: 0,3 µl

(20000U/ml) BamHI HF: 0,3 µl

10X cutsmart buffer: 3 µl

Plasmid DNA (500 ng)

H_2O: up to 30 µl

Digested products were analyzed by gel agarose electrophoresis supplemented with 1X GelRed® (Biotium), and to confirm them maxiprep digested products were sequenced by BMR Genomics.

3.3.5 Transfer of dePAM genes from pEX-A128 to pLXSN vector

This step is necessary as the *pLXSN* vector is used to transform Phoenix cells that will be used next to produce retroviral particles expressing mutagenized genes.

3.3.5.1 Plasmids enzymatic digestion

Plasmids (*pEX-A128 + dePAMgenes and pLXSN*) were digested with their specific enzymes, as described before, and incubated at 37°C for 2 hours. Digested products (*pLXSN* vector and dePAM genes) were analyzed by gel agarose supplemented with 1X GelGreen® (Biotium), visualized and excised from the gel under visible blue light in order to prevent mutations. After excision, DNA gel fragments were purified from gel using Zymoclean™ Gel DNA Recovery Kit (Zymo Research), according to manufacturer's instructions.

3.3.5.2 Plasmid dephosphorylation and ligation

pLXSN vector was dephosphorylated to avoid plasmid closing using Rapid DNA Dephos & Ligation KIT (Roche), as described below.

Component	Volume	Final concentration
Vector DNA	X µl	Up to 1 µg
rAPid Alkaline Phosphatase buffer 10 X	2 µl	1 X
rAPid Alkaline Phosphatase	1 µl	1U
ddH2O	Up to 20 µl	

Reactions were incubated at 37°C for 1 hour and then phosphatase was inactivated at 75°C for 2 minutes. The dephosphorylation mixture was used in the following ligation reaction with a ratio of 1:3 (vector/insert).

Component	Volume	Final concentration
Vector DNA	X µl	50 ng
Insert DNA	X µl	150 ng
DNA dilution buffer	2 µl	10 X
ddH_2O	Up to 10 µl	
Mix thoroughly and add:		
T4 DNA Ligation Buffer 2 X	10 µl	1 X
T4 DNA ligase	1 µl	5 U

Reactions were incubated at 16°C o/n. The ligation mixtures were used for bacterial transformation of TOP10 chemically competent *E. coli* (*pLXSN* + *dePAMgenes*).

3.3.6 Plasmids design

All plasmids were created with Snapgene® software (GSL Biotech LLC)

Retroviral vectors for dePAM genes expression in Cos-1 cells

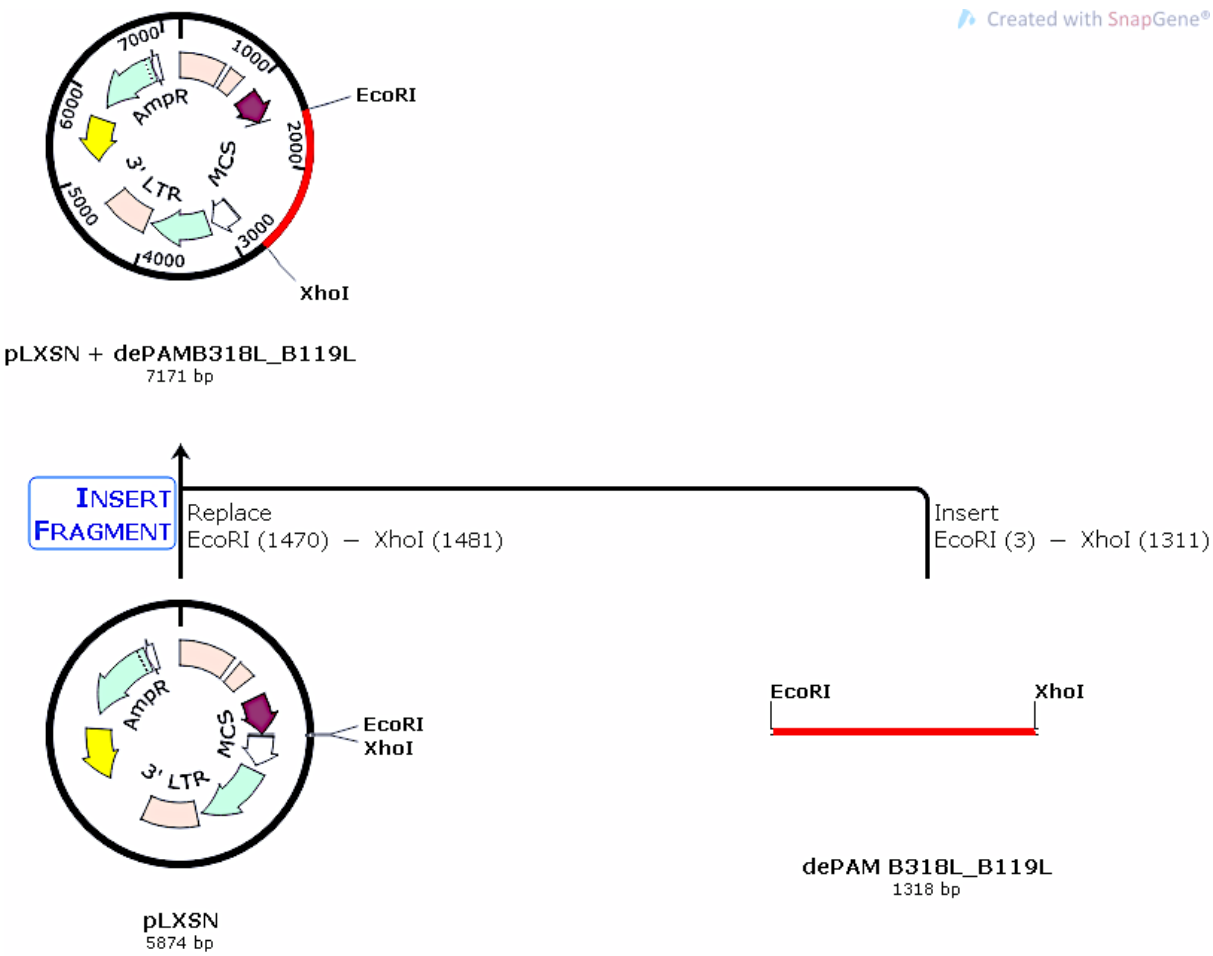

Figure 23 *pLXSN + dePAM_B318L-B119L*

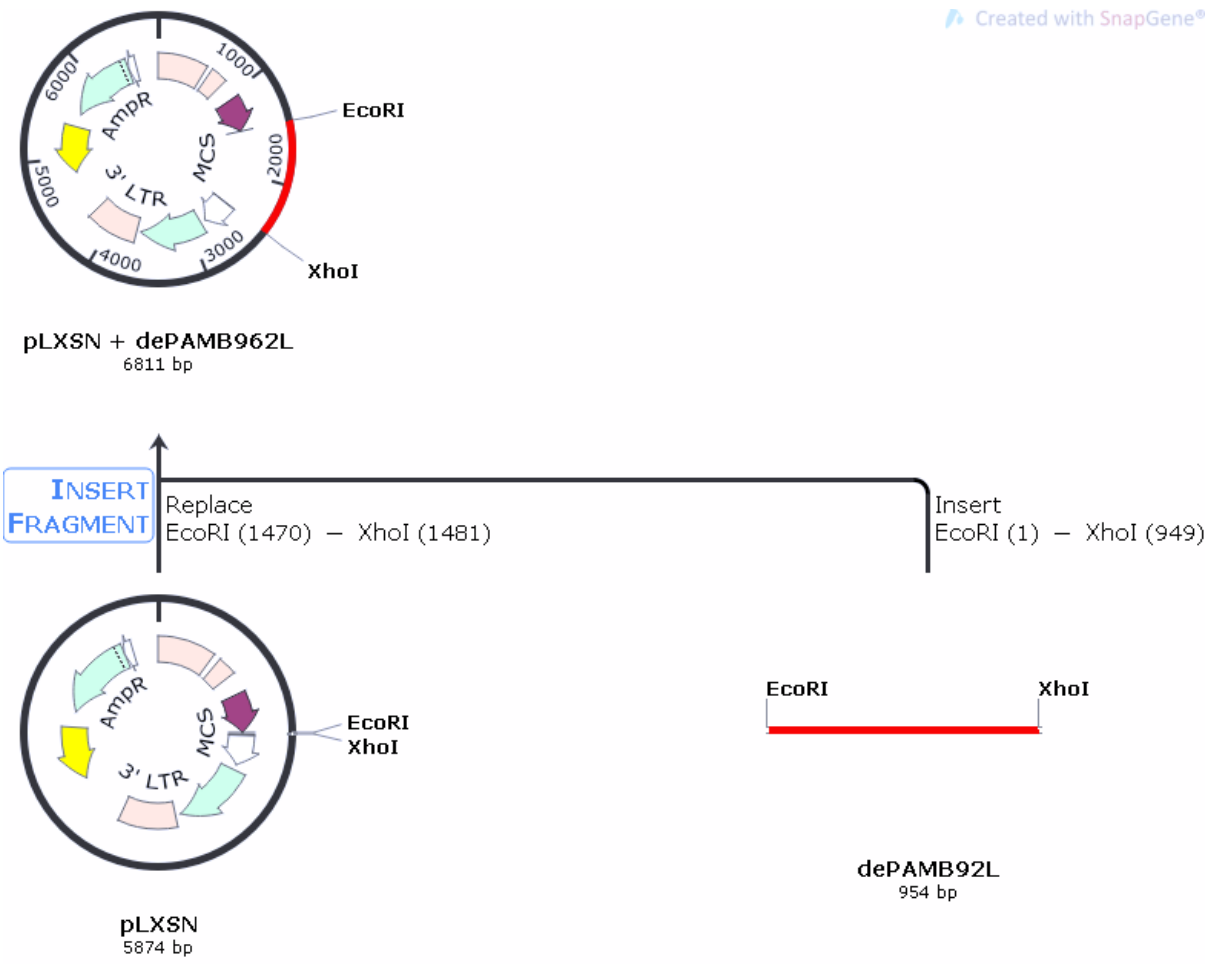

Figure 24 *pLXSN + dePAM_B962L*

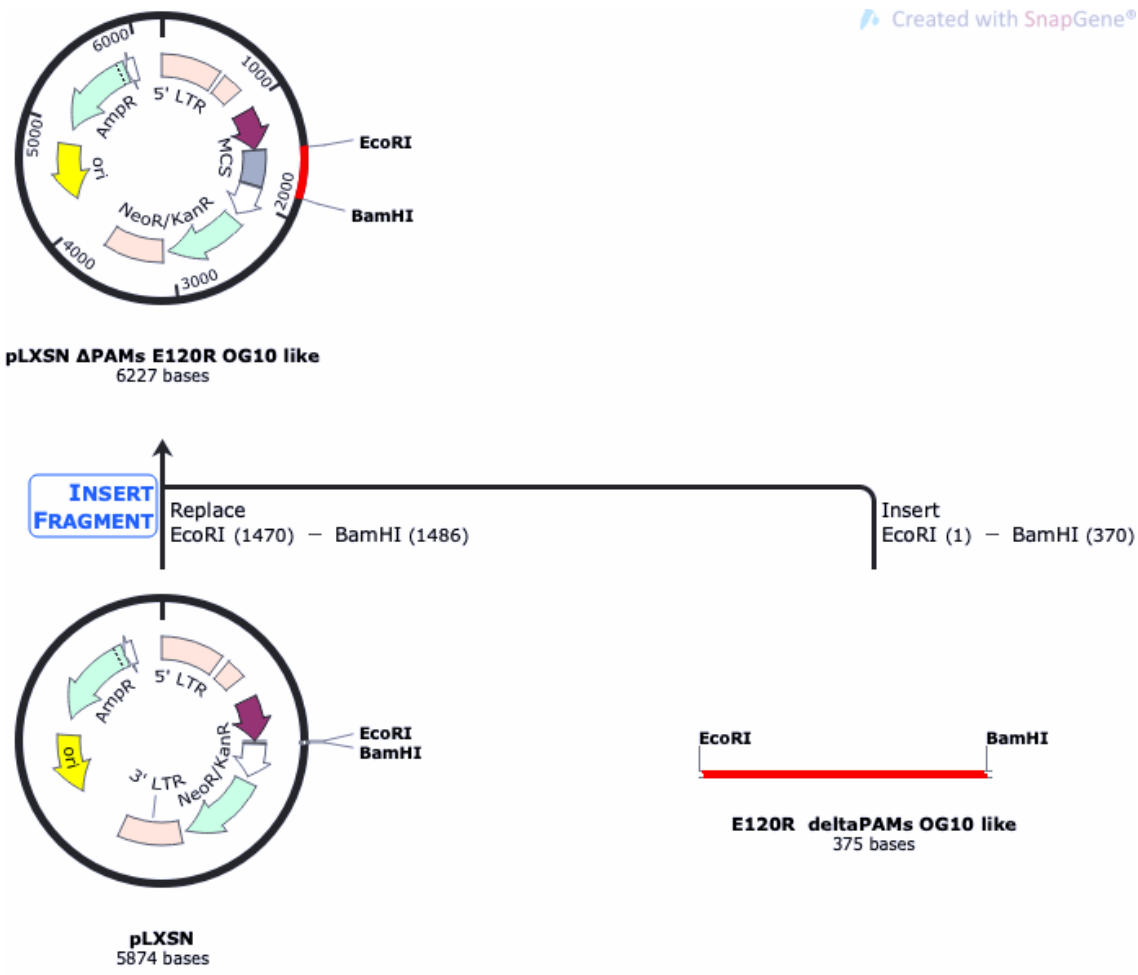

Figure 25 *pLXSN + dePAM_E120R*

3.3.7 Transformation of One ShotTM TOP10™ chemically competent E. coli cells, plasmids extraction and enzymatic digestions

The obtained constructs were used to transform One Shot™ TOP10™ chemically competent *E. coli* cells, as described in paragraph 3.3.2. Once cells were transformed, Small-scale and large-scale preparations of plasmid DNA were performed with Zyppy™ Plasmid Miniprep Kit (Zymo Research) and Zymopure ™ Plasmid Maxiprep Kit (zymo Research) respectively, according to manufacturer's instructions. Subsequently, the obtained miniprep and maxiprep of our constructs were digested with their specific enzyme (see paragraph 3.3.4) in order to verify the presence of inserted genes. Reactions were analyzed by agarose gel electrophoresis. Then, plasmids maxiprep were sequenced by BMR genomics.

3.3.8 Transfection of Phoenix cells

Phoenix cells were transfected using Calphos Mammalian Transfection kit (Clontech) as described in paragraph 3.1.4. Transfection solutions were prepared in 15 ml tubes using different vectors:

- *pLXSN + dePAM_B318L_B119L*
- *pLXSN + dePAM_B962L*
- *pLXSN + dePAM_E120R*
- Empty *pLXSN* (used as a control)

3.3.9 Cos-1 cells infection with retroviral particles

Cos-1 cells were seeded in 10 cm plates two days before infection. Old medium was removed, and filtered retrovirus suspensions were added to. 3 hpi retroviral suspensions were removed from cells and fresh medium was replaced (complete DMEM).

3.3.10 Selection of transduced cells

Selection of transduced cells was started 24 hpi. Cells were splitted according to cell confluence and fresh medium supplemented with 750 µg/ml of G418 selective antibiotic was added. Selection was continued until death of control cells.

3.3.11 RNA extraction from Cos-1 cells and RT-PCR

RNA was extracted from Cos-1 cellular pellet using the RNeasy Mini Kit (Qiagen), following vendor's recommendations. RNA was treated with the DNA-free™ DNase Treatment and Removal Reagents kit (Ambion) and retrotranscribed using the GoScript™ ReverseTranscription System (Promega) or the AffinityScript Multi Temperature cDNA Synthesis Kit (Agilent technologies), following manufacturer's instruction. cDNAs from Cos-1 cells expressing *E120R* and *B318L-B119L* genes were analyzed by RT-PCR to check genes transcription. RT-PCR was performed with Taq DNA polymerasis Kit (Qiagen) according to following conditions.

Components	**volume**	**Final concentration**
10 X CoralLoad buffer	5 µl	1 X
10 mM dNTPs	1 µl	200 µM of each dNTP
10 µM Primer F	1,5 µl	0,2 µM
10 µM Primer R	1,5 µl	0,2 µM
Taq polimerase	0,25 µl	1,25 U
DNA	X µl	100-150 ng
H_2OMQ	Up to 50 µl	

Primers

- B318L-B119L_EcoRI_F (5'ACGAATTCAGCATGGTGCATCTCATCTATATCTCC 3')
- B318L-B119_XhoI_R (5'AACTCGAGTTATAGAGATGACCAGGCTCCAATAAAG 3')

- E120R_BamHI_F (5'CCGGATCCGCAGATTTTAATTCTCCAATC 3')
- E120R_EcoRI_R (5'GCGAATTCTTACTTCGATTTATGCGAGC 3')

PCR profile

Initial activation step	94°C 3'	
Denaturation	94°C 20''	30 cycles
Annealing	55°C 20''	
Extension	72°C 20''	
Final extension	72°C 10'	

PCR products were analyzed by agarose gel electrophoresis and purified with the DNA Clean & concentrator^{TM} Kit (Zymo Research), according to manufacturer's instructions. Samples were sequenced by BMR genomics.

3.3.12 Total proteins extraction from Cos-1 cultured cells

Cell pellet was resuspended in IP Lysis buffer (20 mM Tris-HCl pH 8.0, 200mM NaCl, 1mM EDTA pH 8.0, 0,5% NP-40, Pierce EDTA-Free Protease Inhibitor Tablet) (Thermo Scientific) and incubated on ice for 30 minutes. After centrifugation at 10000 rpm for 10 minutes at 4°C, supernatant was transferred in a new tube. Proteins' quantification of supernatant was carried out using Pierce BCA protein assay kit (Thermo Scientific). Equal amounts of protein extracts were loaded onto SDS-PAGE and subjected to Western immunoblotting.

3.3.13 SDS-Polyacrylamide Gel Electrophoresis (SDS-PAGE)

Proteins were resolved in 10% SDS polyacrylamide gel. Before loading onto gel, proteins were dissolved in 4X Laemmli buffer (8% SDS, 40% Glycerol 99%, 10% β-Mercaptoethanol, 240 mM Tris-HCl pH 6.8, 0,04% Bromophenol blue) and boiled at 95°C for 5-10 min to allow denaturation. Electrophoresis was performed in a Mini-PROTEAN® Tetra Cell system (Bio- Rad) in SDS Running buffer (Trizma base 25mM, Glycin 250mM, SDS 1%) for approximately 2 hours at 140V. After

running, proteins were subjected to Western blot or directly visualized by staining with Commassie SimplyBlue™ SafeStain (Invitrogen Life Technologies).

Separating gel 10% 6 ml

- 2,4 ml dH_2O ml
- 2 ml 30% Acrylamide mix
- 1,6 ml 1,5 M Tris (pH 8.8)
- 0,06 ml 10% SDS
- 0,06 ml 10% APS
- 0,003 ml TEMED

Stacking gel 2ml

- 1,4 ml dH_2O
- 0,33 ml 30% Acrylamide mix
- 0,250 ml 1,0 M Tris (pH 6.8)
- 0,02 ml 10% SDS
- 0,02 ml 10% APS
- 0,002 ml TEMED

3.3.14 Western immunoblotting

After SDS-PAGE, proteins were transferred to a nitrocellulose membrane with Mini Trans- Blot® 3 cell (Bio-Rad). Gels and membranes were equilibrated in transfer buffer 1X (Western blot buffer 10X (Trizma base 25mM, Glycin 192mM, dH20), Methanol and dH2O) and placed between three pieces of filter paper (3MM Whatmann paper). Blotting was performed at 250 mA for one hour at 4°C and membranes were incubated with 5% blocking solution (5% skim milk in PBS-tween 0,05%) for one hour at RT under gentle shacking. After that, membranes were incubated with the primary antibody diluted in 5% blocking solution under gentle shacking at 4°C o/n. After incubation, membranes were washed 3 times for 5-10 minutes with PBS-T (PBS 1X, 0,05% Tween 20) and then incubated with the secondary antibody HRP- conjugated (dilution from 1:2000 to 1:50000 in 5% blocking solution) under gentle agitation at RT for 1 hour. After washes, membranes were developed with Clarity ECL Substrate (50% solution A + 50% solution B) (Bio-Rad), and chemiluminescence was acquired with The ChemiDoc XRS+ System (Bio-Rad). β-Actin antibody was used as a control.

Antibodies

- Anti pE120R monospecific rabbit polyclonal serum (*Andrés et al., 2001*) 1:500
- β-Actin Antibody (Santa Cruz biotechnology) 1:500
- Secondary anti-rabbit HRP (Southern Biotech) 1:50000
- Secondary anti-mouse HRP (southern Biotech) 1:20000

3.3.15 Immunocytochemistry

$3{,}5x10^5$ Cos-1 transduced cells were seeded in SPL Cell Culture borosilicate chamber slides (Euroclone) and let grow until 70-80% of confluence was reached. Cells were fixed in methanol for 15 minutes at 4°C and washed three times with PBS-T. Subsequently, cells were blocked for endogenous peroxidase with Dako REAL Peroxidase-Blocking Solution (S2023, Dako, Glostrup, DK) for 1 hour, then washed three times in PBS-T, and incubated in 2% BSA for one hour. Then, nonspecific binding was blocked with 2.5% normal horse serum (ImmPRESS reagent kit,Vector Labs) for 1 hour. Cells were washed three times in PBS-T and incubated with primary antibody anti-pE120R 1:50 o/n at 4°C. Cells were washed in PBS-T and incubated with secondary anti-rabbit antibody (MP-7500, ImmPRESS reagent kit, Vector Laboratories) for 30 minutes at RT. 3,3'-Diaminobenzidine (DAB) (ImmPACT DAB, Vector Laboratories) was used as chromogen.

3.4 Production of GST-pE120R protein

3.4.1 E120R gene amplification and cloning into pGEX-2T

cDNA from Cos-1 cells transduced with *pLXSN + dePAM_E120R* vector was used as a template to amplify *E120R ORF*.

Primers

- E120R_F_BamHI (5' CCGGATCCGCAGATTTTAATTCTCCAATC 3') (Invitrogen)
- E120R_R_EcoRI (5' GCGAATTCTTACTTCGATTTATGCGAGC 3') (invitrogen)

PCR was carried out using the Taq DNA Polymerase kit (Qiagen) as described below.

Components	volume	Final concentration
10 X coralLoad buffer	5 µl	1 X
10 mM dNTPs	1 µl	200 µM of each dNTP
10 µM Primer F	1,5 µl	0,2 µM
10 µM Primer R	1,5 µl	0,2 µM
Taq polimerase	0,25 µl	1,25 U
DNA	X µl	100-150 ng
H_2OMQ	Up to 50 µl	

PCR profile

Initial activation step	94°C 3'	
Denaturation	94°C 20''	30 cycles
Annealing	55°C 20''	
Extension	72°C 20''	
Final extension	72°C 10'	

Amplified products were analyzed by agarose gel supplemented with GelRed ™ (BIOTIUM) and purified with DNA Clean & concentrator™ Kit (Zymo Research).

3.4.2 Enzymatic Digestions of pGEX-2T vector and PCR purified product

To insert dePAM_*E120R* gene inside *pGEX-2T* vector were both digested with BamHI and EcoRI enzyme (New England Biolab). Samples were incubated at 37°C for 2 hours.

Digestion mixture for dePAM_E120R amplified product:

- (20000U/ml) BamHI HF 0,5 µl
- (20000U/ml) EcoRI HF 0,5 µl
- 10X cutsmart 4,5 µl
- DNA (60 ng/µl) 35 µl
- H_2O 4,5 µl

Digestion mixture for pGEX-2T plasmid:

- (20000U/ml) BamHI HF 0,5 µl
- (20000U/ml) EcoRI HF 0,5 µl
- 10X cutsmart 4,5 µl
- DNA (2µg) 5 µl
- H_2O 34,5 µl

The digested amplify was purified with the DNA Clean & concentrator™ Kit (Zymo Research), instead the digested vector was analyzed by agarose gel supplemented with GelGreen ™ (BIOTIUM) and purified by gel excision with Zymoclean™ Gel DNA Recovery Kit (Zymo Research).

3.4.3 Plasmid dephosphorylation and ligation

pGEX-2T vector was dephosphorylated using Rapid DNA Dephos & Ligation KIT (Roche), as described in paragraph 3.3.5.1. Subsequently, dephosphorylated *pGex-2T* and the digested and purified dePAM_*E120R* product were ligated (see paragraph 3.3.5.2).

3.4.4 Transformation of One ShotTM Stbl3™ chemically competent E. coli (invitrogen) using pGEX-2T + dePAM_E120R

5 µl of ligation mixture were added in each One Shot™ Stbl3™ cell vial. *pUC19* vector was used as control DNA. Samples were incubated on ice for 30 minutes, then shocked at 42°C for 2 minutes and incubated 5 minutes on ice. 250 µl of S.O.C. medium was added, and cells were incubated at 37°C at 200 rpm for 1 hour. Transformed cells were seeded in LB Agar plates supplemented with ampicillin (100 µg/ml) and incubated o/n at 37°C. The day after, several colonies were collected and resuspended il LB supplemented with ampicillin, then incubated o/n at 37°C, 200 rpm. After incubation, plasmid extraction was performed usig Zippy™ Plasmid miniprep Kit (Zymo Research). The obtained miniprep preparations were digested to verify insert presence and sequenced by BMR genomics.

3.4.5 BL21 transformation using TransformAid Bacterial Transformation Kit

Non-competent *BL21* Codon plus *E. coli* cells were transformed with *pGEX-2T + dePAM_E120R* by using the TransformAid Bacterial Transformation Kit (Thermo Fisher Scientific) and following vendor's recommendations. Once plasmid extraction was performed and plasmid digestion confirmed the presence of the dePAM gene, *BL21* transformed cells were used to protein induction.

3.4.6 GST fusion protein expression

Single transformed colonies were grown o/n at 37°C in 3 ml of LB medium supplemented with 100 µg/ml of ampicillin and 34 µg/ml of chloramphenicol. The day after, two 1ml aliquots were collected and resuspended into two separate tubes containing 10 ml of LB supplemented with 100 µg/ml of ampicillin and 34 µg/ml of chloramphenicol. Samples were incubated at 30°C for 3 hours under shaking. At this point, the expression of fusion protein was induced by adding isopropylthio-β-galactoside (UltraPure IPTG-Invitrogen) to a final concentration of 0,1 mM. 1 ml aliquots were collected every hour for 6 hours, splitting pellet from supernatant by centrifugation at 4000 rpm for 10 min. Correct expression of recombinant protein was verified by SDS-PAGE before purification.

3.4.7 GST fusion protein purification

For bacterial lysis and protein purification, a bacterial pellet was resuspended in 1 ml of NETN buffer supplemented with protease inhibitors. Resuspended bacteria were lysed by sonication on ice (4 cycles of 20 sec with 5 sec ON and 5 sec OFF, 50%-70% power) avoiding foam and overheating. The insoluble bacterial debris were removed by centrifugation at 10000 rpm for 10 minutes at 4°C. Supernatant was filtered through a sterile 0.45 μm filter to obtain a clear bacterial extract. Fusion protein was then purified through incubation of lysed bacterial extracts with 75μl of Glutathione Sepharose 4B (GE Healthcare). Glutathione beads were previously washed three times with cold NETN buffer containing 0,5% skim milk. After each washing, beads were collected by centrifugation at 800 rpm for 2 min. Mixtures of bacterial extract and beads were incubated for 1 to 3 hours rocking at 4°C. After incubation, beads were recovered by centrifugation, washed 5 times with cold NETN buffer and stored at -20°C. 10 μl of bead-immobilized recombinant protein was loaded onto SDS-PAGE to verify purification.

3.5 Engineering of *pLXSN* and *pLXSN +dePAM_E120R* vectors

This step has been necessary to develop new vectors containing puromycin antibiotics resistance cassette unlike the G418 resistance that is normally included into *pLXSN* vector. In fact, as they contain geneticin antibiotic resistance gene they cannot be used to transduce our iPAEC cells since they were immortalized with a plasmid (*pLXSN + OaPV3_E6E7*) containing the same antibiotic resistance gene that, for this reason, is integrated into their genome.

3.5.1 Digestion of pLXSN and pLXSN + dePAM_E120R vectors

Two different reactions of digestion were performed. In the first reaction vectors were digested with HindIII-HF enzyme (New England Biolabs). Once digested, vectors were analyzed with gel agarose supplemented with GelGreen™ (BIOTIUM) and purified from gel with Zymoclean ™ Gel DNA Recovery Kit (Zymo Research), according to manufacturer's instructions. Purified plasmids were

digested with NgoMIV enzyme (New England Biolabs), analyzed by agarose gel electrophoresis, and purified as described before.

3.5.2 Puromycin gene amplification from Lenti-CRISPR-V2 plasmid

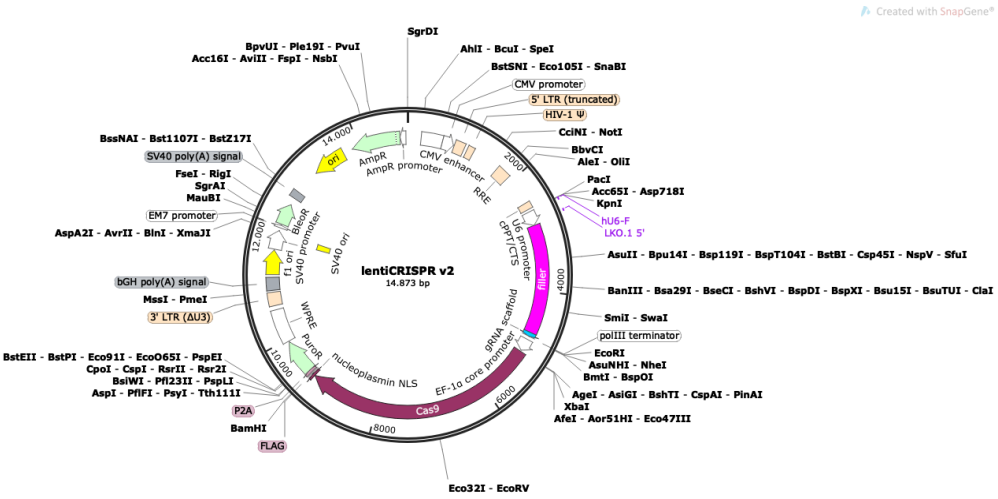

Figure 26 *LentiCRISPR-V2 vector with puromycin resistance gene*

Amplification was performed using *Lenti-CRISPR-V2* plasmid as a DNA template using the Accutaq^{TM} LA DNA Polymerase kit (Sigma), as described below.

Primers

- PuroHindFor (5' AGAAGCTTATGACCGAGTACAAGCCCACGGTG 3')
- PuroNgoMIVRev (5' TAAGCCGGCTCAGGCACCGGGCTTGCGG 3

Components	volume	Final concentration
10 X Accutaq LA buffer	5 µl	1 X
10 mM dNTPs	2,5µl	500 µM of each dNTP
10 µM Primer F	1 µl	600 nM
10 µM Primer R	1 µl	600 nM
Taq polimerase	0,5 µl	0,05 U/µl
DNA	X µl	100-150 ng
H_2OMQ	Up to 50 µl	

PCR profile

Initial activation step	98°C 30''	
Denaturation	94°C 15''	30 cycles
Annealing	65°C 30''	
Extension	68°C 50''	
Final extension	68°C 10'	

The amplified gene was analyzed by agarose gel electrophoresis, purified with DNA Clean & concentrator^{TM} Kit (Zymo Research), digested with HindIII and NgoMIV enzymes and purified.

3.5.3 Dephosphorylation and ligation

pLXSN and *pLXSN+dePAM_E120R* vectors were dephosphorylated to avoid plasmid closing using Rapid DNA Dephos & Ligation KIT (Roche), as described in paragraph 3.3.5.1. Subsequently, the reaction of ligation between dephosphorylated plasmids and digested and purified puromycin resistance gene was performed (see paragraph 3.3.5.1).

3.5.4 Plasmids design

Plasmids were created with Snapgene® software (GSL Biotech LLC).

Retroviral vectors for dePAM genes expression in iPAEC

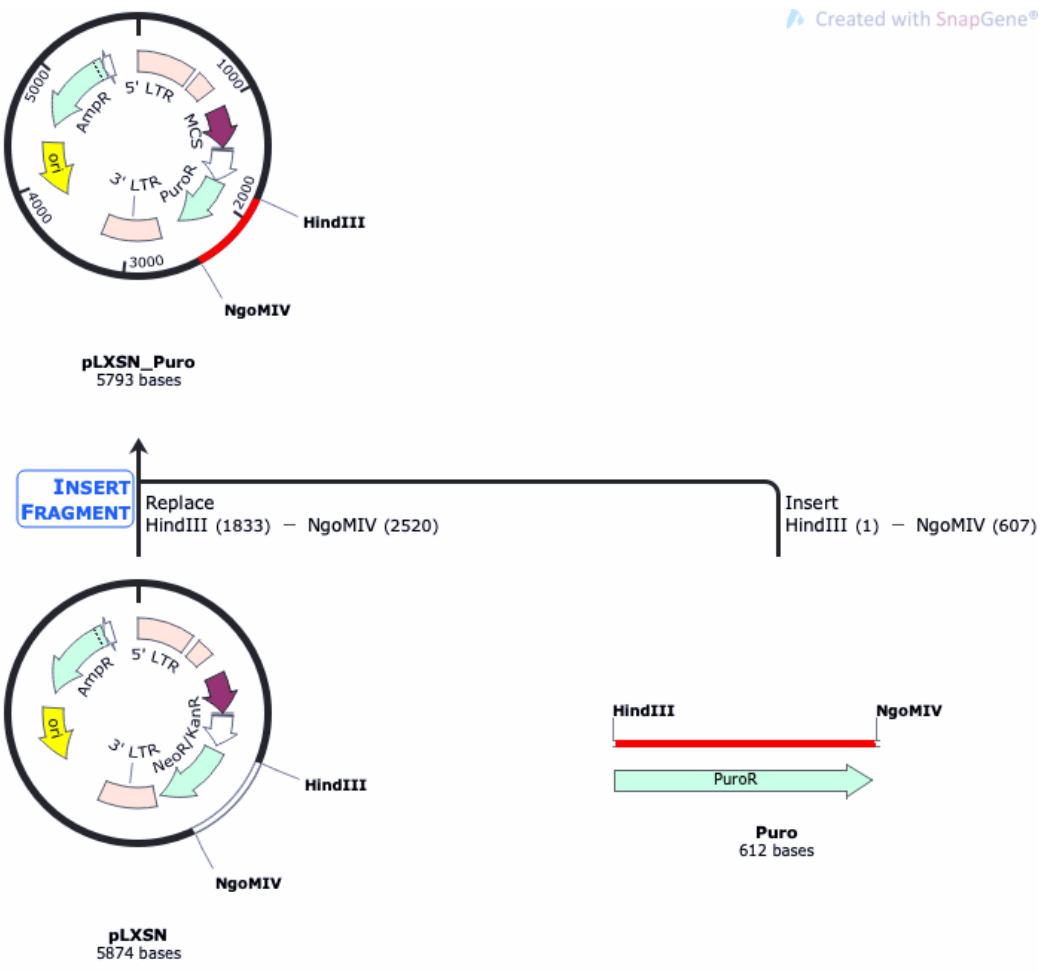

Figure 27 *pLXSN + Puro vector*

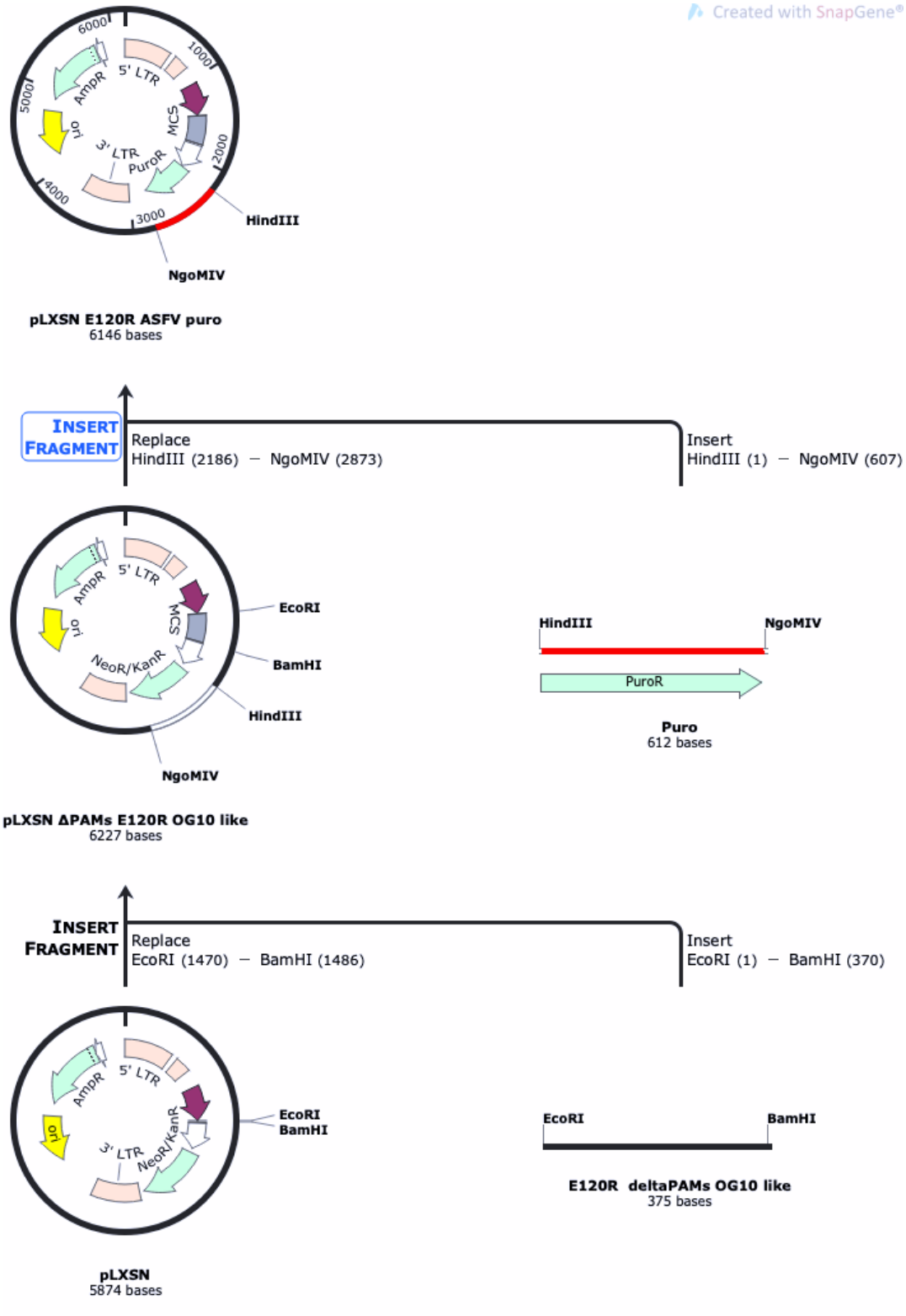

Figure 28 *pLXSN + dePAM_E120R +Puro vector*

3.5.5 Amplification of pLXSN + Puro and pLXSN + dePAM_E120R + Puro plasmids to confirm puromycin resistance gene presence

Amplification of the obtained plasmids was performed using Accutaq ™ LA DNA Polymerase kit (Sigma), as described before (see paragraph 3.5.2)

3.5.6 Phoenix transfection

Phoenix cells were transfected using Calphos Mammalian Transfection kit (Clontech) as described in paragraph 3.1.4. Transfection solutions were prepared in 15 ml tubes using different vectors:

- *pLXSN + Puro*
- *pLXSN + dePAM_E120R + Puro*
- Empty *pLXSN* (used as a control)

3.5.7 iPAEC infection and selection

iPAEC cells were seeded in 10 cm plates two days before infection. Old medium was removed from PAEC immortalized, and filtered retrovirus suspensions was added to. 3 hours post infection retroviral suspensions were removed from the cells and fresh medium was replaced. Selection of transduced cells was started 24 hours post infection. Cells were splitted according to cell confluence and fresh medium supplemented with 0,7 μg/ml of Puromycin selective antibiotic was added.

4. Results

4.1 Primary Porcine Aortic Endothelial Cells isolation and characterization

Primary Porcine Aortic Endothelial cells were collected from porcine aorta using two different enzymatic solutions. The use of dispase enzymatic solution allowed to obtain a numerically high but heterogeneous cell population. Microscope analysis showed a percentage of 30-40% of smooth muscular cells and fibroblasts (Figure 29 D), with a majority of fibroblasts found in cells monolayer. In contrast, the use of collagenase enzymatic solution allowed to obtain a most homogeneous cell population constitute prevalently of Porcine Aortic Endothelial Cells (95%) (Figure 29C). Immediately after cells isolation, PAEC showed a spherical morphology (Figure 29A-B), but after 24-48 hours they acquired their typical phenotype, shaping in cobblestone-like structures. After 60-72 hours cultured primary cells started their exponential growth phase.

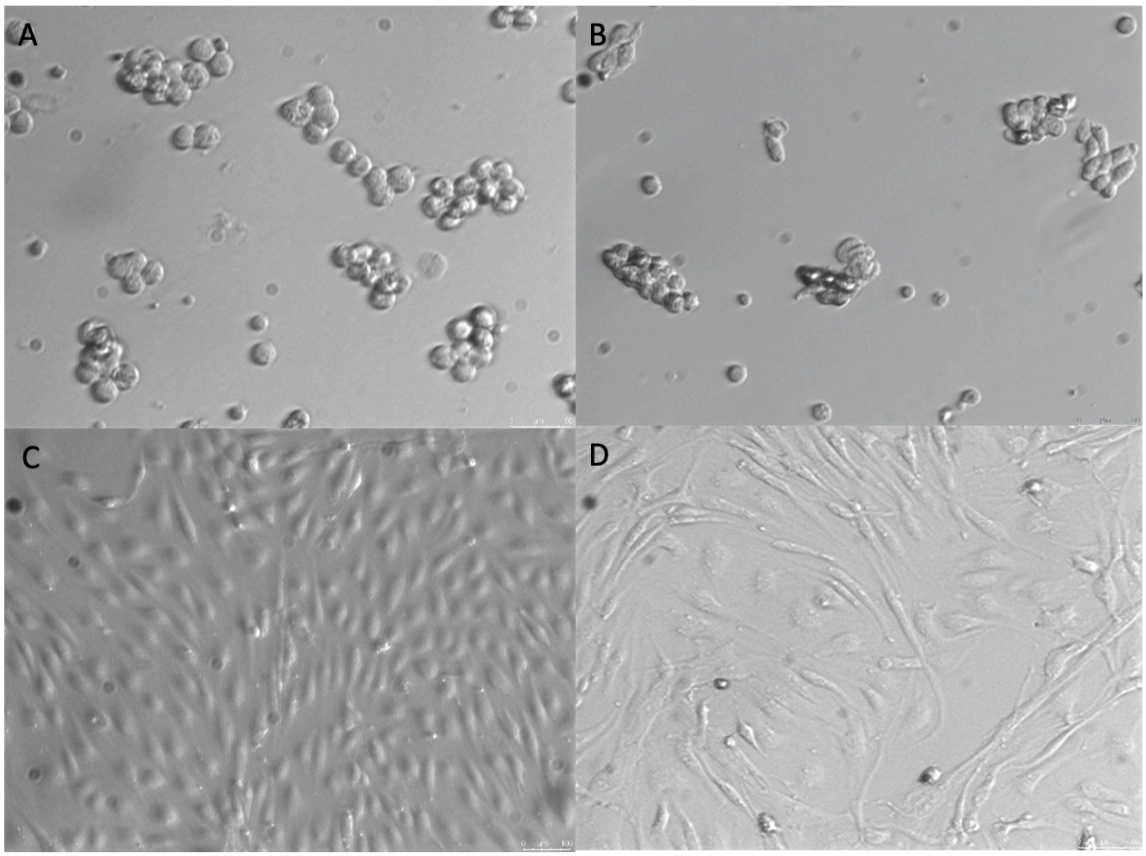

Figure 29 *Primary Porcine Aortic Endothelial Cells (PAEC).* ***A-B:*** *primary PAEC immediately after isolation.* ***C:*** *PAEC isolated with collagenase solution.* ***D:*** *PAEC isolated with dispase solution.*

Characterization of primary PAEC was performed by immunofluorescence using CD31 (Pecam-1) specific endothelial marker (Figure 30). The analysis was carried out with confocal laser scanning microscope Leica SP5 associated with a Leica LAS AF Lite software for pictures acquisition, and it highlighted a high positivity to CD31 marker (96% of cells), especially in their cell junctions.

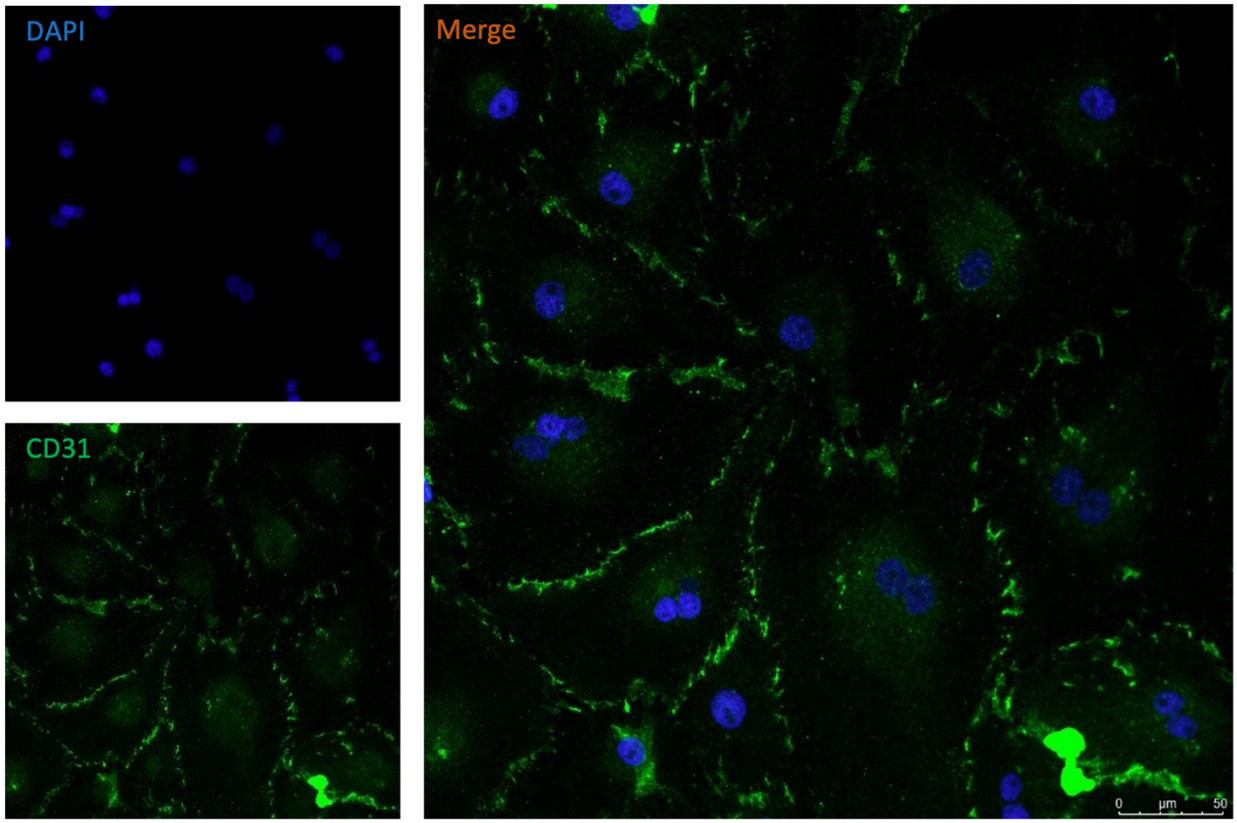

Figure 30 *Immunofluorescence of primary PAEC showing CD31 expression.* In green is shown CD31 signal in cell junctions, while in blue are indicated cells nuclei marked with DAPI.

4.2 Immortalization and characterization of Porcine Aortic Endothelial Cells

Porcine Aortic Endothelial Cells were transduced with two different retroviral vectors: *pLXSN + OaPV3_E6E7* and *pLXSN + OaPV4_E6E7*. *pLXSN* empty vector was used as a negative control. The reaction of infection was performed in duplicate in 6-weel-plates. Cells antibiotic selection was performed with 0,7 mg/ml of G418 for approximately 35 days, though negative control (empty *pLXSN*) stopped proliferating early after selection. Unfortunately, we were able to obtain PAEC immortalization only using the retroviral vector *pLXSN + OaPV3_E6E7*, cause cells transduced with *pLXSN + OaPV4_E6E7* showed senescence signals and cellular suffering and died after one week of antibiotic selection (data not showed). After transduction with *pLXSN + OaPV3_E6*E7 and selection, PAECs expressing OaPV3 oncogenes (Figure 31B-C) showed the same morphology of mock cells (Figure 31A). Cell morphology was evaluated also after frequent steps of freezing and unfreezing to evaluate cell resistance. This showed that cells were still able to proliferate (Figure 31D).

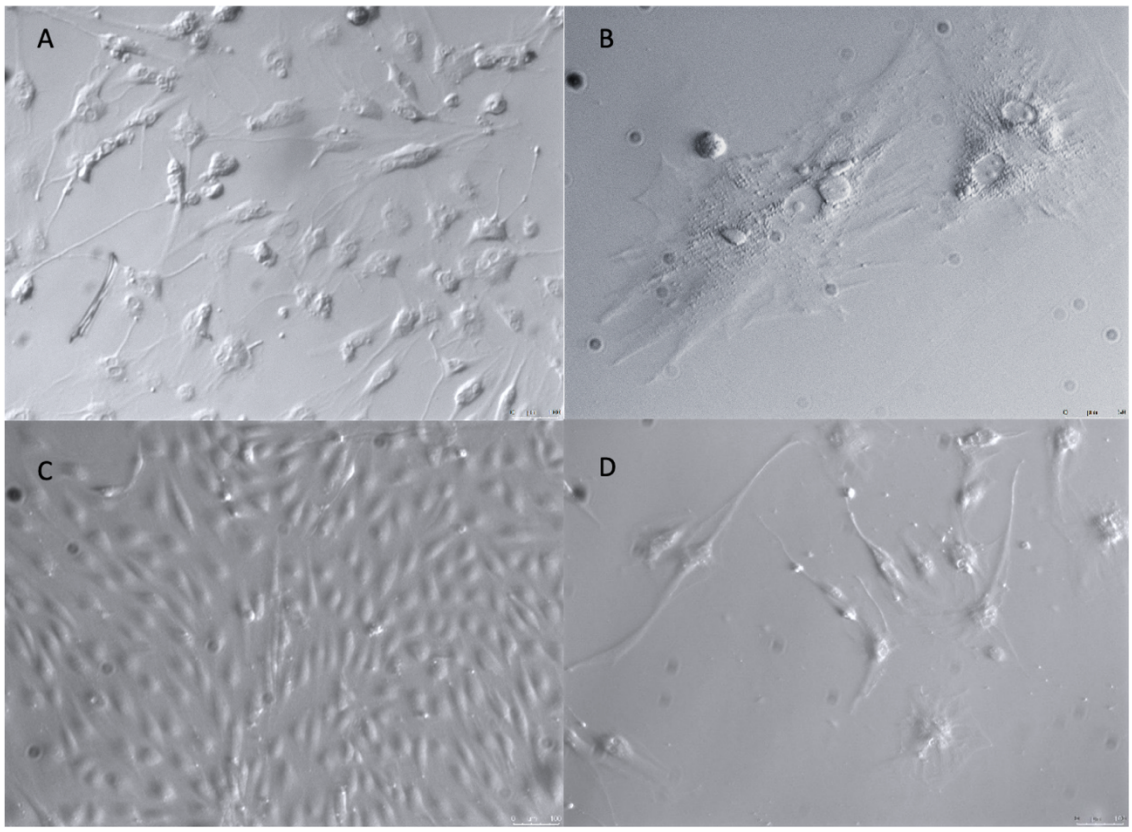

Figure 31 *Morphology of transduced iPAECs.* **A-B** iPAECs immortalized with *pLXSN + OaPV3-E6E7*. **C** Mock. **D** iPAECs morphology after unfreezing.

According to current data, the cell growth profile demonstrates that *E6E7* expression of *OaPV3* has determined a significative increase of Porcine Aortic Endothelial Cells lifespan, as showed in the table below (table 2). In fact, iPAECs transduced with the empty retroviral vector stopped proliferating early after infection: PAEC + *pLXSN* died at PD 5.

Retrovirus	**N° of population doublings in iPAEC cells.**
pLXSN + OaPV3-E6E7	PD 35
Empty *pLXSN*	Dead at PD 5

Table 2 *Population doubling levels in Porcine Aortic Endothelial cells transduced with the indicated recombinant retroviruses.* Data referred to ongoing experiments and are updated to current results.

Graph (Figure 32) of iPAEC cell lines represents the number of population doublings (PDs) at the specified times after infection with the different recombinant retroviruses. PD levels were calculated as described above.

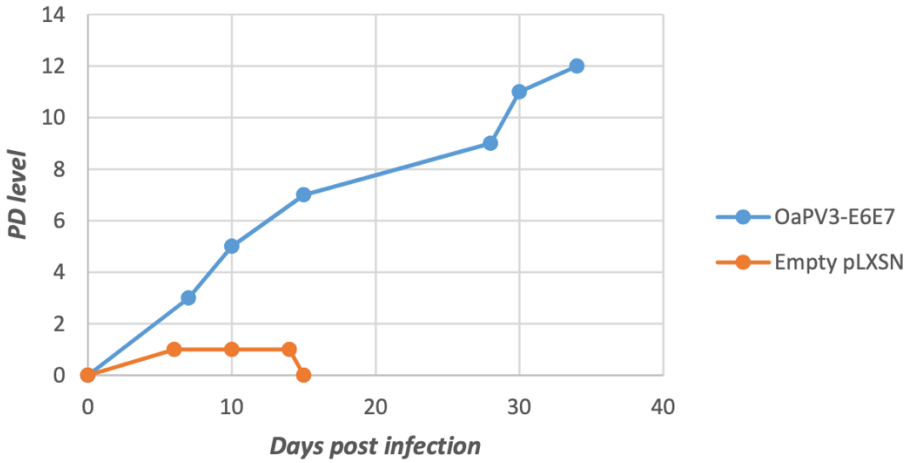

Figure 32 *Growth curve of transduced iPAECs*. PD level indicates the number of times cells have double since their retroviral transduction.

Population doubling time (PD time) (number of days it took each culture to reach 80-90% confluence) of iPAEC expressing E6E7 was significantly statistically shorter compared to mock cells (*pLXSN*). Moreover, iPAEC manifested the shortest time length and the higher proliferative activity (Figure 33).

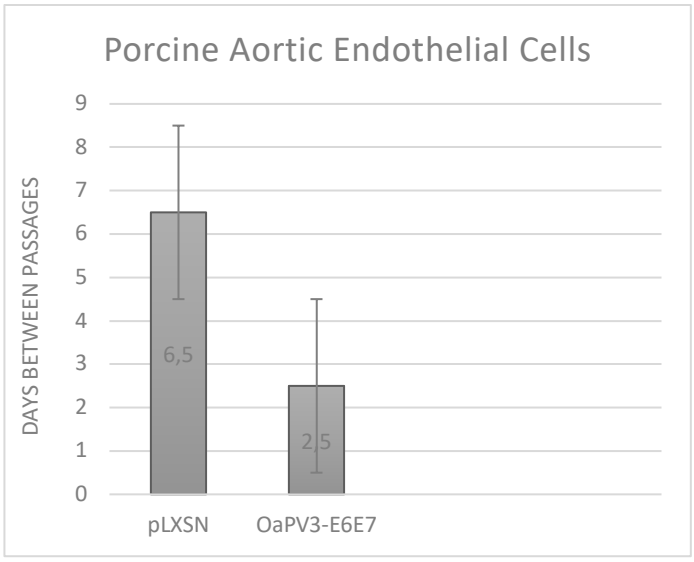

Figure 33 *Time length between post-selection passages of transduced iPAECs.*

E6E7 gene expression was also evaluated. RNA was extracted from transduced cells, retrotranscribed in cDNA and utilized as template for RT-PCR to evaluate gene expression using specific primers. Analysis confirmed *E6E7* expression in transduced iPAECs (Figure 34). Amplicons shown a 100% similarity with *E6E7* gene, confirming cells immortalization.

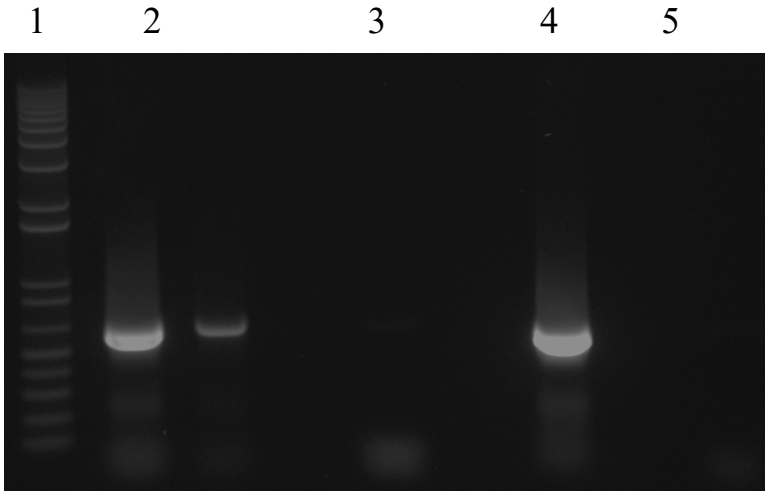

Figure 34 *Agarose gel: RT-PCR of iPAEC transduced with OaPV3-E6E7 showing E6E7 genes expression.* **1**: 1Kb Dna Ladder. **2**: cDNA of iPAEC. **3**: No-retrotrascribed control. **4**: *pLXSN + OaPV3-E6E7* used as a positive control. **5**: H_2O

Characterization of iPAEC was performed by indirect immunofluorescence looking for the presence of endothelial specific marker CD31 (Figure 35). Experiment was performed in triplicate.

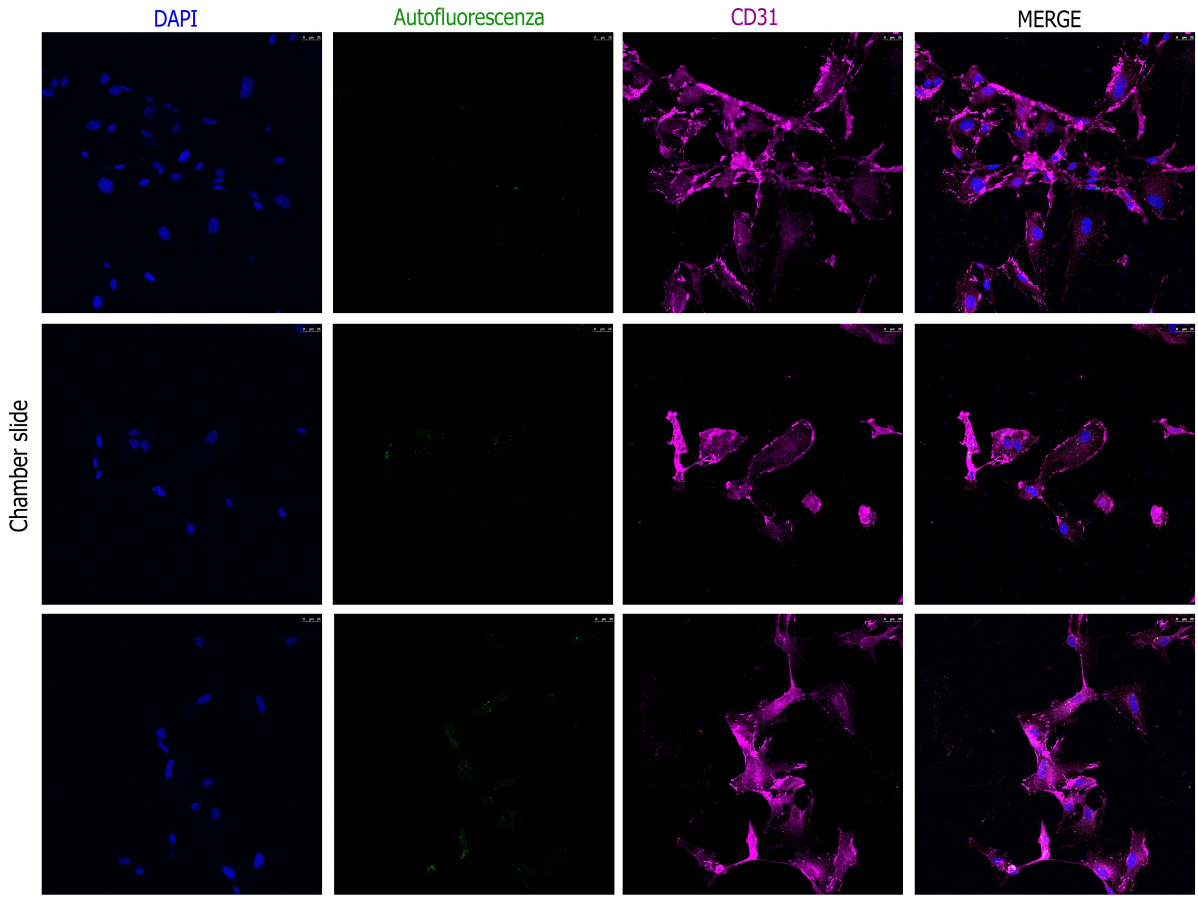

Figure 35 *Immunofluorescence analysis of iPAEC showing CD31 endothelial specific marker.*

4.3 Evaluation of iPAEC susceptibility to *ASFV* infection

Transduced Porcine Aortic Endothelial cells were mock-infected or infected with a virulent Sardinian *ASFV* isolate, *2008 (47/Ss/08)*, and an attenuated isolate, *NH/P68* (from Portugal). Cells were infected at different MOI (1, 2 and 0.2) end stopped after 2-, 4-, 24-, 48-, 72-, 96-hours. A control experiment with Cos-1 cells was performed. Cos-1 are susceptible to different *ASFV* isolates, and they are commonly used to study virus production. Experiments with MOI 1 and 3 were carried out in triplicate while experiments with MOI 0.2 in duplicate. iPAECs infected with MOI 1 and 3 were stopped after 2-, 24-, 48-, 72-hours and, before that, their morphology was evaluated by microscope at 72-hours pi (Figure 36). The analysis showed that the high virulent isolate, virus *2008*, killed

iPAEC cells (Figure 36A) compared with *NH/P68* strain (Figure 36B). This is due because *NH/P68* is an attenuated isolate.

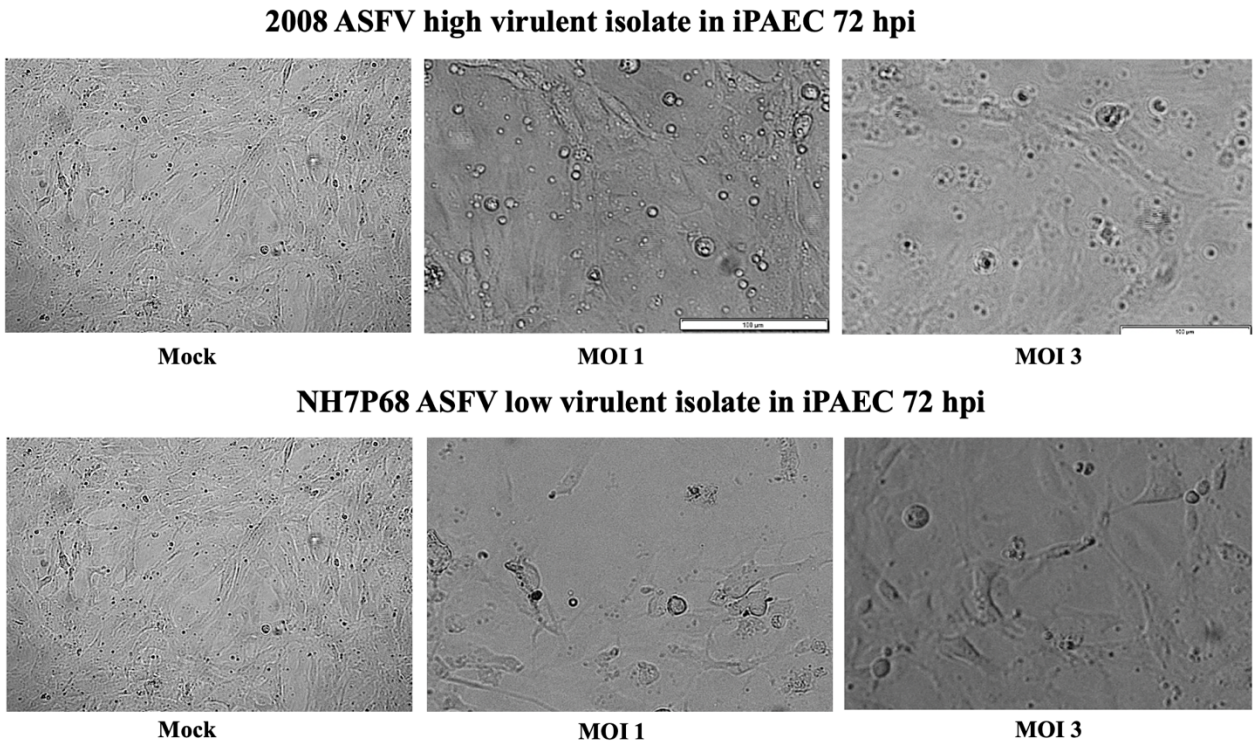

Figure 36 *Morphology evaluation of infected iPAECs.* **A**: iPAEC infected with high virulent *ASFV* isolate (*2008*). **B**: iPAEC infected with low virulent *ASFV* isolate (*NH/P68*).

The qPCR analysis on the DNA extracted from infected cells supernatant with MOI 1 and 3 showed that the total production of both isolates inside iPAEC was quite the same of the Cos-1 cells, with a virus replication increase at 24-hours pi, while the quantity was stable in the next hours (Figure 37).

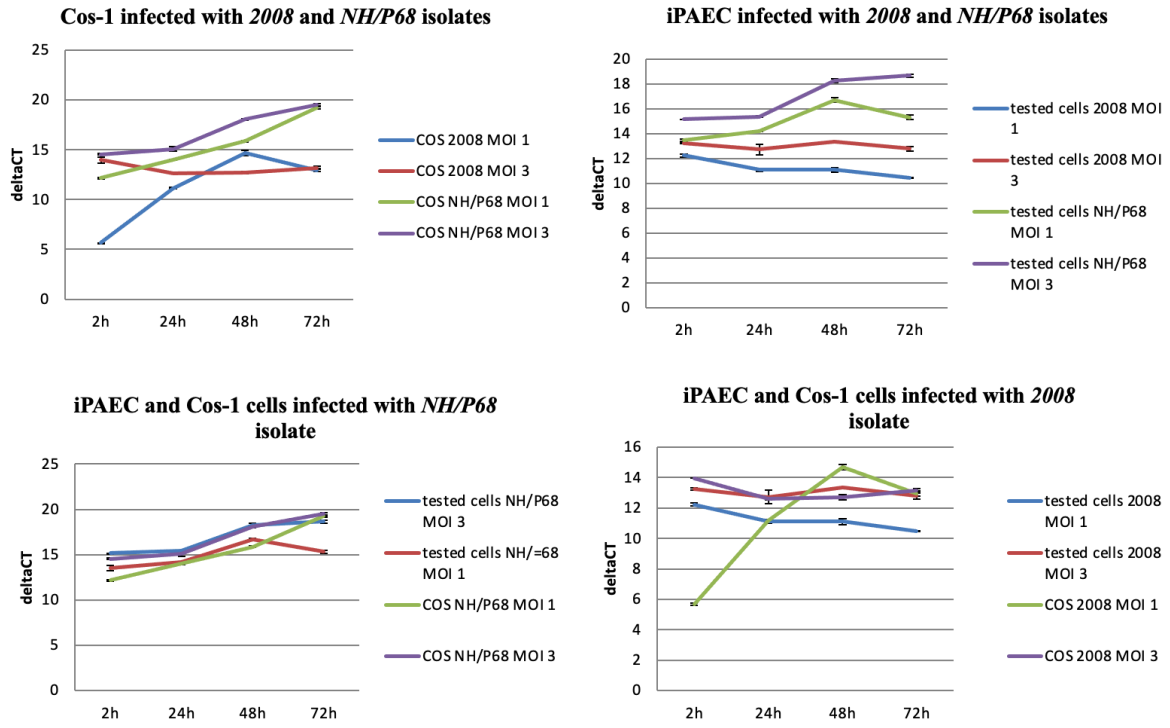

Figure 37 Real-Time PCR analysis on cell pellet and supernatant of infected cells with MOI 1 and 3.

Otherwise, experiments carried out with MOI 0.2 were stopped after 2-, 4-, 24-, 48-, 72- and 96-hours pi. qPCR analysis showed that the total kinetic of virus *2008* production inside iPAEC cells (pellet) is highest, revealing an increase of virus replication after 24-hours, while virus quantity remains stable in the next hours. Instead, the quantity of viral particles found in cell supernatant showed an increase after 4- and 48-hours (Figure 38).

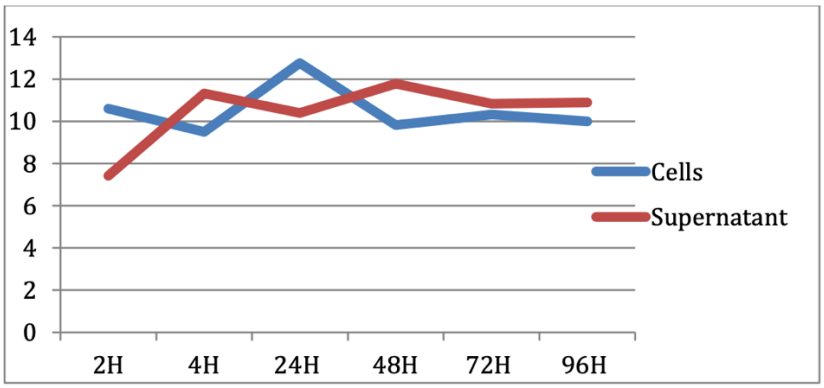

Figure 38 Real-Time PCR analysis on cell pellet and supernatant of iPAECs infected with *2008* strain and with MOI 0.2.

The cytofluorimetric analysis to quantify levels of intracellular p72 virus protein was performed on cellular pellet derived from iPAECs infected with MOI 3 and stopped after 72-hours pi. The analysis showed that iPAEC cells were highly susceptible to virus infection with both *ASFV* isolates (*2008* and *NH/P68*) compared to Cos-1 cells (Figure 39-40). Indeed, as showed in cells morphology analysis, iPAECs infected with the two isolates were died at 72h pi.

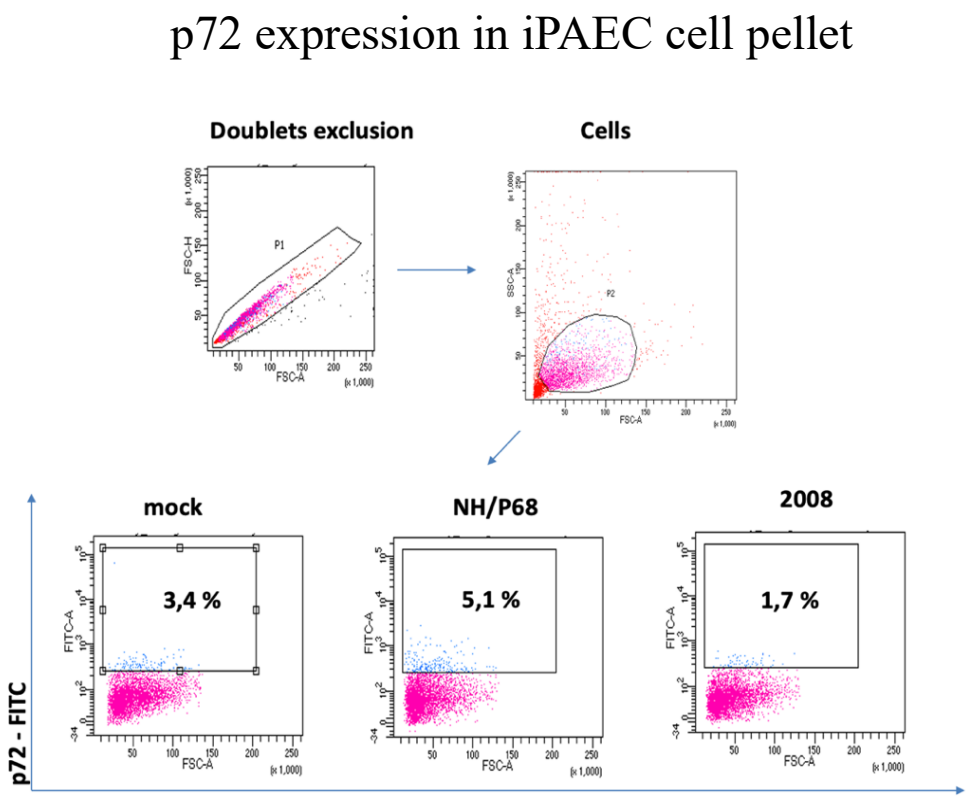

Figure 39 *FACS analysis of infected iPAEC with MOI 3 showing p72 levels*

p72 expression in Cos-1 cell pellet

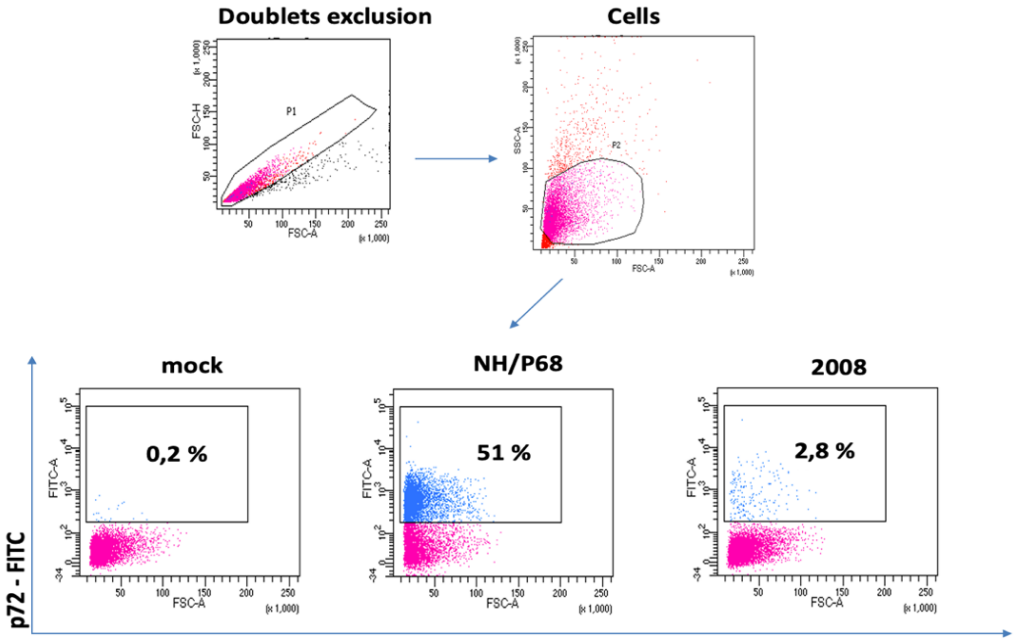

Figure 40 *FACS analysis of infected cells with MOI 3 showing p72 levels.*

4.4 Evaluation of isolates titer after their passage on iPAEC cells

iPAEC cells supernatant at 72-hours pi with MOI 3 was titled on monocytes/macrophages cells. Supernatants collected from infected iPAEC were seeded and titled on monocyte/macrophage cells (back titration). An average title of $10^{-3,18}$ was measured in iPAEC cells supernatant infected with *2008* isolate, and an average title of $10^{-4,68}$ in iPAEC cells supernatant infected with *NH/P68* isolate using Spearman–Kärber formula to calculate the 50% endpoint. For *2008 ASFV* isolate analysis was performed according with its hemo-adsorbing properties, by adding 1% of erythrocyte to macrophages culture evaluating rosette formation (Figure 41).

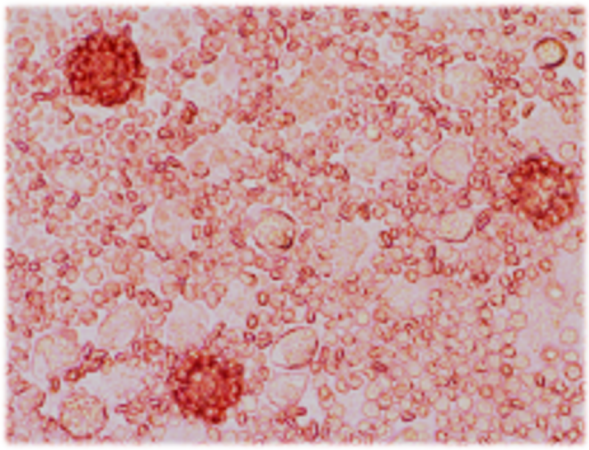

Figure 41 *Rosette developed on macrophage cultured cells.*

For *NH/P68 ASFV* isolate titration was calculated by direct immunofluorescence using an Anti-PSA-Coniugate FITC antibody, since this isolate does not present hemo-adsorbing properties (data not showed).

4.5 Expression of different selected *ASFV* late genes in Cos-1 cells

Selected *ASFV* late genes (*B318L-B119L*, *B962L* and *E120R*) were mutagenized in order to remove PAM sequences to avoid Cas9 bond. dePAMs genes were synthetized from Eurofins and included into *pEX-A128* vector. Subsequently, dePAM genes were successfully cloned into *pLXSN* retroviral vector (Figure 42).

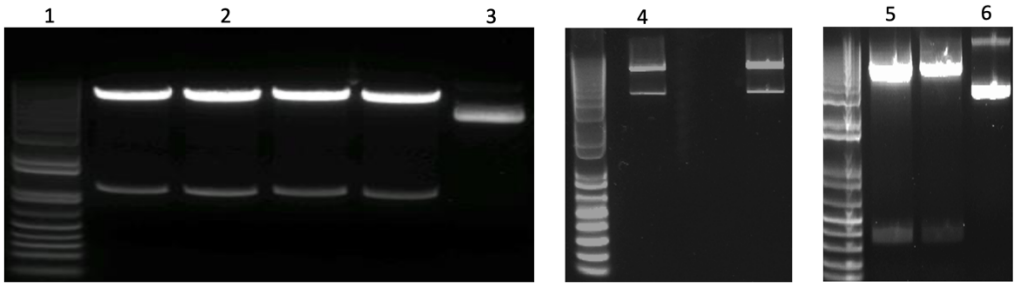

Figure 42 *Agarose gel: analytical digestion of pLXSN + dePAM genes.* **1:** 1 kb plus DNA ladder. **2:** *pLXSN + dePAM_B318L-B119L*. **3:** not digested. **4:** *pLXSN + dePAM_B962L*. **5***: pLXSN + dePAM_E120R*. **6:** not digested.

After transfection of Phoenix cells with retroviral constructs, Cos-1 cells were infected with recombinant retroviral particles collected from Phoenix supernatant and selected with G418 selective

antibiotic. We were able to obtain Cos-1 expressing *dePAM_B318L-B119L* gene and Cos-1 expressing *dePAM_E120R* gene. Unfortunately, Cos-1 infected with *pLXSN + dePAM_ B962L* died early after transduction. PCR was performed with specific primers using cDNAs from transduced Cos-1 as templates (Figure 43).

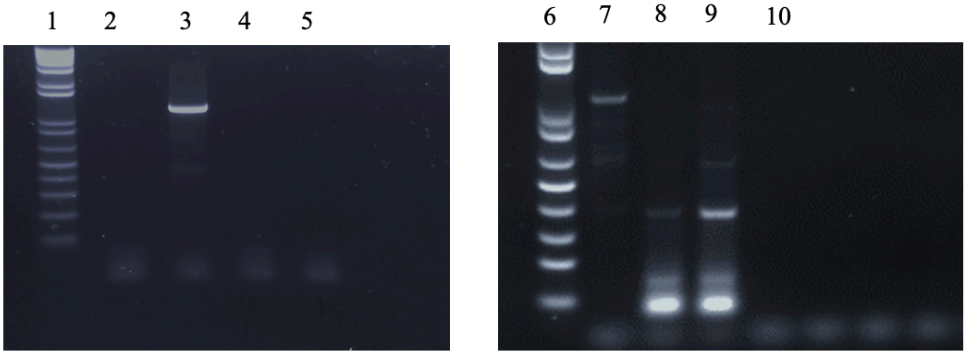

Figure 43 *Agarose gel: RT-PCR confirming genes expression in COS-1 cells.* **1**: 1Kb plus DNA ladder. **2:** empty *pLXSN*. **3:** *pLXSN + dePAM_B318L-B119L (1318 bp)* (72h). **4:** not retrotranscribed. **5:** H20. **6:** 1 Kb plus DNA ladder. **7:** empty *pLXSN*. **8:** *pLXSN +dePAM_E120R (365 bp)* (48 h). **9:** *pLXSN +dePAM_E120R (365 bp)* (72 h). **10:** not retrotranscribed.

PCR products were sequenced by BMR genomics. Amplicons shown a 100% similarity with *B318L-B119L* and *E120R* mutagenized genes, confirming the specificity of transcribed mRNAs. In addition, Cos-1 cells expressing dePAM*_E120R* gene were tested by western immunoblotting analysis. Proteins were extracted from Cos-1 cell pellet and submitted to Western Blot with specific antibody (Figure 44).

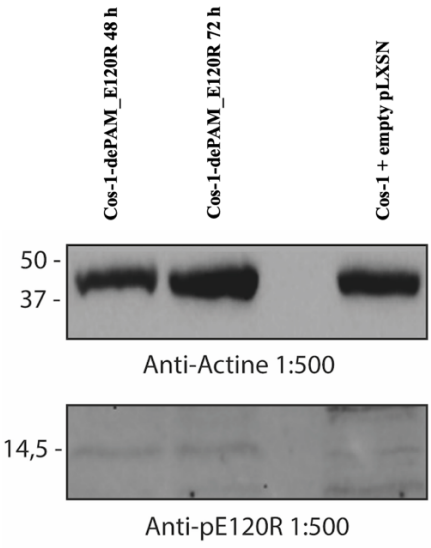

Figure 44 *Western Immunoblotting: pE120R (14.5 kb) expression in transduced COS-1.* Normalization was performed using β-actin.

Cos-1 transduced cells with *pLXSN +dePAM_E120R* were tested also by immunocytochemistry to better understand pE120R localization and its functions (Figure 45).

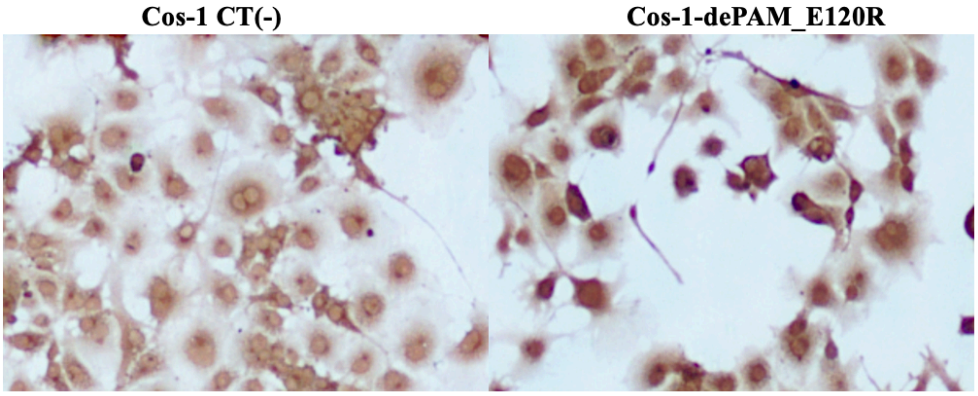

Figure 45 *Immunocytochemistry:* pE120R localization in Cos-1 transduced cells.

The immunocytochemistry analysis showed a high aspecific signal in negative control (Cos-1 transduced with empty *pLXSN*), while Cos-1 expressing pE120R showed, as expected, a positive signal localized into cytoplasm and/or at nuclei border. It is necessary to repeat the analysis to obtain a clearer data.

4.6 GST fusion protein expression and purification

dePAM *E120R* gene was amplified from *pLXSN* vector and successfully cloned into *pGEX-2T* bacterial expression vector in order to generate GST fusion protein (Figure 46).

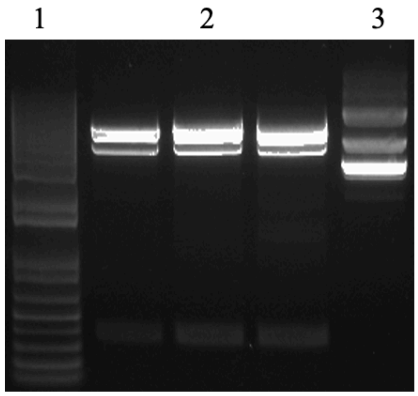

Figure 46 *Agarose gel: analytical digestion of pGEX-2T + dePAM_E120R.* **1**: 1Kb plus DNA ladder. **2**: digested *pGEX-2T + dePAM_E120R*. **3**: not digested.

BL21 Codon plus *E. coli* were transformed with the plasmid mentioned above and induced with IPTG. The correct expression of GST fusion protein was checked on SDS-PAGE before purification (Figure 47). *BL21 E. coli* transformed with *Mycoplasma* MAG 5040 protein were used as a positive control. It is a nuclease $MgCl_2$ dependent, tested before in our laboratory.

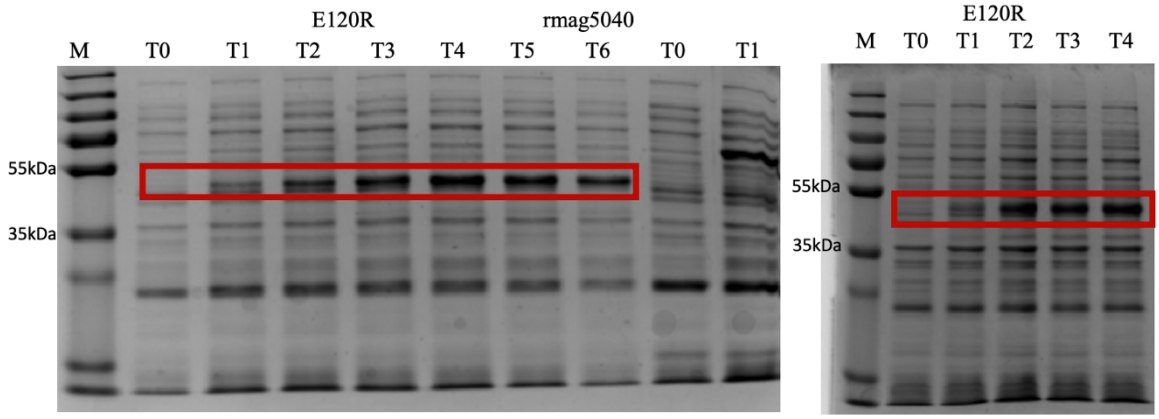

Figure 47 *SDS-Page: pE120R expression (from T0 to T6).* Bl21+rmag5040 used as a positive control.

The GST-pE10R fusion protein (25kDa GST molecular weight + 14.5kDa pE120R molecular weight) reaches its highest expression after induction at 30°C at T4. GST fusion protein was purified using glutathione beads and purification was checked through SDS-PAGE. In order to estimate the amount of purified protein, a BSA curve was included in the running gel (Figure 48)

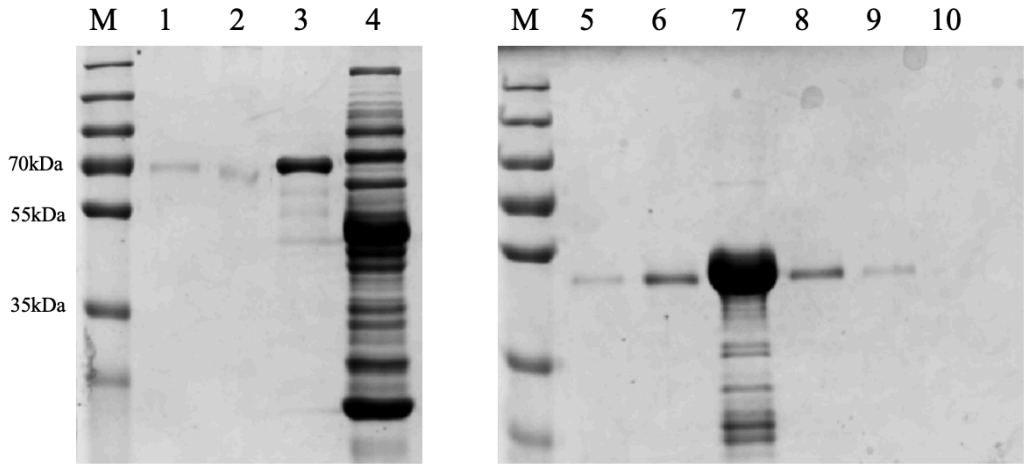

Figure 48 *SDS-Page: GST fusion protein purification.* ***1***: BSA 20 ng/µl; **2**: BSA 100 ng/µl; ***3***: BSA 200 ng/µl; ***4***: unbound; **5**: P1; **6**: P2; **7**: P3; **8**: P4; **9**: P5; **10**: P6. (P= portion of eluted protein).

The highest amount of GST fusion protein during purification process is revealed in the eluted portion 3 (P3).

4.7 Expression of different selected *ASFV* late genes in iPAEC

pLXSN and *pLXSN + dePAM_E120R*, were mutagenized in order to cut out their geneticin antibiotic resistance cassette to insert puromycin antibiotic resistance. This step is necessary to transduce iPAEC cells with dePAM genes selected before since they were immortalized using a vector (*pLXSN + OaPV3_E6E7*) containing geneticin, antibiotic resistance gene that is integrated into iPAEC genome. Puromycin resistance gene was amplified from *Lenti-CRISPR-V2* plasmid and successfully cloned into *pLXSN* and *pLXSN + dePAM_E120R* (Figure 49).

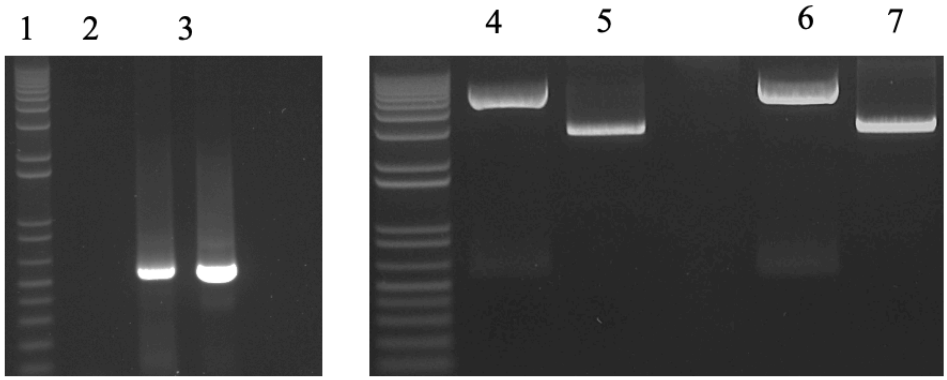

Figure 49 *Agarose gel: amplification of puromycin resistance gene and analytical digestion of pLXSN + Puro and pLXSN + dePAM_E120R + Puro.* **1**: 1Kb plus DNA Ladder. **2**: negative control. **3**: Puromycin resistance gene (612 bp). **4**: digested *pLXSN + Puro*. **5**: not digested. **6**: digested *pLXSN + dePAM_E120R + Puro*. **7**: not digested.

Puromycin resistance gene cloning into indicated vectors was also confirmed by its successfully amplification from designed vectors (Figure 50). Amplicons were sequenced revealing a 100% similarity with puromycin resistance gene.

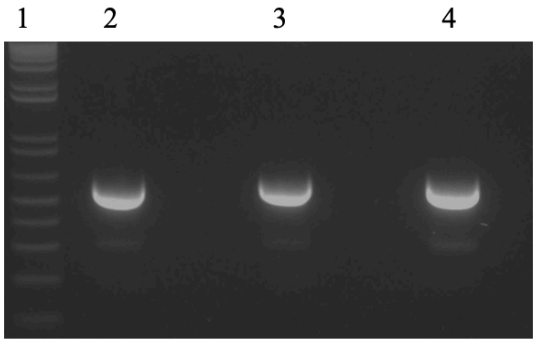

Figure 50 *Agarose gel: Amplification of puromycin resistance gene cloning into vectors.* **1**: 1 Kb plus DNA Ladder. **2**: *pLXSN + Puromycin resistance gene*. **3**: *pLXSN + dePAM_E120R + Puromycin resistance gene*. **4**: positive control (*Lenti-CRISPR-V2* vector).

iPAEC cells were transduced with the obtained vectors, but unfortunately, they died after one week of antibiotic selection. This is probably due to a mutation inside the designed vectors that was not revealed before their employment to infect cells, although plasmids were sequenced before their use, without observing inconsistencies. It is probably that during geneticin resistance gene excision was accidentally cut a portion of *pLXSN* promoter that did not allow puromycin resistance expression in cells. For this reason, at the moment we are considering changing *pLXSN* promoter with another deriving from *pCMV* vector to allow puromycin resistance gene expression (experiments are still in progress).

5. Discussion

African swine fever (ASF) is one of the most important viral diseases of bush pigs (*Potamochoerus porcus* and *P. larvatus*), warthogs (genus *Phacochoerus*), domestic pigs and wild boars, transmitted by *African Swine Fever Virus* (*ASFV*) (*Sánchez-Cordón P.J et al., 2019*). ASF is highly contagious and lethal, and it is considered an economically devasting disease representing the most serious damage for world pork industries (*Dan Murtaugh et al., 2019*). Until today, a vaccine against *ASFV* does not exist and the only weapons to limit its spread are a prompt disease individuation followed by a rapid laboratory diagnosis and stamping out of animals. For forty years, different strategies have been implemented to develop a possible vaccine, but virus complexity and its ability to evade host immune system hampered its setting up (*Sanchez-Vizcaino, et al., 2006; 2015*). Indeed, inactivated vaccines proved to be not effective (*Alejo et al., 2018*), while vaccines created with naturally attenuated virus (*Blome et al., 2014*) or live attenuated virus (LAV) (*Gallardo et al., 2019*) arise important side effects and protect only from isolates derived from the same genotype. Recently, vaccines obtained by deletion of specific genes or by subunit vaccine were developed (*Ramirez-Medina et al., 2019*). An important issue in vaccines development is the identification of *ASFV* genes involved in virulence and the characterization of the viral mechanisms used to elude host immune system. Therefore, the lack of a vaccine limits the options to control the disease and for this reason it is extremely important the development of a vaccine capable of infecting and inducing a long last immunity as well as avoiding the risk of possible recombination with the wild type circulating virus. The principal aim of this project was the development of a DISC (Disabled Infectious Single Cycle) vaccine specific for *ASFV* Sardinian isolates. A DISC vaccine is developed through deletion of target genes to prevent viral replication, resulting in a defective strain unable to replicate in the natural host. This kind of vaccine combines the efficacy of LAV vaccines with the security of inactivated vaccines and could be a good compromise to satisfy vaccine requirements. Vaccines production require the development of suitable continuous cell lines genetically stable to support viral replication. It is important that such cell lines originate from natural host species and from tissues involved in infection, since it has been observed that virus adapting to cell lines derived from different species caused undesired modifications and mutations. In addition, the use of cell lines derived from primates, such as Cos-1 cells, may lead to virus adaptation to primates. The natural target cells for *ASFV* are cells derived from monocytes, in particular macrophages. At present, monocyte/macrophage continuous cell lines permissive to virus replication do not exist.

In the natural host, *ASFV* replicates in endothelial cells as well. For this reason, in this study primary Porcine Aortic Endothelial Cells (PAECs) cultures were developed. PAECs were isolated using two different enzymatic solution, dispase and collagenase, showing that PAECs isolated with collagenase solution showed a most homogeneous cell population prevalently represented by endothelial cells (95%). PAEC cells were characterized by the presence of CD31 marker, which is highly expressed in endothelial cell junctions. We tried to immortalize PAEC cells using *E6* and *E7* oncogenes derived from *OaPV3* and *OaPV4* ovine papillomavirus. The transduction was carried out using two different retroviral vectors, *pLXSN + OaPV3_E6E7* and *pLXSN + OaPV4_E6E7*. Unfortunately, we were able to obtain a stable continuous cell line of Porcine Aortic Endothelial Cells (iPAEC) only with *OaPV3* genes. Cells transduced with *pLXSN + OaPV4_E6E7* showed senescence and cellular suffering dying after one week of antibiotic selection. This was probably due since *OaPV3* is a most virulent strain that is able to transform endothelial cells causing SCC, while *OaPV4* induces only fibropapillomas. Once a stable cell line was obtained, we test their ability to support virus replication. To that aim, we infected iPAECs with two different *ASFV* isolates, *2008* and *NH/P68*, with different MOI. This allowed to verify iPAECs capability to sustain virus replication showing that the high virulent strain, *2008*, was able to kill our cells when infected with MOI 1 and 3. In order to verify the capability to enhance viral titer we infected cells using a lower number of viruses (MOI=0.2). qPCR analysis of infected cells with MOI 1 and 3 showed that the kinetic of total virus production in iPAEC cells is quite the same as the Cos-1 cells, revealing an increase at 24-hours pi, while virus quantity was stable during next hours. Instead, when used a MOI of 0.2, qPCR analysis displayed that the kinetic of virus *2008* production inside iPAEC was highest, revealing an increase of virus replication after 24-hours. FACS analysis as well revealed that iPAECs were high susceptible to both virus using MOI 3, in fact *ASFV* isolates killed the cells, as showed in cell morphology analysis. As described before, the production of a DISC vaccine requires the deletion of selected *ASFV* genes. To this aim, different target late genes were selected (*B962L, B438L, B318L, B119L* and *E120R)*, because of their crucial role during viral particles assembling and budding. Selected genes were mutagenized in order to delete PAM sequences that are necessary to bind Cas9 in CRISPR technology. Defective viruses can replicate only in suitable helper cell lines expressing mutagenized ASFV genes. The helper cell lines represent the cellular substrate in which can be applicated CRISPR-Cas9 technology to interrupt specific late genes. Once genes were mutagenized, they were transduced in Cos-1 cells, in order to test our designed procedure before utilizing it in iPAECs. We were able to obtain Cos-1 stable cell lines expressing *B318L-B119L* and *E120R* genes, as showed by RT-PCR analysis and sequencing of

amplicons. Immunoblotting and immunocytochemistry experiments on Cos-1 expressing dePAM_*E120R* gene confirmed its expression. Unfortunately, a high aspecific signal was detected that did not allow to show satisfactorily its expression and location (Figure 44-45). For this reason, we decided to express *E120R*-GST fusion protein in *E. coli* managing to obtain the recombinant protein to be used to produce more specific antibodies. Unfortunately, due to pandemic situation we were not able to carry on successive experiments. Another thing that absolutely should be done, is the production of specific antibodies to reveal the presence of the selected late proteins, as they are not present available. Furthermore, it is essential to obtain cell lines expressing other selected genes in order to have a more complete cell platform in which delete different genes to arise the efficiency of the projected vaccine. As mentioned earlier, designed procedure may be used in iPAEC cells, and to this aim we projected new vectors in order to express the chosen genes into the obtained cell line. This was necessary since vectors used in Cos-1 cells contain G418 antibiotic resistance that cannot be used in iPAEC, as they have already integrated in their genome this resistance because of the immortalization process. We were able to acquire new vectors containing puromycin resistance cassette, and ready to use to genes expression in iPAEC. Unfortunately, after several attempts, it was impossible to select cells with puromycin resistance. In conclusion, we obtained a stable and continuous Porcine Aortic Endothelial cell line that may be used as a cell platform to develop helper cells expressing different dePAM *ASFV* genes and that will be used to produce a DISC vaccine against Sardinian isolates. Further analyses are clearly required to verify if *ASFV* Sardinian isolates needed to adapt to the new cell line. For this reason, it would be necessary implement virus cultures on the new cell line checking the viral titer obtained. It would be also necessary to confirm isolates genetic stability after their passage on iPAEC by Next Generation Sequencing in order to evaluate the presence of undesired mutations. Finally, we will proceed to DISC vaccine production using our strategy and, subsequently, developing a DIVA test that allow to differentiate between vaccinated animals and those naturally infected.

6. Conclusion

In Sardinia African Swine Fever has been endemic since 1978 and the lack of a suitable vaccine limits the option to control the disease producing devasting effects on Sardinian economy due to commercial limitations. In addition, the high number of wild boars circulating in the region constitutes a serious problem in ASF control. For this reason, the development of a vaccine is necessary to eradicate *Africa Swine Fever Virus*. Until today, attempts to develop an effective and safe vaccine did not have success. This project was aimed to identify a novel strategy to achieve a DISC vaccine able to protect against Genotype I of *ASFV*, as this is the only circulating in Sardinia region. It is extremely important that vaccines are based on the circulating genotype to avoid recombination between different genotypes, for this reason the project make use of a Sardinian isolated, *2008* virus (*47/Ss/08*). Furthermore, until today a stable and continuous swine derived cell line able to support *ASFV* growth did not exist. The virus can be isolated and cultivated on monocytes/macrophages, primary cell lines that are difficult to obtain and to cultivate as a continuous macrophages cell line does not exist. Moreover, the employment of primary macrophages in vaccine production is an expensive procedure and would be impossible to use for veterinary applications. Considering that, we may assert that iPAEC developed in this project represents a suitable cellular substrate for DISC vaccine development and production. In addition, the study of genes mutagenized by PAMs sequences removal in this project may provide further clarifications on their role during infection, as their biological functions are still unknown. The methodology developed in this research may lay the basis to develop a vaccine not only against Genotype I but also against all 23 genotypes. Once inoculated, the virus is not able to express the interrupted gene, for this reason its relating protein can be used as a DIVA test. In fact, vaccinated animals should not produce antibodies against it, unlike animals naturally infected with the wild type virus. Concluding, the immortalized Porcine Aortic Endothelial Cell line here developed represents an important tool to produce a DISC vaccine and until today, is the only stable and continuous porcine cell line developed that may be used to cultivate *African Swine Fever Virus*.

References

Agüero M, Arias M, Romero L J, Zamora MJ, Sánchez-Vizcaíno JM. Molecular differentiation between NS1 gene of a field strain Bluetongue virus serotype 2 (BTV-2) and NS1 gene of an attenuated BTV-2 vaccine. Vet Microbiol. 2002 May 24;86(4):337-41. doi: 10.1016/s0378-1135(02)00011-1. PMID: 11955783.

Ahuja D, Sáenz-Robles MT, Pipas JM. SV40 large T antigen targets multiple cellular pathways to elicit cellular transformation. Oncogene. 2005 Nov 21;24(52):7729-45.

Alejo, A.; Matamoros, T.; Guerra, M.; Andres, G. 2018 A proteomic atlas of the African swine fever virus particle. J. Virol. 92 (23) e01293- 18; DOI: 10.1128/JVI.01293-18

Alejo A, Andrés G, Viñuela E, Salas ML. The African swine fever virus prenyltransferase is an integral membrane trans-geranylgeranyl-diphosphate synthase. J Biol Chem. 1999 Jun 18;274(25):18033-9. doi: 10.1074/jbc.274.25.18033. PMID: 10364254.

Altamura, G., Corteggio, A., Pacini, L., Conte, A., Pierantoni, G.M., Tommasino, M., Accardi, R., Borzacchiello, G., 2016. Transforming properties of Felis catus papillomavirus type 2 E6 and E7 putative oncogenes in vitro and their transcriptional activity in feline squamous cell carcinoma in vivo. Virology 496, 1–8. doi:10.1016/j.virol.2016.05.017

Andrés G. African Swine Fever Virus Gets Undressed: New Insights on the Entry Pathway. J Virol. 2017 Jan 31;91(4):e01906-16. doi: 10.1128/JVI.01906-16. PMID: 27974557; PMCID: PMC5286891.

Andrés G, Alejo A, Salas J, Salas ML. African swine fever virus polyproteins pp220 and pp62 assemble into the core shell. J Virol. 2002 Dec;76(24):12473-82. doi: 10.1128/jvi.76.24.12473-12482.2002. PMID: 12438573; PMCID: PMC136718.

Andres, G., Garcia-Escudero, R., Salas, M.L., Rodriguez, J.M., 2002b. Repression of African swine fever virus polyprotein pp220-encoding gene leads to the assem- bly of icosahedral core-less particles. Journal of Virology 76 (6), 2654–2666.

Andrés G, García-Escudero R, Viñuela E, Salas ML, Rodríguez JM. African swine fever virus structural protein pE120R is essential for virus transport from assembly sites to plasma membrane but not for infectivity. J Virol. 2001 Aug;75(15):6758-68. doi: 10.1128/JVI.75.15.6758-6768.2001. PMID: 11435554; PMCID: PMC114402.

Andres, G., Garcia-Escudero, R., Vinuela, E., Salas, M.L., Rodriguez, J.M., 2001b. African swine fever virus structural protein pE120R is essential for virus transport from assembly sites to plasma membrane but not for infectivity. Journal of Virology 75 (15), 6758–6768.

Andrés G, García-Escudero R, Simón-Mateo C, Viñuela E. African swine fever virus is enveloped by a two-membraned collapsed cisterna derived from the endoplasmic reticulum. J Virol. 1998 Nov;72(11):8988-9001. doi: 10.1128/JVI.72.11.8988-9001.1998. PMID: 9765444; PMCID: PMC110316.

Andrés G, Simón-Mateo C, Viñuela E. Assembly of African swine fever virus: role of polyprotein pp220. J Virol. 1997 Mar;71(3):2331-41. doi: 10.1128/JVI.71.3.2331-2341.1997. PMID: 9032369; PMCID: PMC191342.

Antonsson, A., McMillan, N.A.J., 2006. Papillomavirus in healthy skin of Australian animals. J. Gen. Virol. 87, 3195–3200. doi:10.1099/vir.0.82195-0

Arias M.L., De La Torre A., Dixon L., Gallardo C., Jori F., Laddomada A.4, Martins C.5, Parkhouse M.6, Revilla Y. 7, Rodrìguez F.8, Sànchez-Vizcaìno J.M Blueprint and Roadmap on the possible development of a vaccine for African Swine Fever prepared by the AfricanSwine Fever EU reference laboratory on Commission Request, Brussels, 31 January 2017

Arias, M., Sanchez-Vizcaino, J.M., 2002b. African Swine Fever Eradication: The Span- ish Model. In: Morilla, A., Yoon, K.J., Zimmerman, J.J. (Eds.), Trends in Emerging Viral Infections of Swine, vol. 1. Iowa State Press, Ames, pp. 133–139.

Bacciu, D., Deligios, M., Sanna, G., Madrau, M. P., Sanna, M. L., Dei, G. S., & Oggiano, A. (2016). Genomic analysis of Sardinian 26544/OG10 isolate of African swine fever virus. Virology Report, 6, 81-89. https://doi.org/10.1016/j.virep.2016.09.001

Baroudy, B.M., Venkatesan, S., Moss, B., 1982. Incompletely base-paired flip–flop terminal loops link the 2 DNA strands of the vaccina-virus genome into one uninterrupted polynucleotide chain. Cell 28 (2), 315–324.

Beltran-Alcrudo D, Lubroth J, Depner K, De la Roque S (2008) African swine fever in the Caucasus. FAO EMPRES Watch,1e8, April 2008.

Blome, S.; Gabriel, C.; Beer, M. 2014 Modern adjuvants do not enhance the efficacy of an inactivated African swine fever virus vaccine preparation. Vaccine, 32, 3879–3882.

Boinas FS, Wilson AJ, Hutchings GH, Martins C, Dixon LJ. The persistence of African swine fever virus in field-infected Ornithodoros erraticus during the ASF endemic period in Portugal. PLoS One. 2011;6(5):e20383. doi: 10.1371/journal.pone.0020383. Epub 2011 May 31. PMID: 21655242; PMCID: PMC3105027.

Borca, M.V., Irusta, P.M., Kutish, G.F., Carillo, C., Afonso, C.L., Burrage, A.T., Neilan, J.G., Rock, D.L., 1996. A structural DNA binding protein of African swine fever virus with similarity to bacterial histone-like proteins. Archives of Virology 141 (2), 301–313.

Boshoff, C.I., Bastos, A.D.S., Gerber, L.J., Vosloo, W., 2007. Genetic characterisation of African swine fever viruses from outbreaks in southern Africa (1973–1999). Veterinary Microbiology 121 (1–2), 45–55.

Bottalico, D., Chen, Z., Dunne, A., Ostoloza, J., McKinney, S., Sun, C., Schlecht, N.F., Fatahzadeh, M., Herrero, R., Schiffman, M., Burk, R.D., 2011. The oral cavity contains abundant known and novel human papillomaviruses from the Betapapillomavirus and Gammapapillomavirus genera. J. Infect. Dis. 204, 787–92. doi:10.1093/infdis/jir383

Breese SS Jr, DeBoer CJ. Electron microscope observations of African swine fever virus in tissue culture cells. Virology. 1966 Mar;28(3):420-8. doi: 10.1016/0042-6822(66)90054-7. PMID: 18611474.

Brimer, N., Lyons, C., Wallberg, A.E., Vande Pol, S.B., 2012. Cutaneous papillomavirus E6 oncoproteins associate with MAML1 to repress transactivation and NOTCH signaling. Oncogene 31, 4639–46. doi:10.1038/onc.2011.589

Brookes, S.M., Hyatt, A.D., Wise, T., Parkhouse, R.M., 1998. Intracellular virus DNA distribution and the acquisition of the nucleoprotein core during African swine fever virus particle assembly: ultrastructural in situ hybridisation and DNase- gold labelling. Virology 249 (1), 175–188.

Brookes, S.M., Hyatt, A.D., Wise, T., Parkhouse, R.M.E., 1998a. Intracellular virus DNA distribution and the acquisition of the nucleoprotein core during African swine fever virus particle assembly: ultrastructural in situ hybridisation and DNase- gold labelling. Virology 249 (1), 175–188.

Brookes SM, Sun H, Dixon LK, Parkhouse RM. Characterization of African swine fever virion proteins j5R and j13L: immuno-localization in virus particles and assembly sites. J Gen Virol. 1998 May;79 (Pt 5):1179-88. doi: 10.1099/0022-1317-79-5-1179. PMID: 9603333.

Brookes, S.M., Dixon, L.K., Parkhouse, R.M., 1996. Assembly of African swine fever virus: quantitative ultrastructural analysis in vitro and in vivo. Virology 224 (1), 84–92.

Campo, M.S., 2002. Animal models of papillomavirus pathogenesis, in: Virus Research. pp. 249–261. doi:10.1016/S0168-1702(02)00193-4.

Canivet C, Rhéaume C, Lebel M, Piret J, Gosselin J, Boivin G. Both IRF3 and especially IRF7 play a key role to orchestrate an effective cerebral inflammatory response in a mouse model of herpes simplex virus encephalitis. J Neurovirol. 2018 Dec;24(6):761-768. doi: 10.1007/s13365-018-0666-9. Epub 2018 Aug 9. PMID: 30094631.

Carrasco, L., de Lara, F.C., Martin de las Mulas, J., Gomez-Villamandos, J.C., Hervas, J., Wilkinson, P.J., Sierra, M.A., 1996. Virus association with lymphocytes in acute African swine fever. Veterinary Research 27 (3), 305–312.

Carrascosa, J. L, Carazo, J. M., Carrascosa, A. L., García, N., Santisteban, A., and Viñuela, E. (1984). General morphology and capsid fine structure of African swine fever virus particles. Virology 132, 160-172.

Carrascosa, A.L., Sastre, I., Gonzalez, P., Vinuela, E., 1993. Localization of the African swine fever virus attachment protein P12 in the virus particle by immunoelec- tron microscopy. Virology 193 (1), 460–465.

Casal I, Enjuanes L, Viñuela E. Porcine leukocyte cellular subsets sensitive to African swine fever virus in vitro. J Virol. 1984 Oct;52(1):37-46. doi: 10.1128/JVI.52.1.37-46.1984. PMID: 6384555; PMCID: PMC254486.

Chapman, D.A.G., Darby, A.C., Da Silva, M., Upton, C., Radford, A.D., Dixon, L.K., 2011. Genomic analysis of highly virulent Georgia 2007/1 isolate of African swine fever virus. Emerging Infectious Diseases 17 (4), 599–605.

Chapman, D.A.G., Tcherepanov, V., Upton, C., Dixon, L.K., 2008. Comparison of the genome sequences of nonpathogenic and pathogenic African swine fever virus isolates. Journal of General Virology 89, 397–408.

Chlanda, P., Carbajal, M.A., Cyrklaff, M., Griffiths, G., Krijnse-Locker, J., 2009. Mem- brane rupture generates single open membrane sheets during vaccinia virus assembly. Cell Host Microbe 6 (1), 81–90.

Cobbold, C., Windsor, M., Wileman, T., 2001. A virally encoded chaperone specialized for folding of the major capsid protein of African swine fever virus. Journal of Virology 75 (16), 7221–7229.

Cobbold, C., Wileman, T., 1998. The major structural protein of African swine fever virus, p73, is packaged into large structures, indicative of viral capsid or matrix precursors, on the endoplasmic reticulum. Journal of Virology 72 (6), 5215–5223.

Costard S, Mur L, Lubroth J, Sanchez-Vizcaino JM, Pfeiffer DU. Epidemiology of African swine fever virus. Virus Res. 2013 Apr;173(1):191-7. doi: 10.1016/j.virusres.2012.10.030. Epub 2012 Nov 1. PMID: 23123296.

Dan Murtaugh, D.; Curran, E. 2019 Pig 'Ebola' Virus Sends Shock Waves Through Global Food Chain. Available online:https://www.bloomberg.com/news/articles/2019- 05-02/pig-ebola-virus sends-shock-waves-throughglobal-food-chain (accessed on 3 May 2019).

DeCaprio JA. How the Rb tumor suppressor structure and function was revealed by the study of Adenovirus and SV40. Virology. 2009 Feb 20;384(2):274-84. doi: 10.1016/j.virol.2008.12.010. Epub 2009 Jan 17. PMID: 19150725.

De Matos, A.P., Carvalho, Z.G., 1993. African swine fever virus interaction with micro- tubules. Biologie Cellulaire 78 (3), 229–234.

De Villiers, E.P., Gallardo, C., Arias, M., da Silva, M., Upton, C., Martin, R., Bishop, R.P., 2010. Phylogenomic analysis of 11 complete African swine fever virus genome sequences. Virology 400 (1), 128–136.

De Villiers, E.M., Fauquet, C., Broker, T.R., Bernard, H.U., Zur Hausen, H., 2004. Classification of papillomaviruses. Virology. doi:10.1016/j.virol.2004.03.033.

Díaz-Martín V, Manzano-Román R, Oleaga A, Encinas-Grades A, Pérez-Sánchez R. Cloning and characterization of a plasminogen-binding enolase from the saliva of the argasid tick Ornithodoros moubata. Vet Parasitol 2012;191:301–14.

Dixon, L.K., Alonso, C., Escribano, J.M., Martins, C., Revilla, Y., Salas, M.L., Takamatsu, H., 2012. Asfarviridae Virus Taxonomy: Ninth Report of the International Com- mittee on Taxonomy of Viruses. Elsevier, London, UK, pp. 153–162.

Dixon, L. K., Escribano, J. M., Martins, C., Rock, D. L., Salas, M. L. & Wilkinson, P. J. (2005). Asfarviridae. In Virus Taxonomy, Eighth Report of the ICTV, pp. 135–143. Edited by C. M. Fauquet, M. A. Mayo, J. Maniloff, U. Desselberger & L. A. Ball. London: Elsevier/Academic Press.

Dixon, L.K., Bristow, C., Wilkinson, P.J., Sumption, K.J., 1990. Identification of a vari- able region of the African swine fever virus genome that has undergone separate DNA rearrangements leading to expansion of minisatellite-like sequences. Jour- nal of Molecular Biology 216 (3), 677–688.

Doorbar, J., 2016. Model systems of human papillomavirus-associated disease. J. Pathol. doi:10.1002/path.4656.

EFSA 2010a. Scientific opinion on geographic distribution of tick-borne infections and their vectors in Europe and the other regions of the Mediterranean Basin EFSA Journal, 8 (9) (2010), p. 1723 ISSN 1831-4732.
EFSA 2010b. Scientific opinion on the role of tick vectors in the epidemiology of Crimean-Congo hemorrhagic fever and African Swine Fever in Eurasia.EFSA Journal, 8 (8) (2010), p. 1703 ISSN 1831-4732.

Epifano, C., Krijnse-Locker, J., Salas, M.L., Rodriguez, J.M., Salas, J., 2006a. The African swine fever virus nonstructural protein pB602L is required for forma- tion of the icosahedral capsid of the virus particle. Journal of Virology 80 (24), 12260–12270.

Epifano, C., Krijnse-Locker, J., Salas, M.L., Salas, J., Rodriguez, J.M., 2006b. Generation of filamentous instead of icosahedral particles by repression of African swine fever virus structural protein pB438L. Journal of Virology 80 (23), 11456–11466.

Franzoni, G., Graham, S.P., Dei Giudici, S., Bonelli, P., Pilo, G., Anfossi, A.G., Pittau, M., Nicolussi, P.S., Laddomada, A., Oggiano, A., 2017. Characterization of the interaction of African swine fever virus with monocytes and derived macrophage subsets. Vet. Microbiol. 198, 88-98.

Galindo I, Alonso C. African Swine Fever Virus: A Review. Viruses. 2017 May 10;9(5):103. doi: 10.3390/v9050103. PMID: 28489063; PMCID: PMC5454416.

Galindo, I., E. Vin˜uela, and A. L. Carrascosa. 2000. Characterization of the African swine fever virus protein p49: a new late structural polypeptide. J. Gen. Virol. 81:59–65.

Gallardo, C.; Sanchez, E.G.; Perez-Nunez, D.; Nogal, M.; de Leon, P.; Carrascosa, A.L.; Nieto, R.; Soler, A.; Arias, M.L.; Revilla, Y. 2019 African swine fever virus (ASFV) protection mediated by NH/P68 and NH/P68 recombinant live-attenuated viruses. Vaccine 2018. Vaccines. 7, 56 18 of 20.

Gallardo, C., Anchuelo, R., Pelayo, V., Poudevigne, F., Leon, T., Nzoussi, J., Bishop, R., Perez, C., Soler, A., Nieto, R., Martin, H., Arias, M., 2011b. African swine fever virus p72 genotype IX in domestic pigs, Congo, 2009. Emerging Infectious Diseases 17 (8), 1556–1558.

Gallardo, C., Mwaengo, D.M., Macharia. J. M., Arias, M, Taracha, E.A., Soler, A., Okoth, E., Martin, E., Kasiti, J., Bishop, R.P., 2009. Enhanced discrimination of African swine fever virus isolates through nucleotide sequencing of the p54, p72, and pB602L (CVR) genes. Virus Genes. 38,85-95.

Garciabeato, R., Salas, M.L., Vinuela, E., Salas, J., 1992b. Role of the host-cell nucleus in the replication of African swine fever virus-DNA. Virology 188 (2), 637–649.

García-Escudero R, Andrés G, Almazán F, Viñuela E. Inducible gene expression from African swine fever virus recombinants: analysis of the major capsid protein p72. J Virol. 1998 Apr;72(4):3185-95. doi: 10.1128/JVI.72.4.3185-3195.1998. PMID: 9580160; PMCID: PMC109780.

Giammarioli M, Gallardo C, Oggiano A, Iscaro C, Nieto R, Pellegrini C, Dei Giudici S, Arias M, De Mia GM. Genetic characterisation of African swine fever viruses from recent and historical outbreaks in Sardinia (1978-2009). Virus Genes. 2011 Jun;42(3):377-87. doi: 10.1007/s11262-011-0587-7. Epub 2011 Mar 5. PMID: 21373994.

Gómez-Villamandos JC, Hervás J, Méndez A, Carrasco L, Villeda CJ, Sierra MA, Wilkonson PJ. A pathological study of the perisinusoidal unit of the liver in acute African swine fever. Res Vet Sci. 1995 Sep;59(2):146-51. doi: 10.1016/0034-5288(95)90049-7. PMID: 8525104.

Granberg F, Torresi C, Oggiano A, Malmberg M, Iscaro C, De Mia GM, Belák S. Complete Genome Sequence of an African Swine Fever Virus Isolate from Sardinia, Italy. Genome Announc. 2016 Nov 17;4(6):e01220-16. doi: 10.1128/genomeA.01220-16. PMID: 27856577; PMCID: PMC5114369.

Gross, E., C. S. Sevier, A. Vala, C. A. Kaiser, and D. Fass. 2002. A new FAD-binding fold and intersubunit disulfide shuttle in the thiol oxidase Erv2p. Nat. Struct. Biol. 9:61-67.

Heath, C.M., Windsor, M., Wileman, T., 2001. Aggresomes resemble sites specialized for virus assembly. Journal of Cell Biology 153 (3), 449–455.

Iyer, L.A., Balaji, S., Koonin, E.V., Aravind, L., 2006. Evolutionary genomics of nucleo- cytoplasmic large DNA viruses. Virus Research 117 (1), 156–184.

Iyer, L.M., Aravind, L., Koonin, E.V., 2001. Common origin of four diverse families of large eukaryotic DNA viruses. Journal of Virology 75 (23), 11720–11734.

Jori F, Bastos AD. Role of wild suids in the epidemiology of African swine fever. Ecohealth. 2009 Jun;6(2):296-310. doi: 10.1007/s10393-009-0248-7. Epub 2009 Nov 14. PMID: 19915917.

Jouvenet, N., Windsor, M., Rietdorf, J., Hawes, P., Monaghan, P., Way, M., Wileman, T., 2006. African swine fever virus induces filopodia-like projections at the plasma membrane. Cellular Microbiology 8 (11), 1803–1811.

Jouvenet, N., Monaghan, P., Way, M., Wileman, T., 2004. Transport of African swine fever virus from assembly sites to the plasma membrane is dependent on microtubules and conventional kinesin. Journal of Virology 78 (15), 7990–8001.

Koonin, E.V., Yutin, N., 2010. Origin and evolution of eukaryotic large nucleo- cytoplasmic DNA viruses. Intervirology 53 (5), 284–292.

Koonin, E.V., Wolf, Y.I., Nagasaki, K., Dolja, V.V., 2009. The complexity of the virus world. Nature Reviews Microbiology 7 (3), p. 250.

Kuznar, J., Salas, M.L., Vinuela, E., 1980b. RNAs synthesized invitro by purified African swine fever virus. Archivos de Biologia y Medicina Experimentales 13 (4), 465.

Lewis, T., L. Zsak, T. G. Burrage, Z. Lu, G. F. Kutish, J. G. Neilan, and D. L. Rock. 2000. An African swine fever virus ERV1-ALR homologue, 9GL, affects virion maturation and viral growth in macrophages and viral virulence in swine. J. Virol. 74:1275-1285.

Liu H, Zhu Z, Feng T, Ma Z, Xue Q, Wu P, Li P, Li S, Yang F, Cao W, Xue Z, Chen H, Liu X, Zheng H. African Swine Fever Virus E120R Protein Inhibits Interferon Beta Production by Interacting with IRF3 To Block Its Activation. J Virol. 2021 Aug 25;95(18):e0082421. doi: 10.1128/JVI.00824-21. Epub 2021 Aug 25. PMID: 34190598; PMCID: PMC8387055.

Lubisi, B.A., Dwarka, R.M., Meenowa, D., Jaumally, R., 2009. An investigation into the first outbreak of African swine fever in the Republic of Mauritius. Transboundary and Emerging Diseases 56 (5), 178–188.

Lubisi, B.A., Bastos, A.D.S., Dwarka, R.M., Vosloo, W., 2007. Intra-genotypic resolu- tion of African swine fever viruses from an East African domestic pig cycle: a combined p72-CVR approach. Virus Genes 35 (3), 729–735.

Lubisi, B.A., Bastos, A.D.S., Dwarka, R.M., Vosloo, W., 2005. Molecular epidemi- ology of African swine fever in East Africa. Archives of Virology 150 (12), 2439–2452.

Malmquist, W.A.; Hay, D. Haemadsorbtion and cytopathic e_ect produced by ASFV in swine bone marrow and bu_y coat cultures. Am. J. Vet. Res. 1960, 21, 104–108.

Martínez-Pomares, L., C. Simo´n-Mateo, C. Lo´pez-Ot´ın, and E. Vin˜uela. 1997. Characterization of the African swine fever virus structural protein p14.5: a DNA binding protein. Virology 229:201–211.

Matson SW. DNA helicases of Escherichia coli. Prog Nucleic Acid Res Mol Biol. 1991;40:289-326. doi: 10.1016/s0079-6603(08)60845-4. PMID: 1851571.

Matsuyama T, Takano T, Nishiki I, Fujiwara A, Kiryu I, Inada M, Sakai T, Terashima S, Matsuura Y, Isowa K, Nakayasu C. A novel Asfarvirus-like virus identified as a potential cause of mass mortality of abalone. Sci Rep. 2020 Mar 12;10(1):4620. doi: 10.1038/s41598-020-61492-3. Erratum in: Sci Rep. 2020 May 15;10(1):8378. PMID: 32165658; PMCID: PMC7067878.

McLaughlin-Drubin, M.E., Münger, K., 2009. The human papillomavirus E7 oncoprotein. Virology. doi:10.1016/j.virol.2008.10.006

McVicar JW. Quantitative aspects of the transmission of African swine fever. Am J Vet Res. 1984 Aug;45(8):1535-41. PMID: 6476567.

Mebus CA, Dardiri AH. Additional characteristics of disease caused by the African swine fever viruses isolated from Brazil and the Dominican Republic. Proc Annu Meet U S Anim Health Assoc. 1979;(83):227-39. PMID: 298918.

Montgomery, R.E (1921a). On a form of swine fever occurring in British East Africa (Kenya colony) J. Comp. Pathol. 34, 159-191.

Montgomery, R.E (1921b). On a form of swine fever occurring in British East Africa (Kenya colony) J. Comp. Pathol. 34, 243-262

Moyer, R.W., Graves, R.L., 1981. The mechanism of cytoplasmic orthopoxvirus DNA- replication. Cell 27 (2), 391–401

Munoz, M., Freije, J.M., Salas, M.L., Vinuela, E., Lopez-Otin, C., 1993. Structure and expression in E. coli of the gene coding for protein p10 of African swine fever virus. Archives of Virology 130 (1–2), 93–107.

Mur L, Boadella M, Martínez-López B, Gallardo C, Gortazar C, Sánchez-Vizcaíno JM. Monitoring of African swine fever in the wild boar population of the most recent endemic area of Spain. Transbound Emerg Dis. 2012 Dec;59(6):526-31. doi: 10.1111/j.1865-1682.2012.01308.x. Epub 2012 Jan 16. PMID: 22248024.

Narechania, A., Terai, M., Chen, Z., DeSalle, R., Burk, R.D., 2004. Lack of the canonical pRB-binding domain in the E7 ORF of artiodactyl papillomaviruses is associated with the development of fibropapillomas. J. Gen. Virol. 85, 1243–1250. doi:10.1099/vir.0.19765-0.

Nindl, I., Gottschling, M., Stockfleth, E., 2007. Human papillomaviruses and non-melanoma skin cancer: Basic virology and clinical manifestations. Dis. Markers 23, 247–259.

Nix, R.J., Gallardo, C., Hutchings, G., Blanco, E., Dixon, L.K., 2006. Molecular epidemi- ology of African swine fever virus studied by analysis of four variable genome regions. Archives of Virology 151 (12), 2475–2494.

Ogata, H., Toyoda, K., Tomaru, Y., Nakayama, N., Shirai, Y., Claverie, J.-M., Nagasaki, K., 2009. Remarkable sequence similarity between the dinoflagellate-infecting marine girusand the terrestrial pathogen African swine fever virus. Virology Journal 6, http://dx.doi.org/10.1186/1743-422X-6-178.

OIE (2021) World Organization for Animal Health-African Swine Fever Virus Situation report 3 2021-2022 available on https://www.oie.int/app/uploads/2022/01/asf-situation-report-3.pdf.

OIE (2014) WAHID Database. Disease Information. Available at: http://web.oie.int/wahis/public.php?page1⁄4disease_ immediate_summary (accessed 25 June 2014 2012).

OIE (2012). African Swine Fever. In Manual of Diagnostic Tests and Vaccines for Terrestrial Animals, 7th ed.; Word Organization for Animal Health: Paris, France, 2012; Volume 2, pp. 1067–1079.

OIE (2011) available on https://www.oie.int/app/uploads/2021/03/a-fr-2011-pub.pdf.

Oleaga-Pérez A, Pérez-Sánchez R, Encinas-Grandes A. Distribution and biology of Ornithodoros erraticus in parts of Spain affected by African swine fever. Vet Rec. 1990 Jan 13;126(2):32-7. PMID: 2301109.

Ortin, J., Vinuela, E., 1977. Requirement of cell-nucleus for African swine fever virus- replication in Vero cells. Journal of Virology 21 (3), 902–905.

Pan IC, Hess WR. Virulence in African swine fever: its measurement and implications. Am J Vet Res. 1984 Feb;45(2):361-6. PMID: 6711963.

Pan IC, Hess WR. Virulence in African swine fever: its measurement and implications. Am J Vet Res. 1984 Feb;45(2):361-6. PMID: 6711963.

Penrith ML, Vosloo W. Review of African swine fever: transmission, spread and control. J S Afr Vet Assoc. 2009 Jun;80(2):58-62. doi: 10.4102/jsava.v80i2.172. PMID: 19831264.

Plowright W. Badgers and TB. Nature. 1981 Jan 1;289(5793):8. doi: 10.1038/289008a0. PMID: 7453811.

Ramirez-Medina, E.; Vuono, E.; O'Donnell, V.; Holinka, L.G.; Silva, E.; Rai, A.; Pruitt, S.; Carrillo, C.; Gladue, D.P.; Borca, M.V. 2019 Differential Effect of the Deletion of African Swine Fever Virus Virulence-Associated Genes in the Induction of Attenuation of the Highly Virulent Georgia Strain. Viruses, 11, doi:10.3390/v11070599.

Ran FA, Hsu PD, Lin CY, Gootenberg JS, Konermann S, Trevino AE, Scott DA, Inoue A, Matoba S, Zhang Y, Zhang F. Double nicking by RNA-guided CRISPR Cas9 for enhanced genome editing specificity. Cell. 2013 Sep 12;154(6):1380-9. doi: 10.1016/j.cell.2013.08.021. Epub 2013 Aug 29. Erratum in: Cell. 2013 Oct 10;155(2):479-80. PMID: 23992846; PMCID: PMC3856256.

Rangarajan, A., Talora, C., Okuyama, R., Nicolas, M., Mammucari, C., Oh, H., Aster, J.C., Krishna, S., Metzger, D., Chambon, P., Miele, L., Aguet, M., Radtke, F., Dotto, G.P., 2001. Notch signaling is a direct determinant of keratinocyte growth arrest and entry into differentiation. EMBO J. 20, 3427–3436. doi:10.1093/emboj/20.13.3427

Rodríguez I, Redrejo-Rodríguez M, Rodríguez JM, Alejo A, Salas J, Salas ML. African swine fever virus pB119L protein is a flavin adenine dinucleotide-linked sulfhydryl oxidase. J Virol. 2006 Apr;80(7):3157-66. doi: 10.1128/JVI.80.7.3157-3166.2006. PMID: 16537584; PMCID: PMC1440384.

Rodriguez, J.M., Salas, M.L., Vinuela, E., 1996. Intermediate class of mRNAs in African swine fever virus. Journal of Virology 70 (12), 8584–8589.

Rodríguez, J.M., Yán˜ez, R.J., Almazán, F., Vin˜uela, E., Rodriguez, J.F., 1993. African swine fever virus encodes a CD2 homolog responsible for the adhesion of eryth- rocytes to infected cells. Journal of Virology 67 (9), 5312–5320.

Rowlands, R.J., Michaud, V., Heath, L., Hutchings, G., Oura, C., Vosloo, W., Dwarka, R., Onashvili, T., Albina, E., Dixon, L.K., 2008. African swine fever virus isolate, Georgia, 2007. Emerging Infectious Diseases 14 (12), 1870–1874.

Salas ML, Andrés G. African swine fever virus morphogenesis. Virus Res. 2013 Apr;173(1):29-41. doi: 10.1016/j.virusres.2012.09.016. Epub 2012 Oct 8. PMID: 23059353.

Salas, M.L., Kuznar, J., Vinuela, E., 1981. Polyadenylation, methylation, and capping of the RNA synthesized invitro by African swine fever virus. Virology 113 (2), 484–491.

Salas, M.L., 1999. African swine fever virus. In: Webster, R.G., Granoff, A. (Eds.), Ency- clopedia of Virology., 2nd ed. Academic Press, London, United Kingdom, pp. 30–38.

Salas, M.L., Reycampos, J., Almendral, J.M., Talavera, A., Vinuela, E., 1986. Tran- scription and translation maps of African swine fever virus. Virology 152 (1), 228–240.

Salas, M.L., Kuznar, J., Vinuela, E., 1983. RNA synthesis by African swine fever (ASF) virus. African Swine Fever, Commission of the European Communities, Report EUR 8466 EN, pages 235–239 .

Sánchez-Cordón P.J., Nunez A., Neimanis A., Wikström-Lassa E., Montoya M., Crooke H., Gavier-Widén D. 2019 African swine fever: Disease dynamics in wild boar infected with ASFV isolates belonging to genotype I and II. Viruses.; 11:852.

Sánchez-Vizcaíno JM, Mur L, Gomez-Villamandos JC, Carrasco L. An update on the epidemiology and pathology of African swine fever. J Comp Pathol. 2015 Jan;152(1):9-21. doi: 10.1016/j.jcpa.2014.09.003. Epub 2014 Nov 11. PMID: 25443146.

Sánchez-Vizcaíno JM, Mur L, Martínez-López B. African swine fever (ASF): five years around Europe. Vet Microbiol. 2013 Jul 26;165(1-2):45-50. doi: 10.1016/j.vetmic.2012.11.030. Epub 2012 Nov 29. PMID: 23265248.

Sánchez-Vizcaíno JM, Mur L. African swine fever diagnosis update. Dev Biol (Basel). 2013;135:159-65. doi: 10.1159/000189240. Epub 2013 May 14. PMID: 23689893.

Sánchez-Vizcaíno JM, Mur L, Martínez-López B. African swine fever: an epidemiological update. Transbound Emerg Dis. 2012 Mar;59 Suppl 1:27-35. doi: 10.1111/j.1865-1682.2011.01293.x. Epub 2012 Jan 9. PMID: 22225967.

Sánchez-Vizcaíno J. M and Arias M J.J., (2012) African Swine Fever. In: Diseases of swine. 10th Edit. Zimerman, L. Karriker, A. Ramirez, K. Schwartz, G. Stevenson (Eds.), John Wiley & Sons, Ames, pp. 396-404

Sanchez-Vizcaino, J.M., 2006. African Swine Fever. In: Straw BE, Zimmerman JJ, D'Allaire S,Taylor DJ (eds) Diseases of Swine 9th edition, pp 291-298. Blackwell Publishing, Ames, Iowa.

Sanna G, Dei Giudici S, Bacciu D, Angioi PP, Giammarioli M, De Mia GM, Oggiano A. Improved Strategy for Molecular Characterization of African Swine Fever Viruses from Sardinia, Based on Analysis of p30, CD2V and I73R/I329L Variable Regions. Transbound Emerg Dis. 2017 Aug;64(4):1280-1286. doi: 10.1111/tbed.12504. Epub 2016 May 13. PMID: 27174805.

Sierra, M.A., Bernabe, A., Mozos, E., Mendez, A., Jover, A., 1987. Ultrastructure of the liver in pigs with experimental African swine fever. Veterinary Pathology 24 (5), 460–462.

Simeon-Negrin, R.E., Frias-Lepoureau, M.T., 2002. Eradication of African swine fever in Cuba (1971 and 1980). In: Morilla, A., Yoon, K.J., Zimmerman, J.J. (Eds.), Trends in Emerging Viral Infections of Swine, vol. 1. Iowa State Press, Ames, pp. 125–131.

Simon-Mateo, C., Andres, G., Almazan, F., Vinuela, E., 1997. Proteolytic processing in African swine fever virus: evidence for a new structural polyprotein, pp62. Journal of Virology 71 (8), 5799–5804.

Simon-Mateo, C., Andres, G., Vinuela, E., 1993. Polyprotein processing in African swine fever virus: a novel gene expression strategy for a DNA virus. EMBO Journal 12 (7), 2977–2987.

Singleton MR, Dillingham MS, Wigley DB. Structure and mechanism of helicases and nucleic acid translocases. Annu Rev Biochem. 2007;76:23-50. doi: 10.1146/annurev.biochem.76.052305.115300. PMID: 17506634.

Sogo, J. M., Almendral, J. M., Talavera, A., and Viñuela, E (1984). Terminal and internal inverted repetitions in Africa swine fever virus DNA. Virology 133, 271-275.

Suarez, C., Salas, M.L., Rodriguez, J.M., 2010b. African swine fever virus polypro- tein pp62 is essential for viral core development. Journal of Virology 84 (1), 176–187.

Sullivan CS, Pipas JM. T antigens of simian virus 40: molecular chaperones for viral replication and tumorigenesis. Microbiol Mol Biol Rev. 2002;66(2):179–202.

Tabares, E., Sanchezbotija, C., 1979. Synthesis of DNA in cells infected with African swine fever virus. Archives of Virology 61 (1–2), 49–59.

Thiimmes, P. and Htibscher, U.: Eukaryotic DNA helicases. FEBS Lett. 268(1990)325-328.

Thomson GR. The epidemiology of African swine fever: the role of free-living hosts in Africa. Onderstepoort J Vet Res. 1985 Sep;52(3):201-9. PMID: 3911134.

Tommasino M. The biology of beta human papillomaviruses. Virus Res. 2017 Mar 2;231:128-138.

Tommasino, M., 2014. The human papillomavirus family and its role in carcinogenesis. Semin. Cancer Biol. 26, 13–21. doi:10.1016/j.semcancer.2013.11.002

Tore G, Dore GM, Cacciotto C, Accardi R, Anfossi AG, Bogliolo L, Pittau M, Pirino S, Cubeddu T, Tommasino M, Alberti A. Transforming properties of ovine papillomaviruses E6 and E7 oncogenes. Vet Microbiol. 2019 Mar;230:14-22. doi: 10.1016/j.vetmic.2019.01.010. Epub 2019 Jan 9. PMID: 30827380.

Torresi C, Fiori M, Bertolotti L, Floris M, Colitti B, Giammarioli M, Dei Giudici S, Oggiano A, Malmberg M, De Mia GM, Belák S, Granberg F. The evolution of African swine fever virus in Sardinia (1978-2014) as

revealed by whole-genome sequencing and comparative analysis. Transbound Emerg Dis. 2020 Mar 12. doi: 10.1111/tbed.13540. Epub ahead of print. PMID: 32163673.

Tulman ER, Delhon GA, Ku BK, Rock DL. African swine fever virus. Curr Top Microbiol Immunol. 2009;328:43-87. doi: 10.1007/978-3-540-68618-7_2. PMID: 19216435.

Wilkinson, P. J. (1989). African swine fever virus. In "Virus infections of Porcines", (M. B. Penseaert, Ed.), pp. 17-37. Elsevier Sciences Publishers B. V., Amsterdam, Holland.

Wilkinson PJ, Pegram RG, Perry BD, Lemche J, Schels HF. The distribution of African swine fever virus isolated from Ornithodoros moubata in Zambia. Epidemiol Infect. 1988 Dec;101(3):547-64. doi: 10.1017/s0950268800029423. PMID: 3215286; PMCID: PMC2249407.

Wilkinson PJ, Wardley RC. The replication of African swine fever virus in pig endothelial cells. Br Vet J. 1978 May-Jun;134(3):280-2. doi: 10.1016/s0007-1935(17)33495-4. PMID: 566606.

Yanez, R.J., Rodriguez, J.M., Nogal, M.L., Yuste, L., Enriquez, C., Rodriguez, J.F., Vinuela, E., 1995. Analysis of the complete nucleotide sequence of African swine fever virus. Virology 208 (1), 249–278.

Yánez, R. J., M., R. J., Boursnell, M., Rodríguez, J. F., and Vinuela, E. (1993). Two putative African swine fever virus helicases similar to yeast 'DEAH' pre-mRNA processing proteins and vaccinia virus ATPases D11L and D6R. Gene 134: 161–174.

Yutin, N., Wolf, Y.I., Raoult, D., Koonin, E.V., 2009. Eukaryotic large nucleo- cytoplasmic DNA viruses: clusters of orthologous genes and reconstruc- tion of viral genome evolution. Virology Journal 6, http://dx.doi.org/10. 1186/1743-422X-6-223, Article Number: 223.

Zur Hausen, H., 2002. Papillomaviruses and cancer: from basic studies to clinical application. Nat. Rev. Cancer 2, 342–350. doi:10.1038/nrc798